

Lunbo Duan  
Lin Li

# Oxygen-Carrier- Aided Combustion Technology for Solid-Fuel Conversion in Fluidized Bed

OPEN ACCESS

 Springer

# Oxygen-Carrier-Aided Combustion Technology for Solid-Fuel Conversion in Fluidized Bed

Lunbo Duan · Lin Li

# Oxygen-Carrier-Aided Combustion Technology for Solid-Fuel Conversion in Fluidized Bed

 Springer

Lunbo Duan  
School of Energy and Environment  
Southeast University  
Nanjing, Jiangsu, China

Lin Li  
School of Energy and Environment  
Southeast University  
Nanjing, Jiangsu, China



This project was financially supported by the National Natural Science Foundation of China (No. 51922027).

ISBN 978-981-19-9126-4      ISBN 978-981-19-9127-1 (eBook)  
<https://doi.org/10.1007/978-981-19-9127-1>

© The Editor(s) (if applicable) and The Author(s) 2023. This book is an open access publication.

**Open Access** This book is licensed under the terms of the Creative Commons Attribution 4.0 International License (<http://creativecommons.org/licenses/by/4.0/>), which permits use, sharing, adaptation, distribution and reproduction in any medium or format, as long as you give appropriate credit to the original author(s) and the source, provide a link to the Creative Commons license and indicate if changes were made.

The images or other third party material in this book are included in the book's Creative Commons license, unless indicated otherwise in a credit line to the material. If material is not included in the book's Creative Commons license and your intended use is not permitted by statutory regulation or exceeds the permitted use, you will need to obtain permission directly from the copyright holder.

The use of general descriptive names, registered names, trademarks, service marks, etc. in this publication does not imply, even in the absence of a specific statement, that such names are exempt from the relevant protective laws and regulations and therefore free for general use.

The publisher, the authors, and the editors are safe to assume that the advice and information in this book are believed to be true and accurate at the date of publication. Neither the publisher nor the authors or the editors give a warranty, expressed or implied, with respect to the material contained herein or for any errors or omissions that may have been made. The publisher remains neutral with regard to jurisdictional claims in published maps and institutional affiliations.

This Springer imprint is published by the registered company Springer Nature Singapore Pte Ltd. The registered company address is: 152 Beach Road, #21-01/04 Gateway East, Singapore 189721, Singapore

# Preface

The FBC technology has obvious advantages like fuel adaptability, flexible control of furnace temperature and load (by solid recycle), low-cost control of  $\text{SO}_2/\text{NO}_x$ , etc. It is widely considered as an advanced clean fuel conversion technology for burning inferior fuels. Although FBC technology is claimed to provide uniform temperature distribution, good mass transfer, and mixing, oxygen must be transported from air to the reaction surface of the fuel in a large fluidized bed combustor under relative long time. In industrial-scale CFB combustors, the uneven distributions of oxygen and temperature both horizontally and vertically are still inevitable, leading to large FBC boiler sizes and a combustion efficiency that could be improved. This is noticed in burning high-volatile waste fuels like biomass and MSWs in industrial CFBs.

As a new concept, oxygen-carrier-aided combustion (OCAC) technology proposed in 2013 can alleviate the problem of uneven distribution of oxygen in the reactors. OCAC implies the use of oxygen carriers to replace the inert bed material in the reactor completely or partially. This supplies oxygen from the oxygen carriers via redox reactions (oxygen release and uptake) taking place locally and simultaneously in a single furnace. This technology developed rapidly in the past few years, combustion experiments from laboratory scale—semi-industrial scale—and industrial scale have been accomplished, and results are verified. The oxygen buffering capacity of OCAC has been clearly demonstrated. Therefore, OCAC has corresponding advantages such as low concentrations of unburned hydrocarbons, low CO emission, high sulfur capture rates, and so on. Coupled with oxy-fuel combustion for carbon capture, OCAC can also bring many benefits, one of which is enhanced combustion efficiency at low excess oxygen. Therefore, OCAC is expected to be a promising technique route for improving oxygen and temperature distribution in different conversion processes.

In this book, we firstly introduce the basic working principles of OCAC and then focus on evaluating the presently available experimental work and main findings in a detailed manner. Afterward, special attention has been paid to some issues requiring further investigation, such as benefits (improvement of the boiler operation), costs (OC cost, lifetime, possibilities of regeneration), and criteria for regeneration of bed material in OCAC. Beyond this, some new concepts are proposed, like OCAC with

Oxy-PFBC, OCAC coupled with staged conversion of fuel, OCAC in rotary kilns, and multi-functional OCAC. There will be increasingly more beneficial applications of OCAC in the future. However, so far, tests of OCAC on commercial boilers have only been carried out on low-ash, high-volatile fuels with ilmenite ore as OC. Other conditions can only be discussed superficially, because of lack of experience. Especially the fuel characteristics and the properties of the OC can only be summarized at present, and a wider experience is required. In addition, technical and economic analysis of OCAC has not yet been carried out, including the benefits (improvement of the boiler operation) and costs (the cost, lifetime, and recovery of OC) of OCAC, as well as the regeneration of OC. All these are topics interesting to discuss.

The last part of this book outlines perspectives for future research and development of OCAC. As an emerging technology, there are still many studies and investigations needed to fill in the gaps required for a comprehensive understanding of the technology from fundamental studies to industrial application demonstrations. It is expected that this book provides some novel insights for the readership in the industrial and academic field and that it stimulates follow-up research on this topic.

The publication of this book was financially supported by the National Natural Science Foundation of China (No. 51922027). Last but not the least, we would like to express our sincere thanks to Dr. Dennis Yong Lu (CanmetENERGY-Ottawa, Natural Resource Canada, Canada), Professor Bo Leckner (Chalmers University of Technology, Sweden), Professor Zhenkun Sun (Southeast University, China), Dr. Yueming Wang (Southeast University, China) and Dr. Chun Zhu (Southeast University, China) for their valuable suggestion during the preparation of this book.

Nanjing, China  
25 October 2022

Lunbo Duan  
Lin Li

# Contents

<b>1 Introduction</b> .....	1
1.1 General Background .....	1
1.2 The Objectives of This Book .....	4
References .....	5
<b>2 The Evolution of OCAC and Its Working Principles</b> .....	9
2.1 Three-Way Catalyst (TWC) Technology .....	9
2.2 Chemical Looping Combustion (CLC) Technology .....	10
2.3 Basic Working Principles of OCAC .....	11
2.3.1 OCAC Technology Evolution .....	11
2.3.2 Suggested OCAC Principles .....	12
References .....	17
<b>3 OCAC for Fuel Conversion Without CO<sub>2</sub> Capture</b> .....	19
3.1 Operation Experience .....	19
3.1.1 Combustion Performance .....	19
3.1.2 Oxygen Buffering Ability .....	35
3.2 Emissions .....	37
3.2.1 NO <sub>x</sub> Emission .....	37
3.2.2 SO <sub>x</sub> Emission and Desulfurization .....	40
3.3 Ash-Related Issues .....	42
3.3.1 Bed Agglomeration .....	43
3.3.2 Ash-Layer Formation of OC .....	43
3.4 The Aging of Oxygen Carrier .....	53
3.5 Bed Material Recovery .....	56
3.6 Characteristic Properties of OC .....	59
References .....	60
<b>4 OCAC Technology in Oxy-Fuel Combustion for Carbon Capture</b> .....	65
4.1 Combustion Performance .....	66
4.2 Emissions .....	70

4.2.1	SO <sub>2</sub> Emission and Desulfurization .....	70
4.2.2	NO <sub>x</sub> and N <sub>2</sub> O Emission .....	71
4.2.3	Condensate Liquid Analysis .....	74
4.3	Bed Material Analysis .....	75
	References .....	76
<b>5</b>	<b>Oxygen Carrier Aided Gasification (OCAG) .....</b>	<b>79</b>
5.1	The Proposed of Technical Routes .....	80
5.2	Gasification/Reforming Characteristics .....	83
5.2.1	OC Aided Tar Reforming .....	83
5.2.2	OC Aided Gasification .....	86
5.3	Screening of Bed Materials .....	89
5.4	Ash-Related Effects .....	90
	References .....	94
<b>6</b>	<b>New Concepts for OCAC in Other Applications .....</b>	<b>97</b>
6.1	OCAC with Pressurized Oxy-Fuel Combustion .....	97
6.1.1	Pressurized Oxy-Fuel Combustion .....	97
6.1.2	Oxygen-Carrier-Aided Oxy-PFBC Process .....	99
6.1.3	The Potential Advantages of OC Aided POFC .....	103
6.2	OCAC Coupled with Staged Conversion of Fuel .....	104
6.2.1	Staged Conversion of Fuel .....	104
6.2.2	OCAC Coupled with Staged Conversion of Fuel .....	104
6.3	OCAC Application Beyond Fluidized Bed .....	105
6.4	Multi-functional OCAC .....	108
	References .....	110
<b>7</b>	<b>Perspectives on Future Research .....</b>	<b>115</b>
7.1	Fundamentals Regarding Transport Phenomena and Chemical Reactions .....	115
7.1.1	Heat and Mass Transfer and Reactions .....	115
7.1.2	Problems Associated with Alkali Metals and S .....	116
7.2	Pollutant Transformation Routes and Control Strategies .....	116
7.2.1	NO <sub>x</sub> and SO <sub>x</sub> Formation and Emission Mechanism .....	116
7.2.2	The Emissions of Cl and Dioxin .....	117
7.2.3	Emissions of Mercury, Heavy Metals and PM .....	117
7.3	More Testing and Application of OCAC .....	117
7.3.1	More OC and Fuel Testing .....	117
7.3.2	More Applications of OCAC Technology .....	118
7.4	Techno-economic Analysis of OCAC Technology .....	118
7.5	Process Scale-Up and Optimization .....	119
7.5.1	Process Scale-Up .....	119
7.5.2	Process Optimization .....	120
	References .....	121



## About the Authors

**Lunbo Duan** obtained his doctoral degree in Environmental Engineering from Southeast University in 2010. After that, he worked as a lecturer at the School of Energy and Environment at Southeast University and was appointed as an associate professor and a professor in 2012 and 2018, respectively. Funded by Engineering and Physical Sciences Research Council (EPSRC), he worked as a research fellow at Cranfield University in the UK from 2014 to 2015. He has received funding from various institutions, including the National Natural Science Foundation of China, Ministry of Science and Technology (China), Korean Institute of Energy Research, and Babcock & Wilcox group (USA). He has published more than 200 papers in peer-reviewed journals, and four papers have been selected as “ESI Highly Cited Papers”. He has won the second prize of the Natural Science Award of the Ministry of Education (China) in 2014 (Rank 4) and 2018 (Rank 1). e-mail: [duanlunbo@seu.edu.cn](mailto:duanlunbo@seu.edu.cn)

**Lin Li** received his doctoral degree in Power Engineering and Engineering Thermophysics from Southeast University in 2021. From 2019 to 2020, he worked as a joint training Ph.D. student at the CanmetENERGY-Ottawa, Natural Resources Canada, for 15 months. Now he is a postdoctoral fellow in Southeast University. He has received funding from the National Natural Science Foundation of China, Postdoctoral Innovative Talent Support Program, and Jiangsu Funding Program for Excellent Postdoctoral Talent, and he has published 25 papers in peer-reviewed journals. He has been working with the solid fuel combustion in fluidized bed, oxy-fuel combustion, and oxygen-carrier-aided combustion. e-mail: [101300126@seu.edu.cn](mailto:101300126@seu.edu.cn)

# Chapter 1

## Introduction



### 1.1 General Background

In gas–solid fluidization theory, solid particles become fluidized when an ascending gas imposes a high enough drag force to overcome the downward force of gravity. Fluidized bed reactor (FBR) is an apparatus developed based on the fluidization theory, which has been applied to many kinds of multiphase chemical reactions for energy conversion, chemical, petroleum, metallurgy, and nuclear industries [1, 2]. Fluidized bed reactors have been operated commercially since the 1920s, with the advent of the Winkler coal gasifier in Germany [3]. The first attempt to burn solid fuels in a fluidized bed combustor (FBC) was made in the Soviet Union in the 1950s to develop boilers for industry and district heating. After that, the FBC technology experienced extensive development again from the 1970s [4–6].

During a typical process in FBC, fuel and desulfurization adsorbents, typically limestone, are injected into the lower part of the combustor to be quickly dispersed with the high-temperature bed material fluidized by the combustion gases. Fluidization gas, usually air, is blown into the bed through the air distributor from the wind box at the bottom of the furnace [5]. The fuel is immediately heated due to the high heat transfer coefficient, followed by drying, ignition, volatiles combustion, and char combustion. The limestone is decomposed and absorbs the  $\text{SO}_2$  generated from fuel combustion. With the increase of the fluidizing gas velocity, a bed will experience different fluidization states: fixed bed, bubbling fluidized bed, turbulent fluidized bed, fast bed, and pneumatic conveying.

Generally, large-scale FB reactors employ circulating fluidized bed (CFB) to achieve a satisfactory combustion performance, sulphur removal, and operation reliability [6]. In a CFB combustor, the bottom of the furnace is usually a bubbling or turbulent fluidized bed, while the upper part is normally a fast bed or pneumatic conveying. The small particles (bed material, char, fine ash, and desulfurization absorbent) can be carried out of the furnace by gas flow. They are then captured by a cyclone separator and recirculated to the furnace. This ensures higher combustion and

desulfurization efficiencies. The CFB combustion technology shows many advantages: flexible fuel applicability, stable temperature control, flexible load control, low  $\text{NO}_x$  formation, efficient desulfurization in the boiler, high combustion efficiency, and so on [4, 7–12].

Over the last several decades, fluidized combustion has attracted widespread attention, and a large number of investigations have been done, including hydrodynamic and mixing characteristics [5, 13–17], combustion behavior [18–24], heat and mass transfer enhancement [25–31], pollutant emission controls [5, 32–37], scale-up [6, 11, 12, 38, 39], and so on. It has been used successfully to burn a variety of solid fuels, including high-sulfur petroleum coke, different ranks of coal, and solid wastes [40–43]. In recent years, integrating CFB technology with oxy-fuel combustion (including pressurized oxy-fuel combustion) [44–56] or chemical looping combustion (CLC) [57–62] for carbon capture has become highlighted research topics due to the demand for tackling global warming.

Gas–solid mixing is always an important topic in fluidized bed combustors since it determines heat and mass transfer, combustion behavior, combustion efficiency, and pollutant emissions [11, 24, 63]. The mass transfer in a fluidized bed combustor is a complicated phenomenon. After many years of development, it is generally accepted that oxygen in the bubble phase must pass through inert bed material to reach the fuel surface in the emulsion phase [64], which is different from the direct contact between fuel and oxygen in pulverized coal combustor (Fig. 1.1). The dense phase of the fluidized bed reactor presents an anoxic atmosphere on the whole, thus the char combustion in the dense bed is mainly controlled by oxygen diffusion. In the upper part of the reactor, namely in the transport zone, a core annular structure with a dilute phase surrounding the fuel particle is usually proposed, and the air supply, e.g., the secondary air, needs to reach the fuel in the center of the furnace. Generally, increasing bed voidage and disturbances can enhance the mass transfer, provided that the gas and fuel are evenly distributed in the bed [65, 66].

It should be noted that there are still some problems related to poor mixing, especially in large-scale CFB combustors. In a typical CFB process, the fuel is fed from the wall of the furnace, while the primary air is injected over the cross-section through the distributor [5]. The dispersion of fuel in the bed as well as the uniformity of the air supply determines the fluidization conditions and the distribution of heat release in the bed. According to the experiment and simulation studies on both lab- and industrial-scale CFB combustors, it is found that the effective lateral fuel dispersion coefficient ( $D_{sr}$ ) increases gradually with the increase of the boiler size until reaching a stable value [11, 63, 67–70]. The value of  $D_{sr}$  for fuel particles in industrial CFB boilers is of the order of  $0.1 \text{ m}^2/\text{s}$ , which is affected by the fluidization velocity, the static bed height, the bed particle size, etc. [11, 63]. The fuel is usually introduced from the furnace wall in one or several feed points, sometimes air assisted. The fuel has to travel over the furnace cross section, a distance depending on boiler size. Therefore, the fuel distribution in the fluidized-bed combustor becomes more uneven when the boiler capacity is further increased to electric utility size. In addition to the lateral dispersion, light fuels, such as biomass and solid wastes, tend to be

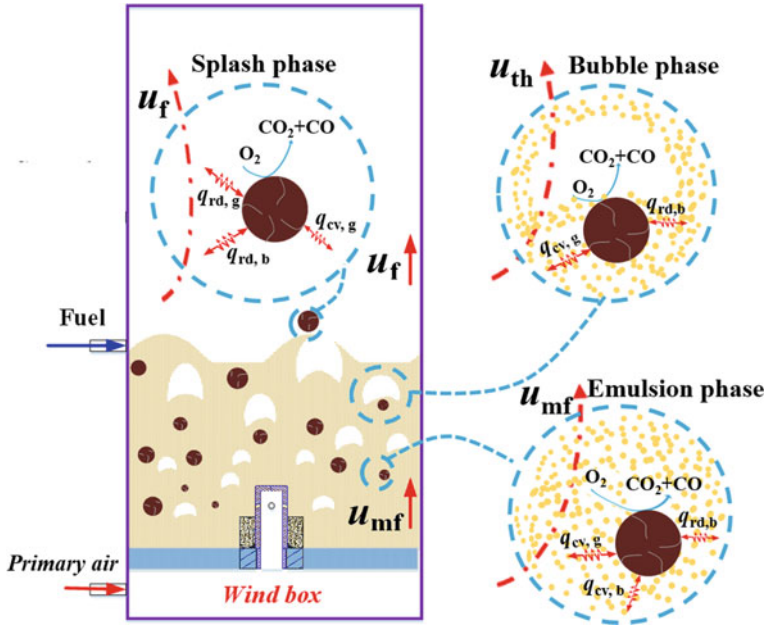


**Fig. 1.1** Heat and mass transfer as a function of the location of the char particle in the bed.  $u_f$ ,  $u_{mf}$  and  $u_{th}$  are the fluidization velocity, minimum fluidization velocity and the velocity through the bubble, respectively

subject to more segregation and bad mixing of fuel and oxygen because of the rapid release of volatiles [71–76].

Poor gas–solid mixing may bring many operational problems, such as local defluidization, uneven temperature distribution, agglomeration, low burnout rate, large excess air ratio, high pollutant emission, and so on [5]. Such issues not only reduce the efficiency of the boiler but also cause safety and environmental problems. Even though technical measures have been introduced to improve the spatial mixing characteristics of boilers, such as optimizing the size distribution of fuel particles, increasing the number of fuel feed points, improving the air distributor performance to ensure even primary air supply, increasing secondary air momentum, etc. Here is still room for improvements.

In 2013, Thunman et al. [77] from Chalmers University of Technology proposed the innovative technology concept of oxygen-carrier-aided combustion (OCAC), which aims of improving the distribution of oxygen throughout the combustion chamber. In this concept, the conventional inert bed inventory (usually silica sand and ash) is partially or completely replaced by reactive particles, like metal oxides. Such so-called oxygen carriers can react with fuels via redox reactions. As a result, the redox reactions taking place on oxygen carriers can transfer oxygen from an oxidizing zone to a reducing region, which can improve the uniformity of the spatial oxygen distribution. The OCAC technology is a technical adjustment based on the traditional

fluidized-bed reactor, which can be applied to various fuel conversion technologies, such as coal-fired large-scale CFB combustion, combustion/gasification technology for low-quality fuels (such as biomass and solid waste), oxy-CFB combustion for carbon capture and storage (CCS), and so on.

## 1.2 The Objectives of This Book

FBC technology with the advantages of flexible fuel applicability, stable temperature control, inherently low gas-pollutant emissions, etc. is an advanced fuel-conversion technology, applied in industry, and in heat and electric utilities. Theoretically, FBC has good gas–solid mixing and a resulting uniform temperature distribution. In the actual FBC operation, however, especially in large-scale reactors, the mixing of oxygen and fuel is still limited by the lateral solids dispersion coefficient ( $D_{sr}$ ) and gas penetration. Such an issue not only reduces the combustion efficiency but also brings a series of problems related to the operation, such as excessive emissions and bed agglomeration.

OCAC technology, which is using oxygen carrier particles to partially or completely replace the traditional inert bed materials in fluidized-bed reactors. The oxygen carrier particles act as oxygen buffers to take up oxygen into their lattice from oxidizing regions and to subsequently react with volatiles in reducing areas, where  $\text{CO}_2/\text{CO}$  and  $\text{H}_2\text{O}/\text{H}_2$  are generated. This technology is aiming to improve combustion efficiency, enhance operational safety, and reduce pollutant emission by promoting the uniformity of the oxygen and temperature distributions in a fluidized-bed reactor. Benefiting from the oxygen buffering characteristic of oxygen carrier particles, OCAC can significantly improve the oxygen distribution throughout the combustion chamber, which can reduce CO and hydrocarbon emissions.

At present, the OCAC technology has already gone through a series of experimental studies at different scales and is considered feasible and economical. The main research institutions on the technology include the Chalmers University of Technology, CanmetENERGY-Ottawa and Vienna University of Technology, etc. Chalmers University of Technology's research mainly focuses on the oxygen carrier aided air combustion, CanmetENERGY mainly investigates the OC aided oxy-fuel (natural gas, biomass, and coal) combustion, whereas Vienna University of Technology mainly investigates the OC aided gasification. The scientific concerns, including combustion and emission characteristics, ash-related problems, OC reactivation, and so on.

In this book, we intent to summarize the evolution and working principle of OCAC firstly, and then introduce the development status of OC aided solid fuel conversion technology critically from three aspects: OCAC without  $\text{CO}_2$  capture and with  $\text{CO}_2$  capture, and OC aided gasification. Some new concepts like OCAC coupled with staged conversion of fuel, OCAC with rotatory kiln, and multi-functional OCAC, are also proposed for the potential applications of OCAC technology. In addition, the future research directions as well as the possible extended strategies based on

OCAC technology are outlooked. This is expected to promote a rapid development of OCAC technology in both fundamental research and practical applications.

## References

1. Trambouze PE (2004) Chemical reactors: from design to operation. Editions Technip, Paris
2. Howard JR (1989) Fluidized bed technology: principles and applications. Adam Higler, New York
3. Leckner B (2016) Developments in fluidized bed conversion of solid fuels. *Therm Sci* 20:S1–S18
4. Koornneef J, Junginger M, Faaij A (2007) Development of fluidized bed combustion—an overview of trends, performance and cost. *Prog Energy Combust Sci* 33:19–55
5. Leckner B (1998) Fluidized bed combustion: mixing and pollutant limitation. *Prog Energy Combust Sci* 24:31–61
6. Yue G, Cai R, Lu J, Zhang H (2017) From a CFB reactor to a CFB boiler—the review of R&D progress of CFB coal combustion technology in China. *Powder Technol* 316:18–28
7. Anthony EJ (1995) Fluidized bed combustion of alternative solid fuels; status, successes and problems of the technology. *Prog Energy Combust Sci* 21:239–268
8. Basu P (2006) Combustion and gasification in fluidized beds. CRC Press, Boca Raton
9. Basu P (1999) Combustion of coal in circulating fluidized-bed boilers: a review. *Chem Eng Sci* 54:5547–5557
10. Yue G, Lu J, Zhang H, Yang H, Zhang J, Liu Q, Li Z, Joos E, Jaud P (2005) Design theory of circulating fluidized bed boilers. In: 18th international conference on fluidized bed combustion, pp 135–146
11. Leckner B, Szentannai P, Winter F (2011) Scale-up of fluidized-bed combustion—a review. *Fuel* 90:2951–2964
12. Basu P (2013) Fluidized bed boilers: design and application
13. Peirano E, Leckner B (1998) Fundamentals of turbulent gas-solid flows applied to circulating fluidized bed combustion. *Prog Energy Combust Sci* 24:259–296
14. Shen L, Johnsson F, Leckner B (2004) Digital image analysis of hydrodynamics two-dimensional bubbling fluidized beds. *Chem Eng Sci* 59:2607–2617
15. Sasic S, Leckner B, Johnsson F (2007) Characterization of fluid dynamics of fluidized beds by analysis of pressure fluctuations. *Prog Energy Combust Sci* 33:453–496
16. Johansson A, Johnsson F, Leckner B (2007) Solids back-mixing in CFB boilers. *Chem Eng Sci* 62:561–573
17. Johnsson F, Larsson G, Leckner B (2002) Pressure and flow fluctuations in a fluidized bed—interaction with the air-feed system. *Chem Eng Sci* 57:1379–1392
18. Kullendorff A, Andersson S (1986) A general review on combustion in circulating fluidized beds. In: Basu P (ed) *Circulating fluidized bed technology*. Pergamon, Oxford, pp 83–96
19. Wang L, Hustad JE, Skreiberg Ø, Skjevraak G, Grønli M (2012) A critical review on additives to reduce ash related operation problems in biomass combustion applications. *Energy Procedia* 20:20–29
20. Nevalainen H, Jegeroff M, Saastamoinen J, Tourunen A, Jäntti T, Kettunen A et al (2007) Firing of coal and biomass and their mixtures in 50kW and 12MW circulating fluidized beds—phenomenon study and comparison of scales. *Fuel* 86:2043–2051
21. Cai R, Zhang M, Mo X, Lyu J, Yang H, Lei X et al (2018) Operation characteristics of external heat exchangers in the 600MW supercritical CFB boiler. *Fuel Process Technol* 172:65–71
22. Sivakumar R, Saravanan R, Elaya Perumal A, Iniyan S (2016) Fluidized bed drying of some agro products—a review. *Renewable and Sustainable Energy Reviews* 61:280–301
23. Chern JS, Hayhurst AN (2012) Fluidised bed studies of: (i) Reaction-fronts inside a coal particle during its pyrolysis or devolatilisation, (ii) the combustion of carbon in various coal chars. *Combust Flame* 159:367–375

24. Agarwal PK, La Nauze RD (1989) Transfer processes local to the coal particle: a review of drying, devolatilization and mass transfer in fluidized bed combustion. *Chem Eng Res Des* 67:457–480
25. Gómez-Barea A, Ollero P, Leckner B (2007) Mass transport effects during measurements of gas–solid reaction kinetics in a fluidised bed. *Chem Eng Sci* 62:1477–1493
26. Abdelmotalib HM, Youssef MAM, Hassan AA, Youn SB, Im I-T (2015) Heat transfer process in gas–solid fluidized bed combustors: a review. *Int J Heat Mass Transf* 89:567–575
27. Andersson B-Å, Leckner B (1992) Experimental methods of estimating heat transfer in circulating fluidized bed boilers. *Int J Heat Mass Transf* 35:3353–3562
28. Scala F (2007) Mass transfer around freely moving active particles in the dense phase of a gas fluidized bed of inert particles. *Chem Eng Sci* 62:4159–4176
29. Parmar MS, Hayhurst AN (2002) The heat transfer coefficient for a freely moving sphere in a bubbling fluidised bed. *Chem Eng Sci* 57:3485–3494
30. Hayhurst AN, Parmar MS (2002) Measurement of the mass transfer coefficient and Sherwood number for carbon spheres burning in a bubbling fluidized bed. *Combust Flame* 130:361–375
31. Chao J, Lu J, Yang H, Zhang M, Liu Q (2015) Experimental study on the heat transfer coefficient between a freely moving sphere and a fluidized bed of small particles. *Int J Heat Mass Transf* 80:115–125
32. Ke X, Cai R, Zhang M, Miao M, Lyu J, Yang H (2018) Application of ultra-low NO<sub>x</sub> emission control for CFB boilers based on theoretical analysis and industrial practices. *Fuel Process Technol* 181:252–258
33. Leckner B, Åmand LE, Lücke K, Werther J (2004) Gaseous emissions from co-combustion of sewage sludge and coal/wood in a fluidized bed. *Fuel* 83:477–486
34. Wu L, Qin W, Hu X, Dong C, Yang Y (2015) Mechanism study on the influence of in situ SO<sub>x</sub> removal on N<sub>2</sub>O emission in CFB boiler. *Appl Surf Sci* 333:194–200
35. Cui J, Duan L, Zhou L, Zhao C (2018) Effects of air pollution control devices on the chlorine emission from 410 t/h circulating fluidized bed boilers co-firing petroleum coke and coal. *Energy Fuels* 32:4410–4416
36. Cui J, Duan L, Jiang Y, Zhao C, Anthony EJ (2018) Migration and emission of mercury from circulating fluidized bed boilers co-firing petroleum coke and coal. *Fuel* 215:638–646
37. Duan L, Cui J, Jiang Y, Zhao C, Anthony EJ (2017) Partitioning behavior of arsenic in circulating fluidized bed boilers co-firing petroleum coke and coal. *Fuel Process Technol* 166:107–114
38. Knowlton TM, Karri SBR, Issangya A (2005) Scale-up of fluidized-bed hydrodynamics. *Powder Technol* 150:72–77
39. Detamore MS, Swanson MA, Frender KR, Hrenya CM (2001) A kinetic-theory analysis of the scale-up of circulating fluidized beds. *Powder Technol* 116:190–203
40. Desroches-Ducarne E, Marty E, Martin G, Delfosse L (1998) Co-combustion of coal and municipal solid waste in a circulating fluidized bed. *Fuel* 77:1311–1315
41. Arena U (2012) Process and technological aspects of municipal solid waste gasification. A review. *Waste Management* 32:625–639
42. Chen J, Lu X (2007) Progress of petroleum coke combusting in circulating fluidized bed boilers—a review and future perspectives. *Resour Conserv Recycl* 49:203–216
43. Leckner B, Lind F (2020) Combustion of municipal solid waste in fluidized bed or on grate—a comparison. *Waste Manage* 109:94–108
44. Lupion M, Alvarez I, Otero P, Kuivalainen R, Lantto J, Hotta A et al (2013) 30 MWth CIUDEN Oxy-cfb boiler—first experiences. *Energy Procedia* 37:6179–6188
45. Seddighi KS, Pallarès D, Normann F, Johnsson F (2013) Progress of combustion in an oxy-fuel circulating fluidized-bed furnace: measurements and modeling in a 4 MWth boiler. *Energy Fuels* 27:6222–6230
46. Tan Y, Jia L, Wu Y, Anthony EJ (2012) Experiences and results on a 0.8MWth oxy-fuel operation pilot-scale circulating fluidized bed. *Applied Energy* 92:343–347
47. Jia L, Tan Y, Anthony EJ (2010) Emissions of SO<sub>2</sub> and NO<sub>x</sub> during Oxy–Fuel CFB combustion tests in a mini-circulating fluidized bed combustion reactor. *Energy Fuels* 24:910–915

48. Duan L, Sun H, Zhao C, Zhou W, Chen X (2014) Coal combustion characteristics on an oxy-fuel circulating fluidized bed combustor with warm flue gas recycle. *Fuel* 127:47–51
49. Leckner B, Gómez-Barea A (2014) Oxy-fuel combustion in circulating fluidized bed boilers. *Appl Energy* 125:308–318
50. Anthony EJ, Preto F (1995) Pressurized combustion in FBC systems. In: Cuenca MA, Anthony EJ (eds) *Pressurized fluidized bed combustion*. Springer, Dordrecht, pp 80–120
51. Cai N, Zhang M, Li D, Fu W (1994) Research and development on PFBC-CC in China and Jiawang pilot plant project. *J Therm Sci* 3:205–210
52. Lasek JA, Janusz M, Zuwała J, Glód K, Iluk A (2013) Oxy-fuel combustion of selected solid fuels under atmospheric and elevated pressures. *Energy* 62:105–112
53. Lasek JA, Glód K, Janusz M, Kazalski K, Zuwała J (2012) Pressurized oxy-fuel combustion: a study of selected parameters. *Energy Fuels* 26:6492–6500
54. Wang J, Duan Y, Duan L, Yan Y, Tong S, Zhao C (2019) Sulfur enrichment in particulate matter generated from a lab-scale pressurized fluidized bed combustor. *Energy Fuels* 33:603–611
55. Duan Y, Duan L, Wang J, Anthony EJ (2019) Observation of simultaneously low CO, NO<sub>x</sub> and SO<sub>2</sub> emission during oxy-coal combustion in a pressurized fluidized bed. *Fuel* 242:374–381
56. Li L, Duan Y, Duan L, Xu C, Anthony EJ (2018) Flow characteristics in pressurized oxy-fuel fluidized bed under hot condition. *Int J Multiph Flow* 108:1–10
57. Ishida M, Jin H (1994) A new advanced power-generation system using chemical-looping combustion. *Energy* 19:415–422
58. Lyngfelt A, Leckner B, Mattisson T (2001) A fluidized-bed combustion process with inherent CO<sub>2</sub> separation; application of chemical-looping combustion. *Chem Eng Sci* 56:3101–3113
59. Adanez J, Abad A, Garcia-Labiano F, Gayan P, de Diego LF (2012) Progress in chemical-looping combustion and reforming technologies. *Prog Energy Combust Sci* 38:215–282
60. Song T, Shen L (2018) Review of reactor for chemical looping combustion of solid fuels. *Int J Greenhouse Gas Control* 76:92–110
61. Xiao R, Song Q, Song M, Lu Z, Zhang S, Shen L (2010) Pressurized chemical-looping combustion of coal with an iron ore-based oxygen carrier. *Combust Flame* 157:1140–1153
62. Wang X, Wang X, Kong Z, Shao Y, Jin B (2020) Auto-thermal operation and optimization of coal-fueled separated gasification chemical looping combustion in a pilot-scale unit. *Chem Eng J* 383:123159
63. Liu D, Chen X (2010) Lateral solids dispersion coefficient in large-scale fluidized beds. *Combust Flame* 157:2116–2124
64. Salinero J, Gómez-Barea A, Fuentes-Cano D, Leckner B (2018) Measurement and theoretical prediction of char temperature oscillation during fluidized bed combustion. *Combust Flame* 192:190–204
65. Breault RW (2006) A review of gas–solid dispersion and mass transfer coefficient correlations in circulating fluidized beds. *Powder Technol* 163:9–17
66. Agarwal PK, Mitchell WJ, La Nauze RD (1988) Transport phenomena in multi-particle systems—III. Active particle mass transfer in fluidized beds of inert particles. *Chemical Engineering Science* 43:2511–2521
67. Winaya INS, Shimizu T, Yamada D (2007) A new method to evaluate horizontal solid dispersion in a bubbling fluidized bed. *Powder Technol* 178:173–178
68. Chirone R, Miccio F, Scala F (2004) On the relevance of axial and transversal fuel segregation during the FB combustion of a biomass. *Energy Fuels* 18:1108–1117
69. Niklasson F, Thunman H, Johnsson F, Leckner B (2002) Estimation of solids mixing in a fluidized-bed combustor. *Ind Eng Chem Res* 41:4663–4673
70. Schlichthaerle P, Werther J (2001) Solids mixing in the bottom zone of a circulating fluidized bed. *Powder Technol* 120:21–33
71. Duan L, Li L, Liu D, Zhao C (2019) Fundamental study on fuel-staged oxy-fuel fluidized bed combustion. *Combust Flame* 206:227–238
72. Dennis JS, Hayhurst AN, Scott SA (2006) The combustion of large particles of char in bubbling fluidized beds: the dependence of Sherwood number and the rate of burning on particle diameter. *Combust Flame* 147:185–194



73. Scala F (2009) A new technique for the measurement of the product CO/CO<sub>2</sub> ratio at the surface of char particles burning in a fluidized bed. *Proc Combust Inst* 32:2021–2027
74. Qin K, Thunman H, Leckner B (2017) Mass transfer under segregation conditions in fluidized beds. *Fuel* 195:105–112
75. Larsson A (2014) Fuel conversion in a dual fluidized bed gasifier. PhD thesis, Chalmers University of Technology
76. Cooke RB, Goodson MJ, Hayhurst AN (2003) The combustion of solid wastes as studied in a fluidized bed. *Process Saf Environ Prot* 81:156–165
77. Thunman H, Lind F, Breitholtz C, Berguerand N, Seemann M (2013) Using an oxygen-carrier as bed material for combustion of biomass in a 12-MW<sub>th</sub> circulating fluidized-bed boiler. *Fuel* 113:300–309

**Open Access** This chapter is licensed under the terms of the Creative Commons Attribution 4.0 International License (<http://creativecommons.org/licenses/by/4.0/>), which permits use, sharing, adaptation, distribution and reproduction in any medium or format, as long as you give appropriate credit to the original author(s) and the source, provide a link to the Creative Commons license and indicate if changes were made.

The images or other third party material in this chapter are included in the chapter's Creative Commons license, unless indicated otherwise in a credit line to the material. If material is not included in the chapter's Creative Commons license and your intended use is not permitted by statutory regulation or exceeds the permitted use, you will need to obtain permission directly from the copyright holder.



# Chapter 2

## The Evolution of OCAC and Its Working Principles



The technical route proposed by Thunman et al. [1] to use OC to aid fluidized bed combustion is very creative, although it is likely that the OCAC technology was inspired by chemical looping combustion (CLC) technology developed at the same department of Chalmers University of Technology [2]. OCAC shares many characteristics with CLC as well as with three-way catalyst (TWC) technology in terms of adopting the oxygen-carrying material, gas–solid redox reaction, improving fuel conversion and reducing pollutants, et al. Therefore, the TWC and CLC will be briefly reviewed here to provide some preliminary knowledge before introducing working principle of OCAC.

### 2.1 Three-Way Catalyst (TWC) Technology

The OCs in OCAC technology are similar to the oxygen storage material of three-way catalysts (TWC) in gasoline engines, which was developed to simultaneously reduce CO, hydrocarbons, and NO<sub>x</sub> in a combustion situation close to the stoichiometric ratio [3]. In the TWC technology, the catalyst not only acts as an oxygen buffer to ensure the complete combustion of fuel, but it also catalyzes the NO<sub>x</sub> reduction [4, 5]. During the catalysis, the continuous fluctuation of the air–fuel ratio in the engine alternates between atmospheres of mild reduction and mild oxidation. Therefore, the catalyst can oxidize unburnt species in a reducing atmosphere with the donation of oxygen, but it absorbs oxygen back to its original state in an oxidizing atmosphere [6]. A schematic of TWC technology is shown in Fig. 2.1.

At present, almost all catalytic converters for automobiles have an integral honeycomb structure, and the catalyst support is divided into a ceramic carrier and a metal carrier. Commonly used catalysts are precious metals such as Pt, Pd, Rh, and rare-earth metals [6]. The three-way catalyst contains about 0.1–0.15% of precious metals, and some metal oxides, such as La<sub>2</sub>O<sub>3</sub>, BaO, CeO<sub>2</sub>, and Zr are used as auxiliary catalysts to improve the catalytic efficiency and catalyst lifespan. Generally, the main

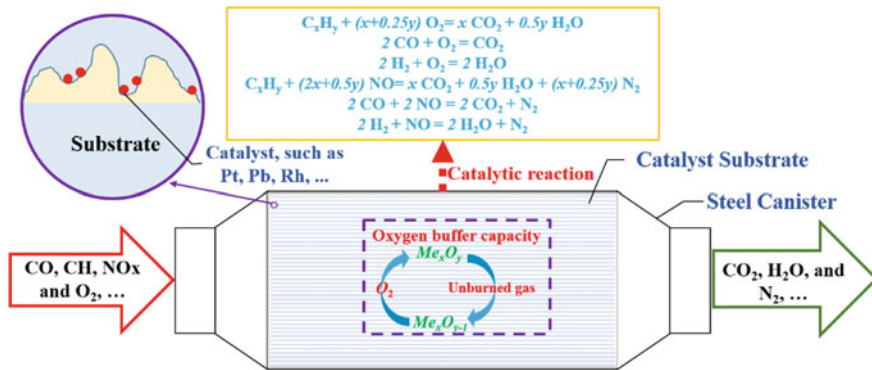


Fig. 2.1 Schematic illustration of TWC technology

factors affecting the life time and conversion efficiency performance of the catalytic converter are the working temperature of the catalytic converter and the content of Pb, P and S in the fuel [3]. Excessive Pb, P, S and other elements in the fuel may results in catalyst poisoning, because high temperature will lead to a chemical reaction between the noble metal and the support, and to sintering of the catalyst etc., which can further lower the lifetime and conversion efficiency. In order to reduce the cost of catalysts while ensuring adequate reactivity and longevity, researchers have focused on the development of catalysts by using cheaper high-performance transition metals with lowered metal loading [3].

## 2.2 Chemical Looping Combustion (CLC) Technology

The concept of CLC technology for CO<sub>2</sub> capture was realised by Ishida et al. [7] from Tokyo Institute of Technology in the middle of 1990s, but it was only when Lyngfelt and coworkers [2] developed the subject and in continuation promoted it in the form of several research projects, supported by the European Union, that it was spread internationally. Then, research activities started to develop. In the European Union projects there is a requirement to co-operate between the European countries and to involve research organizations and companies, and that was done. Much knowledge on CLC was accumulated and spread in publications among many researchers, particularly Lyngfelt et al. and Adánez et al. from Instituto de Carboquímica de Spain [8]. Subsequently, CLC technology was spread back to Asia (for instance, Laihong Shen [9] got the idea during a stay at Chalmers University) and to America.

The CLC system consists of two interconnected fluidized bed reactors (air reactor and fuel reactor) and cyclic transport of OCs between them, which can avoid direct contact between the fuel and air [2]. As shown in Fig. 2.2, the OCs are oxidized by air in the air reactor, then the oxidized OCs enter the fuel reactor and react with the fuel, finally, the reduced OCs are returned to the air reactor to complete the

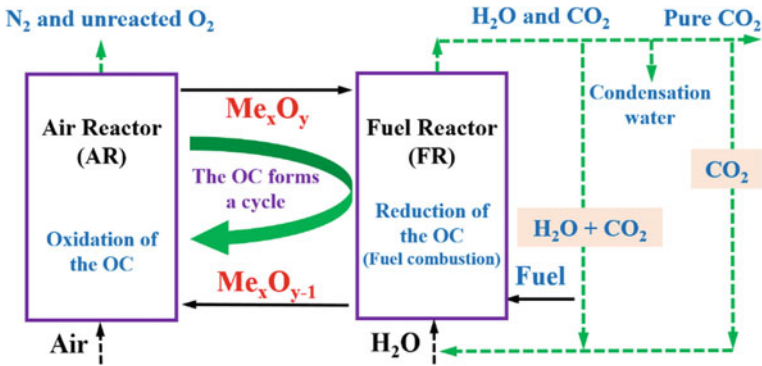


Fig. 2.2 Schematic illustration of CLC technology

cycle [8, 10]. In this system, the exhaust gas from the fuel reactor is mainly CO<sub>2</sub> and H<sub>2</sub>O. High concentration of CO<sub>2</sub> is obtained after the condensation of water vapour, which is conducive to CO<sub>2</sub> capture, storage, and utilization (CCSU). In the CLC process, a solid oxygen carrier supplies the oxygen needed for completing combustion to CO<sub>2</sub> and water, and this leads to a nitrogen-free CO<sub>2</sub> mixture. As a result, the requirement of CO<sub>2</sub> separation from flue gases, a major cost for CO<sub>2</sub> capture, is circumvented. Furthermore, since there is no N<sub>2</sub> in the fuel reactor, the formation of NO<sub>x</sub> is also reduced. Economic assessments have suggested that the CLC technology holds great promise for combustion processes with the potential for achieving efficient and low-cost CO<sub>2</sub> capture compared to other CCS processes [11].

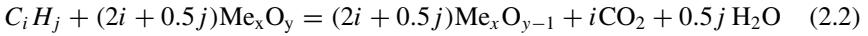
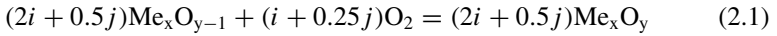
The availability of high-performing and scalable oxygen carriers has become one of the crucial concerns in scaling up and demonstrating the CLC applications. An oxygen carrier is typically formed by a reactive metal oxide and inert support, which provide, respectively, oxygen storage and mechanical strength, but also simple natural ores are used. Over the last 15 years, many research groups have been studying the formulation and preparation of active and stable oxygen carriers.

## 2.3 Basic Working Principles of OCAC

### 2.3.1 OCAC Technology Evolution

The main innovation of OCAC technology is to use oxygen carriers (OCs) as bed material instead of using inert bed material. When the OCs undergo oxidation and reduction reactions at different spots of a CFB reactor, the distribution of oxygen becomes more even, and its utilization efficiency is improved [1]. A schematic diagram is displayed in Fig. 2.3. In the CFB operation, the OCs, typically natural ores, are injected into the CFB and heated up. The lattice oxygen reacts with combustible

gaseous reactants in an oxygen-lean region, resulting in the reduction of OCs and the formation of  $\text{CO}_2$  and  $\text{H}_2\text{O}$ . Then, the reduced oxygen carriers are oxidized by oxygen from the air in oxidizing regions, resulting in fully oxidized OCs with reactive lattice oxygen. As the OCs move throughout the reactor, redox reactions take place cyclically. Ideally, the primary gas can provide enough oxygen for the OC oxidation, but not enough for fuel combustion in the dense bed. When the oxidized metal (Me) OCs (denoted as  $\text{Me}_x\text{O}_y$ ) are transported upward and downward through the entire combustor, the  $\text{Me}_x\text{O}_y$  will be reduced by combustible gases to reduced OC particles (denoted as  $\text{Me}_x\text{O}_{y-1}$ ). These small size reduced OC particles are separated from the flue gas by the cyclone separator and returned to the bottom of the dense bed. Then they are re-oxidized in the oxidizing regions of the combustor [12]. The entire process of oxidation and reduction of OCs during reaction with hydrocarbons  $\text{C}_i\text{H}_j$  can be expressed as:



The OCs are capable of taking up and donating oxygen, which can improve the uniformity of oxygen distribution and the homogeneity of the oxygen-fuel mixture in the combustion chamber. Many advantages may be achieved. Less excess air can be one of those.

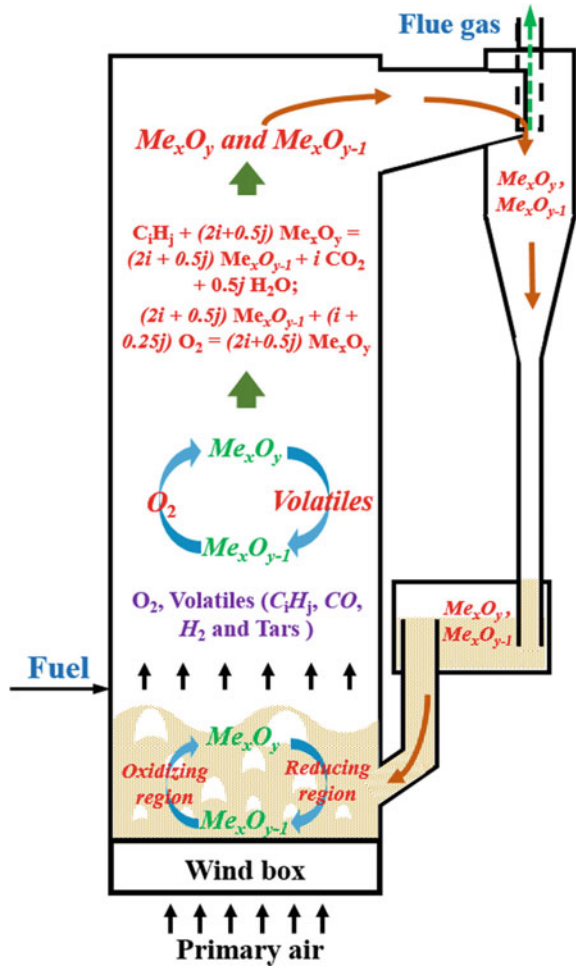
Theoretically, the role of OC is to transport oxygen from an  $\text{O}_2$ -rich region to an  $\text{O}_2$ -lean region. In the real CFB reactor operation, the dense bed presents a reducing atmosphere with local oxidizing spots. Thus, the redox reactions between  $\text{Me}_x\text{O}_y$  and combustible gases always take place in the reducing regions of the dense bed. Similarly, the volatiles can also react with OCs ( $\text{Me}_x\text{O}_y$ ) in the riser. Due to the typical arrangement of secondary air in the boiler, the oxygen in the upper part of the combustor oxidizes the OCs ( $\text{Me}_x\text{O}_{y-1}$ ).

Compared to CLC, the OCAC has a simpler process system, which only contains one FB reactor, and there is no capture of  $\text{CO}_2$ . Therefore, during the OCAC process, the role of the OCs is to donate and acquire oxygen while moving between the reducing and oxidizing regions in the same reactor. The OCAC technology shows great advantages in application potential such as (1) it can be directly adapted to the existing CFB boilers without system modification; (2) the knowledge of OC materials selection and applicability from CLC investigations [13, 14] provides valuable experience for the application of OCAC technology [12].

### 2.3.2 Suggested OCAC Principles

OCAC is a relatively new concept derived from the use of solid OCs as bed material in assisting fuel conversion. Although the fundamental study and practical application

Fig. 2.3 Schematic illustration of OCAC technology



of this technology are rapidly progressing, the principles of the OCAC process are still vague to some extent. The concept of OCAC still lacks a fixed and precise definition. OCAC is similar to the technologies of oxidation catalysis (e.g., the TWC) and CLC in some aspects, but there are also considerable differences. The differences among the three processes are mainly in the following aspects: the reaction time interval, the spatial characteristics, and the reaction temperatures in oxidation and reduction, as well as in the way of generating the desired products (see Table 2.1).

It has been accepted that the reactions involved in the oxidation catalysis either follow the Mars-Van Krevelen (MvK) or Langmuir-Hinshelwood (LH) mechanisms, in which the former is more widely accepted [15]. When it follows the MvK mechanism, the catalyst is oxidized and reduced promptly and almost simultaneously with the progress of the reaction. At this stage, the catalyst behaves as an oxygen vector

**Table 2.1** Comparisons between various aspects of TWC, CLC and OCAC technologies

Technologies	The turnover time between redox reactions	Spatial characteristics of redox reactions	Reaction temperature	Product generation (excluding heat)	The functions of OCs/catalysts towards oxygen	OCs/catalysts arrangement	OCs/catalysts requirements
TWC	Transient turnover time; reduction and oxidation are hardly differentiated by time	Reduction and oxidation both occur in localized microscale active sites of a catalyst within a single reactor	Reduction and oxidation take place isothermally and almost simultaneously	Desired products are generated due to the synergy between reduction and oxidation	Oxygen buffering and catalytic reduction of NO <sub>x</sub>	Catalysts are stationary and fixed at a given location within the reactor	Can be cheap or expensive, containing a minimized amount of noble metals, moderate mechanical strength, responding timely and sensitively to P <sub>O2</sub> change, long lifetime
CLC	Turnover time spans from seconds to even hours depending on the residence time of OCs in air and fuel reactor	Reduction and oxidation reactions take place in two or more different reactors	Temperatures for reduction and oxidation can be the same or different depending on the reactor and process design	Desired products are produced from either oxidation or reduction reactions or both	Oxygen transfer between reactors	OCs are circulated vigorously among different reactors via a designed path	Low-cost without using any noble metals, strong mechanical strength, an appropriate response to P <sub>O2</sub> change, which can be less sensitive than TWC and OCAC, long lifetime

(continued)

Table 2.1 (continued)

Technologies	The turnover time between redox reactions	Spatial characteristics of redox reactions	Reaction temperature	Product generation (excluding heat)	The functions of OCs/catalysts towards oxygen	OCs/catalysts arrangement	OCs/catalysts requirements
OCAC	Turnover time falls in between the ones of TWC and CLC	Reduction and oxidation reactions occur in reducing and oxidizing regions of a single reactor	Redox reactions take place within an isothermal reactor, while the temperature of reduction and oxidation can be slightly different	Desired products are generated mostly from the OC reduction	Oxygen transfer from oxidizing to reducing regions within a single reactor, oxygen storage and buffering	OCs moves randomly inside a single reactor	Low-cost with no tolerance to using noble metals, high mechanical strength, prompt and sensitive response to $P_{O_2}$ change, expected to have strong recyclability, long lifetime



transferring oxygen radicals, atoms, ions or molecules among different reactants. However, the time intervals between oxidation and reduction reactions are too short to be separated in terms of time during observations. From the functional point of view, oxidation catalysis requires the synergy between the oxidation and reduction reactions to obtain the desired products. As a result, the redox reactions, i.e., the oxidation and reduction reactions, cannot be spatially segregated during the oxidation catalysis. On the contrary, the oxidation and reduction reactions are always segregated spatially during the CLC process. They take place either simultaneously or in sequence depending on the reactor and process design of the CLC processes. Unlike oxidation catalysis, the desired products of the CLC process can be generated from either oxidative or reductive reaction or even both [8]. Nevertheless, the OC involved in the CLC process functions similarly to the catalyst for oxidation catalysis, but transports oxygen among different physicochemical environments in terms of multiple reactors. The reaction temperature is another obvious difference between oxidation catalysis and CLC. The redox reactions always take place isothermally in oxidation catalysis, while the reaction temperatures for the oxidation and reduction reactions can be varied in the CLC processes.

Despite its own characteristics, the OCAC shares several similarities with the oxidation catalysis and the CLC technologies. The redox reactions of oxidation and reduction for the OCAC process always take place isothermally within the same reactor but can be distinguished both timely and spatially, which is significantly different from the oxidation catalysis and CLC technologies [1]. In general, the OCAC technology can be deemed a versatile process, in which OC materials are employed in delivering the oxygen species from one physicochemical environment to another. Besides, such oxygen transportation is accomplished via space and time-resolved redox reactions in terms of reductive and oxidative reactions within a single isothermal reactor. Benefiting from the ability of the OCAC technology in transporting the oxygen species from oxygen-enriched regions to the oxygen-deficient areas, the reactants, which are usually solid and gaseous fuels, can be oxidized more evenly and efficiently within the reactor. Although the current oxygen transferring materials used in OCAC technology are mostly derived from the CLC processes, it raises higher requirements for OCs in response to the subtle environment change. In the CLC system, the oxygen partial pressure ( $P_{O_2}$ ) and temperature can be significantly different among the different reactors. Hence, the reductive and oxidative reactions which take place on the OCs in the CLC process can be altered easily due to the wide changes of  $P_{O_2}$  and temperature. However, the  $P_{O_2}$  and temperature vary only slightly in different regions inside the OCAC reactor since only a single isothermal reactor is concerned. Therefore, the OCs designed for OCAC should respond to a change of  $P_{O_2}$  and temperature much more sensitively in order to alter the reactions promptly between oxidation and reduction. Moreover, the time in which the OC materials are retained at different physicochemical environments within the OCAC reactor is much shorter than the residence time of OCs in CLC reactors. Therefore, the reaction rate of OCs during either reduction or oxidation reaction should be much faster in OCAC than that in a CLC system. The major differences between the TWC, CLC, and OCAC technologies are summarized in Table 2.1.

## References

1. Thunman H, Lind F, Breitholtz C, Berguerand N, Seemann M (2013) Using an oxygen-carrier as bed material for combustion of biomass in a 12-MW<sub>th</sub> circulating fluidized-bed boiler. *Fuel* 113:300–309
2. Lyngfelt A, Leckner B, Mattisson T (2001) A fluidized-bed combustion process with inherent CO<sub>2</sub> separation; application of chemical-looping combustion. *Chem Eng Sci* 56:3101–3113
3. Rood S, Eslava S, Manigrasso A, Bannister C (2020) Recent advances in gasoline three-way catalyst formulation: a review. *Proceedings of the Institution of Mechanical Engineers, Part D: Journal of Automobile Engineering* 234:936–949
4. Heck RM, Farrauto RJ (2003) Gulati ST (2009) *Catalytic air pollution control: commercial technology*. Wiley 9:N28
5. Singh MP (2016) A review on catalytic converter for automotive exhaust emission. *Int J Sci Eng Res* 7(2):927–932
6. Twigg MV (2007) Progress and future challenges in controlling automotive exhaust gas emissions. *Appl Catal B* 70:2–15
7. Ishida M, Jin H (1994) A new advanced power-generation system using chemical-looping combustion. *Energy* 19:415–422
8. Adanez J, Abad A, Garcia-Labiano F, Gayan P, de Diego LF (2012) Progress in chemical-looping combustion and reforming technologies. *Prog Energy Combust Sci* 38:215–282
9. Shen L, Zheng M, Xiao J, Xiao R (2008) A mechanistic investigation of a calcium-based oxygen carrier for chemical looping combustion. *Combust Flame* 154(3):489–506
10. Song T, Shen L (2018) Review of reactor for chemical looping combustion of solid fuels. *Int J Greenhouse Gas Control* 76:92–110
11. Hossain MM, de Lasa HI (2008) Chemical-looping combustion (CLC) for inherent CO<sub>2</sub> separations—a review. *Chem Eng Sci* 63:4433–4451
12. Gyllén A (2019) Oxygen carrier aided combustion: implementation of oxygen carriers to existing industrial settings. Doctoral dissertation, Chalmers University of Technology
13. Lyngfelt A (2014) Chemical-looping combustion of solid fuels—status of development. *Appl Energy* 113:1869–1873
14. Adánez J, de Diego LF, García-Labiano F, Gayán P, Abad A, Palacios JM (2004) Selection of oxygen carriers for chemical-looping combustion. *Energy Fuels* 18:371–377
15. Demoulin O, Navez M, Gaigneaux EM, Ruiz P, Mamede A-S, Granger P et al (2003) Operando resonance Raman spectroscopic characterisation of the oxidation state of palladium in Pd/ $\gamma$ -Al<sub>2</sub>O<sub>3</sub> catalysts during the combustion of methane. *Phys Chem Chem Phys* 5:4394–4401

**Open Access** This chapter is licensed under the terms of the Creative Commons Attribution 4.0 International License (<http://creativecommons.org/licenses/by/4.0/>), which permits use, sharing, adaptation, distribution and reproduction in any medium or format, as long as you give appropriate credit to the original author(s) and the source, provide a link to the Creative Commons license and indicate if changes were made.

The images or other third party material in this chapter are included in the chapter's Creative Commons license, unless indicated otherwise in a credit line to the material. If material is not included in the chapter's Creative Commons license and your intended use is not permitted by statutory regulation or exceeds the permitted use, you will need to obtain permission directly from the copyright holder.



# Chapter 3

## OCAC for Fuel Conversion Without CO<sub>2</sub> Capture



Since 2013, various research institutions, including Chalmers University of Technology, University of Cambridge, Tsinghua University, Friedrich-Alexander-University and University of Nottingham, have conducted a series of studies on OCAC technology. It is worth mentioning that Chalmers University of Technology has complied with most of these studies from laboratory to industry scales. In particular, they carried out a series of semi-industrial scale experiments in the 12 MW<sub>th</sub> CFB boiler (as shown in Fig. 3.1), which is well-known research boiler. In this section, all summarized studies were performed under traditional air-combustion conditions without much consideration of CO<sub>2</sub> capture. The relevant experimental studies with detailed information are summarized in Table 3.1.

### 3.1 Operation Experience

#### 3.1.1 Combustion Performance

In 2014, Chadeesingh and Hayhurst [2] investigated the methane combustion in a bubbling fluidized bed with three kinds of bed material: silica sand (1.9 kg), silica sand (1.9 kg) + Fe<sub>2</sub>O<sub>3</sub> (2.5 g) and silica sand (1.9 kg) + Fe<sub>2</sub>O<sub>3</sub> (25 g). Although the term of OCAC has not been used in this work, it was actually an early trial of using OCs as bed material to facilitate fuel conversion. When there was only silica sand in the bed, sharp and loud “popping” noises were clearly heard, which seemed to be caused by the deflagration of hot CH<sub>4</sub> bubbles above the bed [19, 20]. The sound was still present when 2.5 g Fe<sub>2</sub>O<sub>3</sub> was added to the bed material, while it disappeared when the share of Fe<sub>2</sub>O<sub>3</sub> increased to 25.0 g. When only silica sand was used as the bed material, the combustion of hydrocarbon gases (such as CH<sub>4</sub> and C<sub>3</sub>H<sub>8</sub>) is inhibited. This is because silica sand provides a large surface area, on which free radicals readily recombine [21, 22]. As a result, the methane hardly burned in the dense bed. Instead, it burned in the splash zone. This assumption can be proven by the

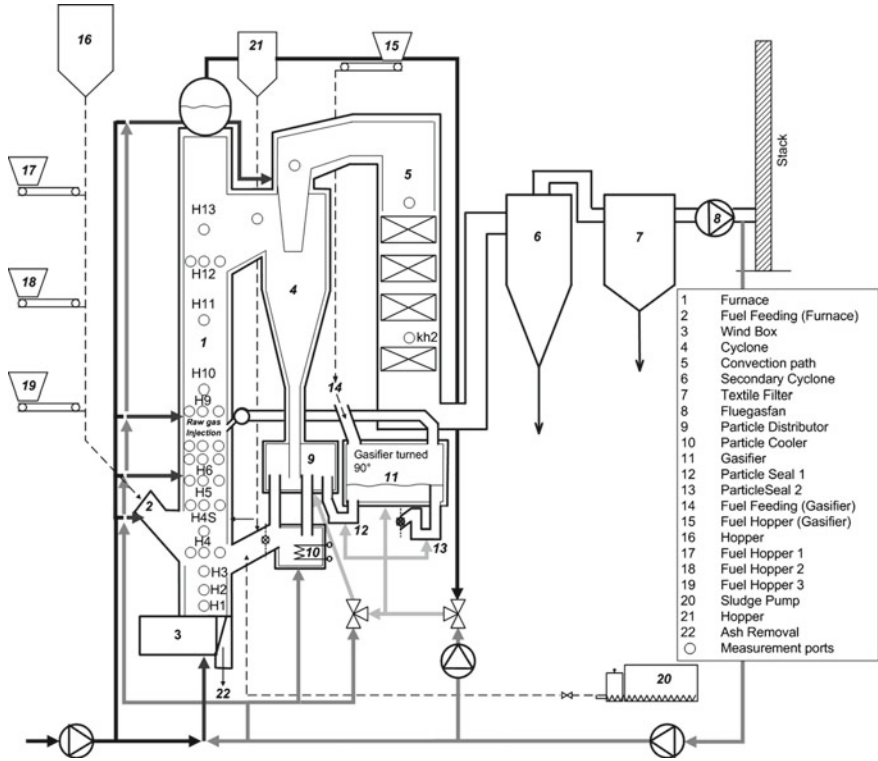


Fig. 3.1 Chalmers boiler/gasifier reactor system (reprinted from [1] with permission of Elsevier)

temperature distribution in the reactor (as shown in Fig. 3.2a). When Fe<sub>2</sub>O<sub>3</sub> particles were present in the dense bed, a portion of CH<sub>4</sub> can be oxidized on the surface of the Fe<sub>2</sub>O<sub>3</sub> particles, resulting in gaseous products of CO, CO<sub>2</sub> and trace C<sub>2</sub>H<sub>4</sub> detected in the bed, as shown in Fig. 3.2c–e. Therefore, the oxidation of methane is promoted when Fe<sub>2</sub>O<sub>3</sub> is added to the bed, even if the Fe<sub>2</sub>O<sub>3</sub>/silica sand ratio was small (<0.1 wt%). This important study demonstrated that the chemical-looping combustion of CH<sub>4</sub> can be achieved with either Fe<sub>2</sub>O<sub>3</sub> or metallic Fe even in a single fluidized-bed reactor.

Schneider et al. [6] investigated the combustion of methane in a bubbling fluidized bed (the schematic illustration is shown in Fig. 3.3) with silica sand and ilmenite as bed materials. As shown in Fig. 3.4, the in-bed CO<sub>2</sub> yield can be significantly increased by replacing the sand with ilmenite at different excess-air ratios. With silica sand as a bed material, the combustion of fuel in the bed was very weak, and occurred mostly above the bed surface. When the silica sand was replaced with ilmenite, the proportion of fuel conversion in the bed increased, and the combustion proportion above the surface of the bed decreased correspondingly, and the deflagration disappeared. With OC as a bed material, the proportion of fuel conversion in dense zone increased with

**Table 3.1** Summary of relevant experimental studies on the use of OC

Scale	Centre and Location	Reactor	Fuel	Bed material	Operating conditions	References
Lab-scale	University of Cambridge, UK (2014)	Bubbling bed (I.D. 121 mm)	Methane (continuous feeding)	Silica sand + Fe <sub>2</sub> O <sub>3</sub> powder (0, 2.5 g and 25 g); Totally: 1.7 kg	700 °C, $u/u_{mf} = 2.5$ air-to-fuel ratio was 6.0	Chadeesingh and Hayhurst [2]
	CUT <sup>a</sup> , Sweden (2015)	Circulating fluidized bed, 300 W	Methane (continuous feeding)	Silica sand + Manganese ores (0 and 50%; UMK and SIB); $d_p$ : 90 - 212 $\mu$ m	800 °C, 850 °C, $u/u_{mf} = N/A$ , air-to-fuel ratio was 0.99 - 1.13	Källén et al. [3]
	CUT, Sweden (2015)	Bubbling bed (I.D. 22 mm)	Wood char (batch feeding)	60% Sand + 40% ilmenite ore (CI, NI and SI) <sup>b</sup> , $d_p$ : 125–180 $\mu$ m); Totally: 15 g	850 °C, $u/u_{mf} = N/A$ , air-to-fuel ratio was 0.6 - 1.3	Pour et al. [4]
	Tsinghua University, China & CUT, Sweden (2017)	Bubbling bed (I.D. 22 mm)	Wood char (batch feeding)	Silica sand, ilmenite ore, AQS <sup>c</sup> , LDs <sup>d</sup> , manganese ore; Totally: 15 g	850 °C, $u/u_{mf} = 5-12$ , air-to-fuel ratio was 0.6 - 1.5	Wang et al. [5]
	FAUEN <sup>e</sup> , Germany (2021)	Bubbling bed (I.D. 100 mm)	Methane (continuous feeding)	Silica sand, ilmenite ore; static bed height: 200 mm and 300 mm	800 °C, $u/u_{mf} = 2.5-7.5$ , air-to-fuel ratio was 0.75 - 2	Schneider et al. [6]

(continued)



Table 3.1 (continued)

Scale	Centre and Location		Reactor	Fuel	Bed material	Operating conditions	References
	Centre	Location					
	CUT, Sweden (2018)		12 MW <sub>th</sub> CFB boiler	Wood - chips	Sand ilmenite ore and rock ilmenite ore	850 °C, the bed samples were taken every day, the test period was 15 days	Corcoran et al. [12]
	CUT, Sweden (2018)		12 MW <sub>th</sub> CFB boiler	Wood chips	Ilmenite ore	850 °C, the bed samples were collected from 5 up to 364 h after start-up	Corcoran et al. [13]
	CUT, Sweden (2018)		12 MW <sub>th</sub> CFB boiler	Wood chips and wood pellets	Manganese ore ( $d_p$ : 100–400 $\mu\text{m}$ )	850–870 °C, air-to-fuel ratio was 1.07 -1.17, the bed samples (from three points) and fly ash samples (from two points) were taken every day	Hanning et al. [14]
	CUT, Sweden (2019)		12 MW <sub>th</sub> CFB boiler	Wood chips	LD-slag ( $d_p$ : 150–400 $\mu\text{m}$ )	850–860 °C, the bed samples were taken at least two times a day, elementary sulfur had been added to the furnace from the fourth day	Hildor et al. [15]

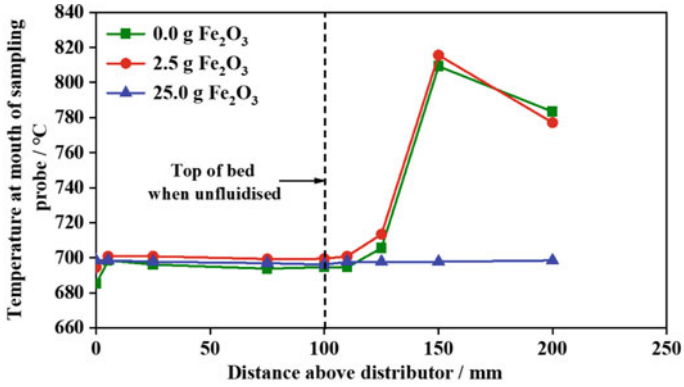
(continued)

Table 3.1 (continued)

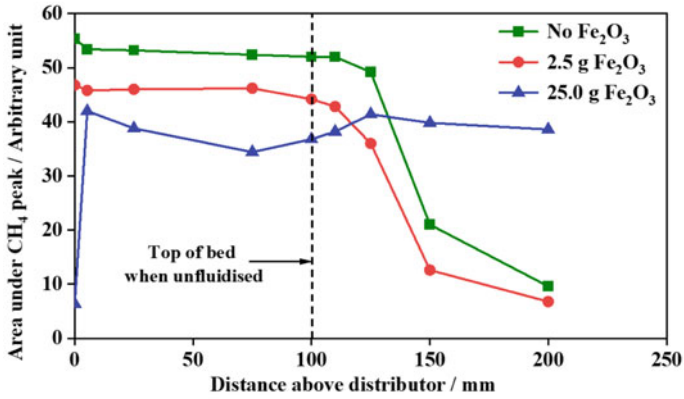
Scale	Centre and Location	Reactor	Fuel	Bed material	Operating conditions	References
Industrial-scale	CUT, Sweden (2020)	12 MW <sub>th</sub> CFB boiler	Wood chips	Rock ilmenite ore (100–300 µm)	860–880 °C, the test was carried out for 2 weeks, S in the form of granules was added into boiler (1.5 kg/h)	Vigoureux et al. [16]
		75 MW <sub>th</sub> CFB boiler	MSW <sup>§</sup>	Silica sand, ilmenite ore	The test period was 12,000 h, the net boiler load was 75–80 MW <sub>th</sub> , the O <sub>2</sub> concentration in flue gas was 5.0–8.0%	Lind et al. [17]
	CUT, Sweden (2018)	115 MW <sub>th</sub> CFB boiler	Waste wood	Silica sand + ilmenite ore (from 0 to more than 90%)	The test period was 3 weeks, the net boiler load was 115–123 MW <sub>th</sub> , the O <sub>2</sub> concentration in flue gas was 1.8–3.0%, bed samples were collected about three times per day, a roll belt magnetic separator was used to separate the magnetic fraction	Moldenhauer et al. [18]

<sup>a</sup>Chalmers University of Technology; <sup>b</sup>CI represents Canadian Ilmenite, NI represents Norwegian Ilmenite and SI represents Ilmenite from South Africa, respectively; <sup>c</sup>the tailings from separation of iron steel slag; <sup>d</sup>LD stone, a waste product from steelmaking; <sup>e</sup>Friedrich-Alexander-University Erlangen-Nuremberg; <sup>f</sup>the 12MW<sub>th</sub> research CFB boiler at CUT; <sup>§</sup>Municipal solid waste

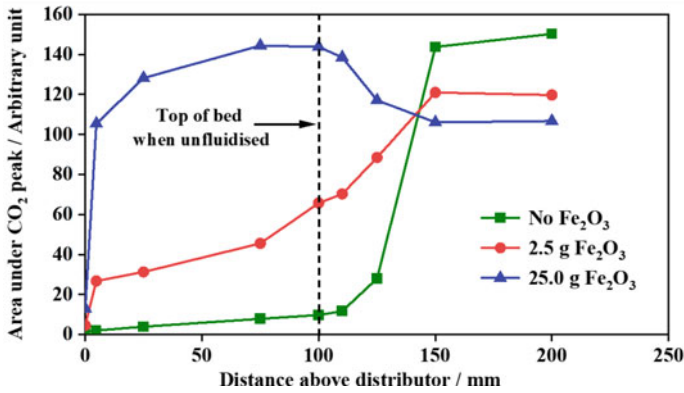




(a) Temperature



(b) CH<sub>4</sub> concentration



(c) CO<sub>2</sub> concentration

Fig. 3.2 Plots of relevant parameter against height above the distributor (adapted from [2])

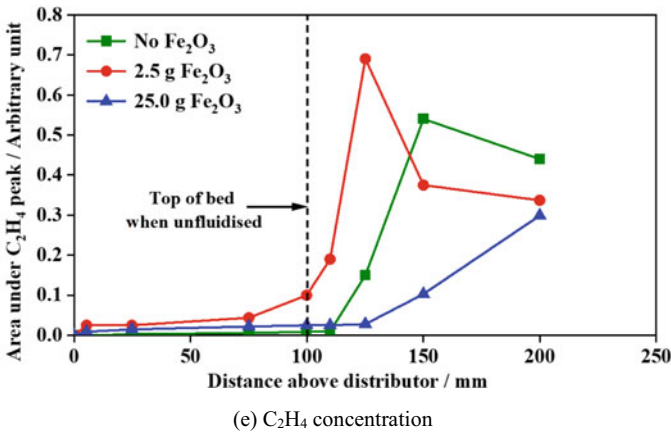
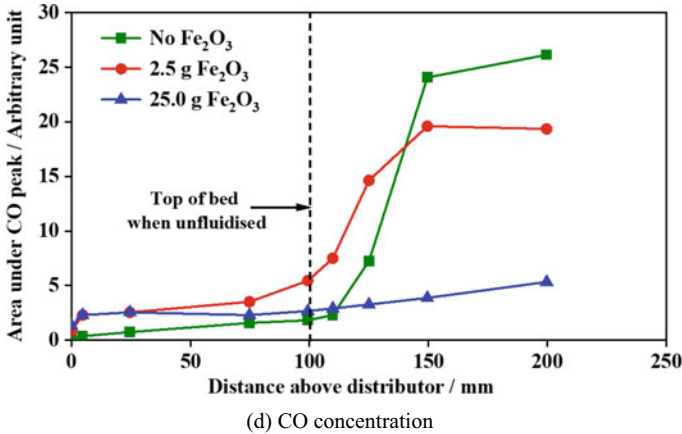
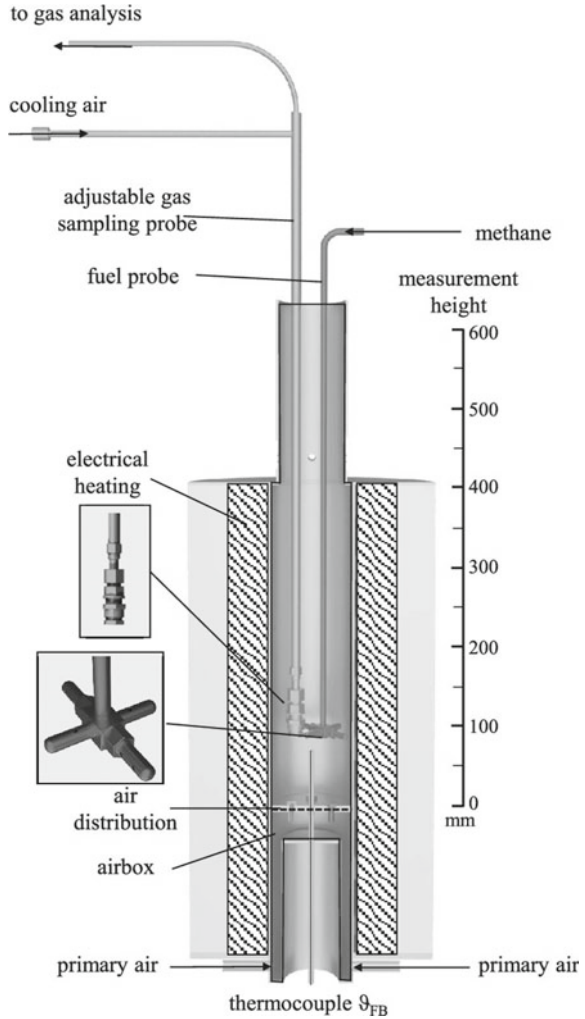


Fig. 3.2 (continued)

the increase of bed height. In addition, the results also indicate that OCAC has more advantages in the application at low excess-air ratio.

In 2014, Källén et al. [3] used two kinds of manganese ore as bed material to investigate the performance of OCAC in a 300 W CFB combustor. The measured concentrations of CO and O<sub>2</sub> in the gas exhaust are shown in Fig. 3.5. When the bed material was solely silica sand, the CO concentration remained at a few hundred ppm until the air-to-fuel ratio decreased below 1.05. As the air-to-fuel ratio approached 1, the concentration of CO reached several thousand ppm at the two investigated temperatures. The same tests were repeated while shifting the bed material to a mixture of manganese ore and silica sand at 50/50 mass ratio. The CO concentration was significantly reduced in both cases when these two manganese ores were used as bed materials, especially at the lower air-to-fuel ratios. The study found that both manganese ores can release gaseous oxygen in the inert atmosphere, because the oxygen concentration of the exhaust gas in the cases of Mn ore were higher than that

**Fig. 3.3** The schematic illustration of the bubbling fluidized bed reactor (reprinted from [6] with permission of American Chemical Society)



in sand case. This study demonstrated the great advantages of OCAC, yielding higher fuel conversion at low air-to-fuel ratios, resulting in higher combustion efficiency and lower energy consumption due to lower air supply.

The improved combustion performance of the OCAC process was also validated in a small bubbling fluidized bed with batch feeding of biomass char. Pour et al. [4] employed three kinds of ilmenite ore as bed material for the tests. Compared with the case of 100% sand as bed material, less oxygen was found in the outlet of the reactor for all ilmenite ore cases, and the fuel conversion increased, which means that the oxygen supply was used more efficiently. The OCAC processes using ilmenite ores as OCs displayed enhanced combustion characteristics regardless of the ore type. Wang et al. [5] investigated the effects of diverse OCs, including ilmenite, manganese ore

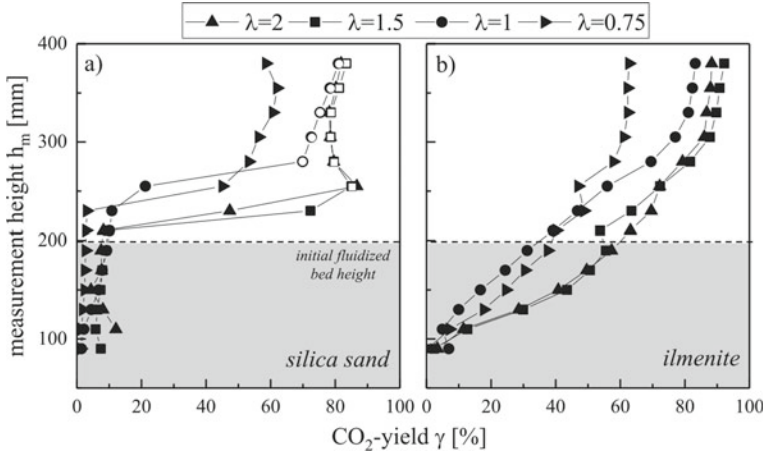


**Fig. 3.4** CO<sub>2</sub> yield depending on excess-air ratio and height for silica sand and ilmenite.  $u/u_{mf} = 2.5$ , and bed temperature = 800 °C, the CO<sub>2</sub> in the bed is oxidized by CO (reprinted from [6] with permission of American Chemical Society)

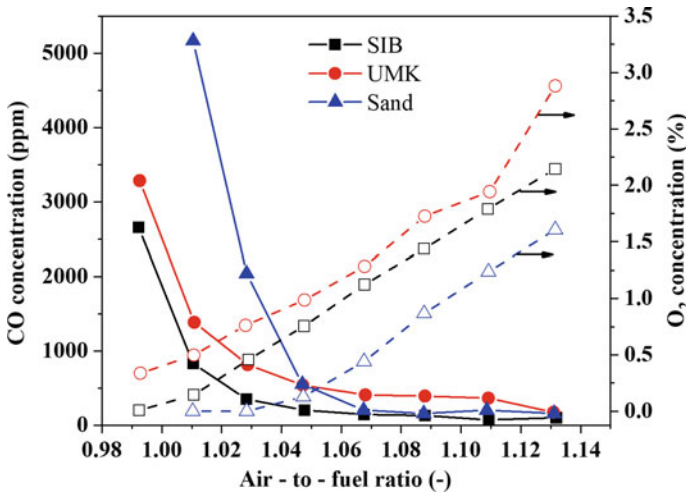
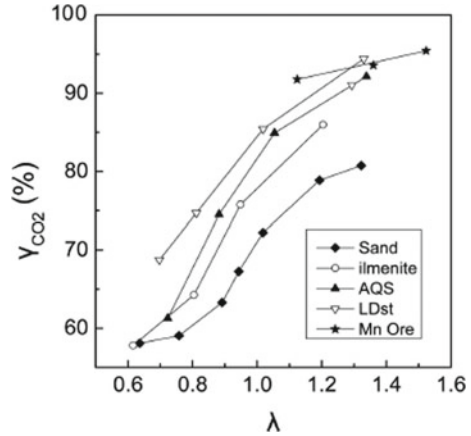


**Fig. 3.5** Measured outlet concentrations of CO and O<sub>2</sub> as a function of air-to-fuel ratio during operation with 100 wt% sand, 50 wt% Mn ore in the sand, SIB and UMK are two kinds of Mn ores from Sibelco and UMK companies (Adapted from [3])

and two industrial iron oxide scales (AQS and LDst), during the OCAC of biomass char at different air-to-fuel ratios. The combustion evidenced by the CO<sub>2</sub> yield (as shown in Fig. 3.6) and unburned volatiles showed that the various OCs perform differently. The promotion effect of OCs follows the order: Mn ore > LDst > AQS > ilmenite > sand.

**Fig. 3.6** Average  $\text{CO}_2$  yields of solid fuel combustion at different  $\lambda$  values (reprinted from [5] with permission of American Chemical Society)



Garcia et al. [7] used silica sand and ilmenite as bed material and a mixture of bituminous coal and wheat straw as fuel to investigate the combustion of OCAC in a 30 kW<sub>th</sub> BFB combustor (the schematic diagram and photo of the pilot-scale BFB combustion system are shown in Fig. 3.7). The results verified that OCAC technology leads to lower CO emissions and smaller efficiency loss. Compared with 100% quartz sand, the combustion loss in 100% ilmenite case caused by CO emission and unburned carbon decreased from 0.2% and 2.59% to 0.17% and 1.76%, respectively. In addition, the results showed that the OCAC operation could slow down bed agglomeration. Compared with the operation of silica sand as a bed material, much less and smaller agglomerates were found in the case of ilmenite, and the agglomerates formed in the OCAC operation appeared to be weak and easily broken.

In 2013, Thunman et al. [1] carried out an OCAC combustion test by using ilmenite ore as OC, which was the first attempt at a semi-industrial scale CFB boiler (12 MW<sub>th</sub>). The gas composition was measured at different heights of the furnace as well as at different intervals along the convection path. The results verified the expectation that CO can be reduced if the inert bed material is replaced by ilmenite ore. Figure 3.8 shows the change of CO concentration in the convection path after OCs were used to replace different proportions of quartz sand in the bed. The CO concentration in the exhaust gas was lower when more silica-sand was replaced by OCs. Compared to the 100% silica-sand case, the CO concentration in the exhaust gas was reduced by 80% when the OC content in the bed material was 40 wt%. By measuring CO and hydrocarbons at different positions of the boiler, it was found that the addition of OC can not only promote the oxidation of fuel, but it also improves the mixing of fuel and oxygen in a cross-section of the furnace. In addition, more fuel was oxidized within the furnace and less combustible gas was released to the cyclone, which is another benefit of OCAC: it avoids serious post-combustion.

Rydén et al. [9, 11] and Hildor et al. [15] did similar experimental studies on the same CFB boiler, while calcined manganese ore and steel slag were used as OCs instead of ilmenite ore. However, the conclusions of the investigators seem

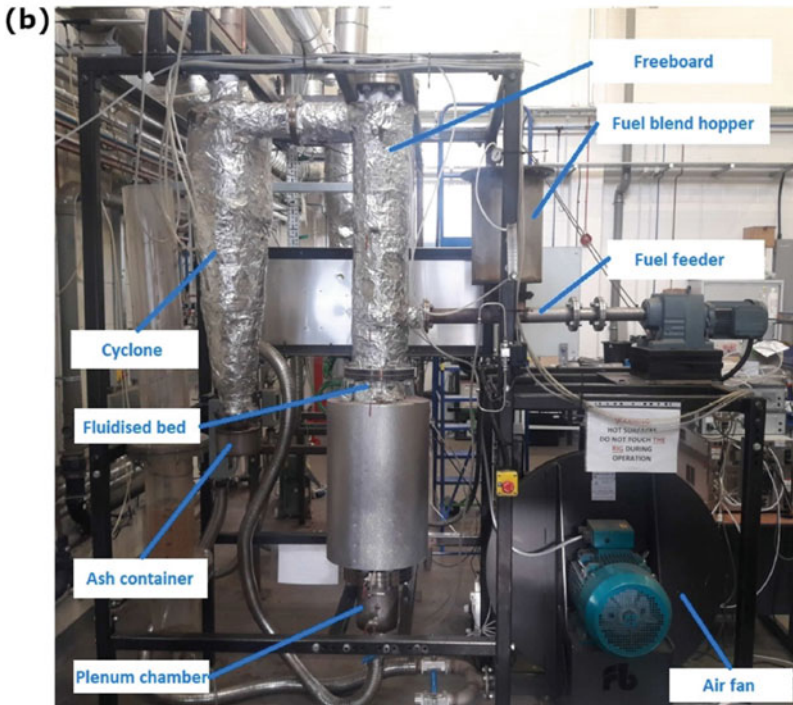
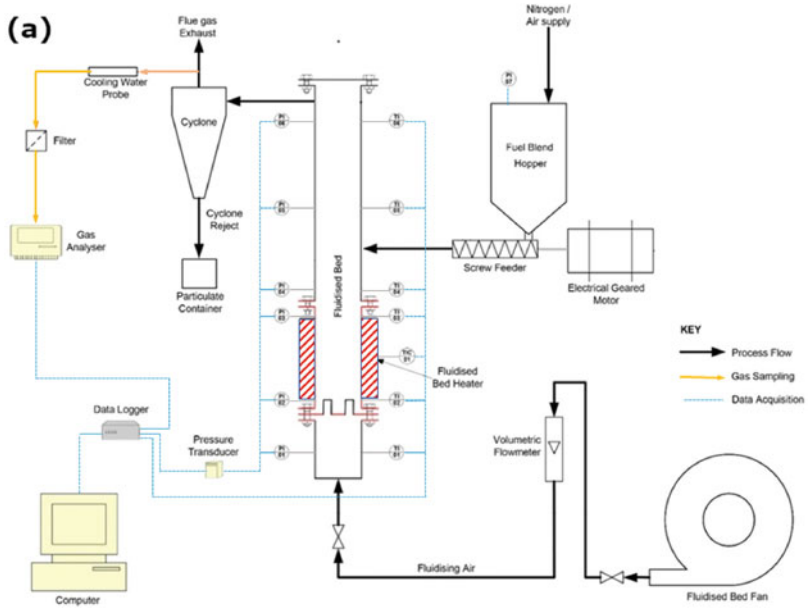
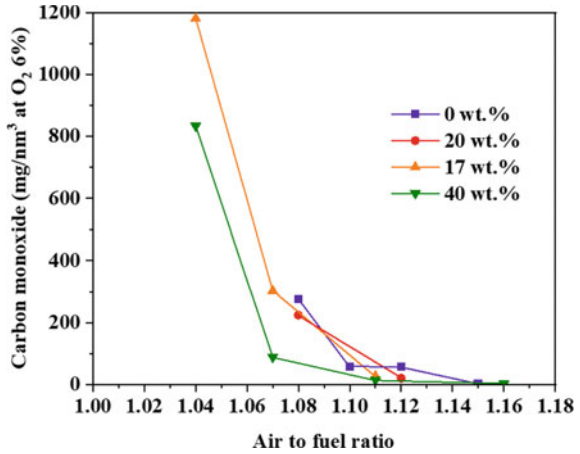


Fig. 3.7 a Schematic diagram and b photo of the pilot-scale BFB combustion system (reprinted from [7] with permission of Elsevier)

**Fig. 3.8** The CO concentration in the convection path ( $\text{mg}/\text{nm}^3$ , at 6%  $\text{O}_2$ ) versus air-to-fuel ratio, the curves show different fractions of OC (adapted from [1])

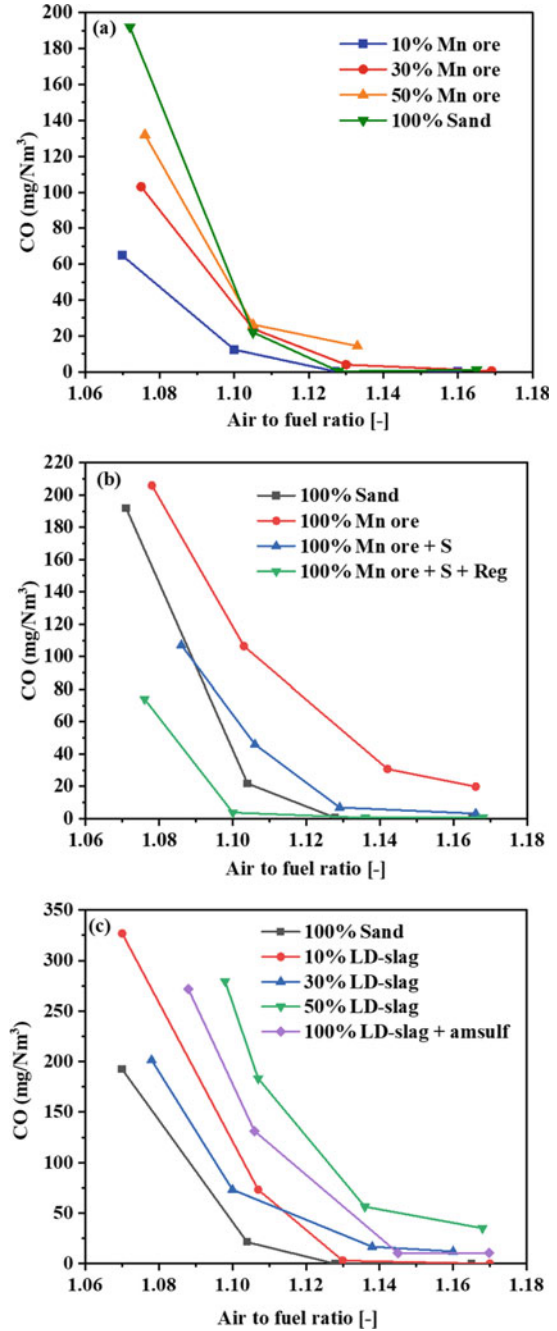


different. Figure 3.9 shows the CO emission when different OC ratios were added to the bed material. The results indicate that the manganese ore and steel slag show excellent performance when used as OC, which facilitated the fuel conversion inside the boiler. On the other hand, the CO emission did not decrease monotonously with the increase of the OC content in the bed material. This is because both OCs have a poor ability to absorb alkali metals, and there is a high concentration of alkali metals (such as K) entering the gas phase, which according to the authors might inhibit the oxidation of CO [23–25]. To confirm this hypothesis, the authors measured the change of CO emission by adding sulfate to the furnace to reduce the alkali metals. When all bed materials were replaced by OCs, the addition of sulfate or ammonium sulfate reduced the CO emission. At the same time, the concentrations of K and S in the fly ash increased significantly. This indicates that the post-added sulfate reacts with the K salts to form a stable solid  $\text{K}_2\text{SO}_4$  [23], which may reduce the inhibition of CO oxidation by alkali compounds in the flue gas [16]. In fact, sulfate fed to biomass boilers is occasionally applied to reduce CO emission [24, 25], but the authors pointed out that this explanation was not proven yet.

Lind et al. [17] conducted an OCAC test in a 75  $\text{MW}_{\text{th}}$  CFB boiler for burning municipal solid waste (MSW) using ilmenite ore as OCs, the study showed that the CFB boiler could be operated well, and the logistics were manageable. With over 12,000 h of operation, it has been demonstrated that the OCAC technology not only drastically reduced the CO concentration in the flue gas, but it can also improve the combustion of volatiles at the top of the combustion chamber. Particularly, compared with the 100% sand case, the average CO concentration was reduced by more than 45% (Fig. 3.10).

Moldenhauer et al. [18] reported an OCAC operation in a commercial CFB boiler using rock ilmenite OC as bed material. CFB-boiler is located in the south of Sweden and consists of a biomass fired CHP cycle (112 bar, 540 °C) with a nominal thermal capacity of 115  $\text{MW}_{\text{th}}$ . The amount of bed material in the system is about 60 tons under normal operation. The cross-section of the furnace is 2.2 m × 8.8 m at the

**Fig. 3.9** CO Concentrations in the convection path (mg/nm<sup>3</sup>, at 6% O<sub>2</sub>) as a function of air-to-fuel ratio (adapted from [9, 11])





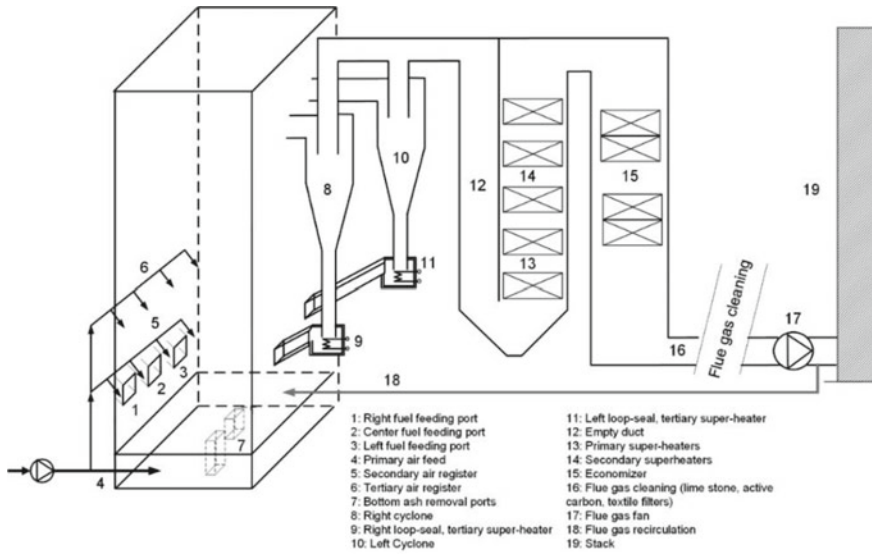


**Fig. 3.10** Schematic representation of the 75 MW<sub>th</sub> CFB-boiler [17]

height of the fluidization nozzles and expands to 5.5 m × 8.8 mm in the upper part of the furnace. The height from of the furnace is 28.4 m. Furnace and separators are equipped with ammonia injection (SNCR) systems to reduce the emissions of NO<sub>x</sub>. A schematic of the system is illustrated in Fig. 3.11.

As shown in Figs. 3.12 and 3.13, compared to the conventional operation with silica sand, the OCAC process made it possible to reduce the excess air by up to 30%, evidenced by the decrease of O<sub>2</sub> concentration at the outlet from 2.5 to 1.8%, while the boiler load increased from 115 to 123 MW<sub>th</sub>. The total airflow in the OCAC operation at 123 MW<sub>th</sub> was approximately the same as that in the conventional operation at 113 MW<sub>th</sub> by silica sand. Consequently, the boiler can be operated in overload mode without increasing the gas velocity in the boiler and convection path. At the same load, OCAC operation significantly reduced the airflow volume, which improves the economics of operation. Keeping the proper gas velocity was also beneficial for the anti-erosion of the heat-transfer surfaces in the furnace.

Combined with the studies of the OCAC technology from lab-scale, semi-industrial, and industrial scale, it is found that the employment of OCs as bed material significantly promotes the combustion and reduces the CO emission compared to traditional FBC technology, especially at low air-to-fuel ratios. This provides the possibility to operate the boiler with low excess air, reducing the energy consumption. However, it should be pointed out that the type of OC, the mass fraction of OC in the bed material, the absorption properties of OC over alkali, and the fuel characteristics need to be comprehensively considered, since they can affect the CO emission.

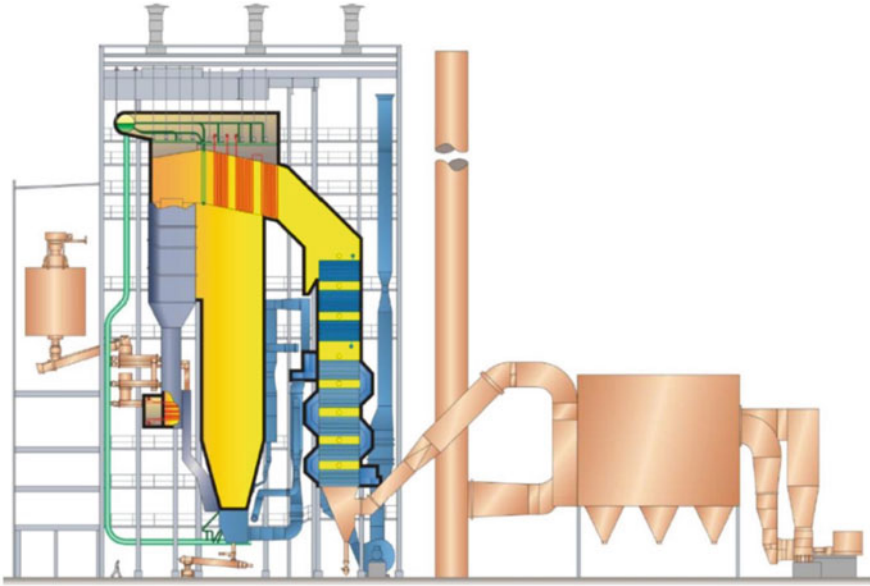


**Fig. 3.11** Schematic representation of the 115 MW<sub>th</sub> CFB-boiler [18]

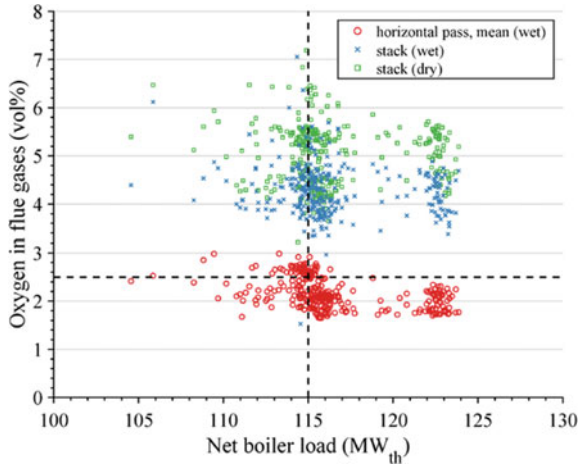
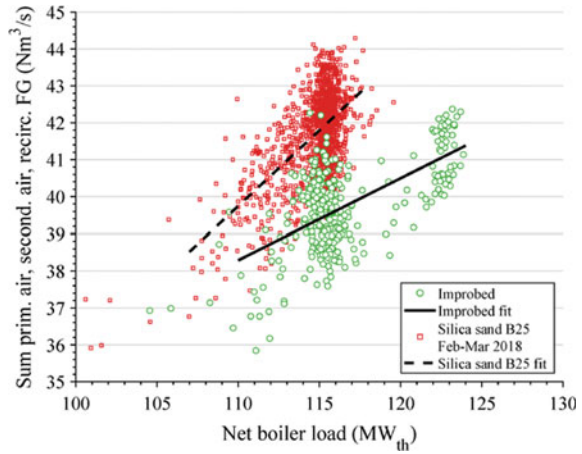


**Fig. 3.12** O<sub>2</sub> concentration during ilmenite operation in the horizontal pass for moist gas and O<sub>2</sub> fractions in the stack for dry and wet gas as a function of the net boiler load (dashed lines symbolizes set points for normal silica-sand operation, i.e. average O<sub>2</sub> and average net boiler load) [18]

**Fig. 3.13** Total gas flow as primary air, secondary air, and recirculated flue gas as a function of the net boiler load during operation with ilmenite and silica-sand [18]



### 3.1.2 Oxygen Buffering Ability

In OCAC technology, the OCs transfer oxygen from oxidizing to reducing regions, thereby improving the uniformity of the oxygen distribution inside the boiler. It acquires oxygen in the oxidizing regions, while donating its stored oxygen in the reducing regions. Therefore, the oxygen buffering ability of OC is an important index for evaluating the OC performance in OCAC technology. An OC with desired oxygen buffering ability not only can improve the combustion efficiency of the boiler but also the stability and safety of boiler operation. For example, during the operation of a commercial CFB boiler, fluctuations in supply air and fuel-feeding inevitably occur. Under such circumstances, using OCs can provide a large amount of oxygen in a short time and so maintaining smooth boiler operation and providing valuable recovery time for the operator.

Lind et al. [10] investigated the oxygen buffering ability of ilmenite ore in the CUT 12 MW<sub>th</sub> CFB boiler. During the test, the boiler load was first stable at 6 MW<sub>th</sub>, then a step response of the process was studied by introducing a fuel pulse corresponding to an increase in fuel load to 8 MW<sub>th</sub> in 5 s, as shown in Fig. 3.14. The response of unburnt fuel and oxygen in dry flue gases are shown in Fig. 3.15 and Fig. 3.16. When the fuel pulse was introduced, the oxygen concentration was reduced regardless of using OC or silica sand as bed materials. The CO concentration shows a significant peak during the fuel injection when using silica sand, while it was almost constant when using OC. The same pulse of fuel injection was repeated three times, all showing consistent results. The constant CO concentration during the fuel injection was attributed to the oxygen buffering ability of ilmenite ore, which has been proven to be significant. Figure 3.16a also confirmed that when the available oxygen in the furnace was not globally sufficient to fully convert the fuel pulse, the oxygen in

the OCs can make up for the lack of oxygen in space and time in the furnace. In addition, the OC can be re-oxidized to the initial stage and capable of oxygen buffering when the pulse of volatiles disappeared and gaseous oxygen becomes available.

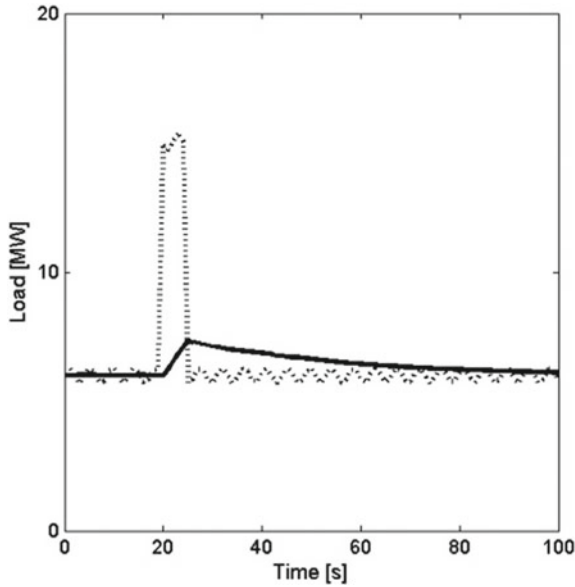


**Fig. 3.14** The load of fuel feed (dashed line) and volatile release (solid line) as function of time (reprinted from [10] with permission of Elsevier)

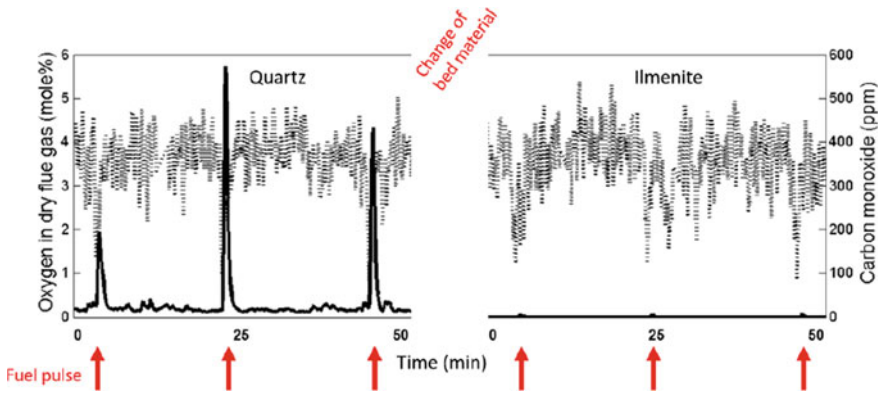
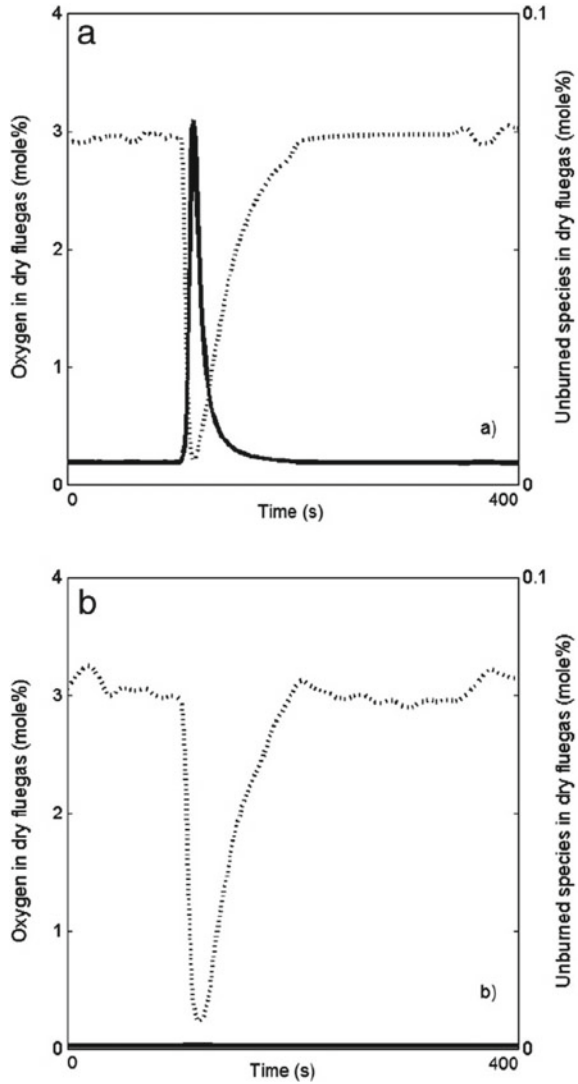


**Fig. 3.15** Response of unburnt fuel (CO (ppmv), solid line) and oxygen (% , dashed line) in dry flue gases. The O<sub>2</sub> concentration in the flue gas was 3.5 mol % on dry basis (reprinted from [10] with permission of Elsevier)

**Fig. 3.16** Evaluated dynamic response of oxygen (dashed line) and unburnt components (solid line) in flue gases during the fuel pulse, **a** silica sand, **b** MeO (reprinted from [10] with permission of Elsevier)

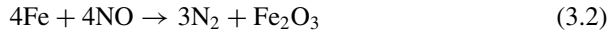
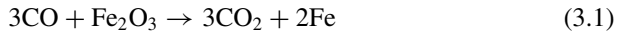


## 3.2 Emissions

### 3.2.1 NO<sub>x</sub> Emission

The characteristics for the formation and emission of NO<sub>x</sub> during typical OCAC processes have been studied in fluidized bed units on the scale of bubbling fluidized bed, 12 MW<sub>th</sub> CFB, and 115 MW<sub>th</sub> CFB. However, the results related to the NO<sub>x</sub> emission during OCAC investigated at different scales seem inconsistent.

Wang et al. [5] investigated the effect of different OCs as bed materials on the NO emission by varying air-to-fuel ratio for burning wood char in a bubbling bed. Under the same oxidation conditions (the same CO concentration), a lower NO emission was observed during operation with OCs compared to operation with sand (as shown in Fig. 3.17). At the same time, lower release of unburned volatiles and ammonia was observed in the outlet of the reactor in the OCAC case (as shown in Fig. 3.18), which means that more ammonia and NO were consumed. The mechanism of this reduction is not clear, and a possible inference is that the metal oxides with variable metal valence states contained in the OCs might promote the reduction of NO via catalytic reactions, which is widely accepted in selective catalytic reduction (SCR) technology [5]. Taking iron oxide as an example, the reaction could be as follow:



Therefore, when there was CO in the reactor, even if the temperature was as high as the bed temperature, the metal oxide can still catalyze the reaction between NO and CO [26, 27]. This was also the reason why iron oxides have been widely used as additives in reburning technology for denitration [28].

Based on an investigation in the CUT 12 MW<sub>th</sub> CFB boiler (fuel: wood chips), Thunman et al. [1] also found that the OCAC process with ilmenite as OC could significantly reduce the NO emission, as shown in Fig. 3.19. However, it was not clear whether the formation of NO was reduced, or if the reduction of NO was enhanced. Interestingly, a lower NO concentration was achieved in the case of 17 wt% ilmenite ore than with 20 wt%. It should be noted that the residence time of the ilmenite in the reactor at 17 wt% case was longer than that in the 20 wt% case. According to the relevant knowledge on the ilmenite ore in CLC, the continuous redox cycles of

**Fig. 3.17** NO emission as a function of the CO concentration for different bed materials (reprinted from [5] with permission of American Chemical Society)

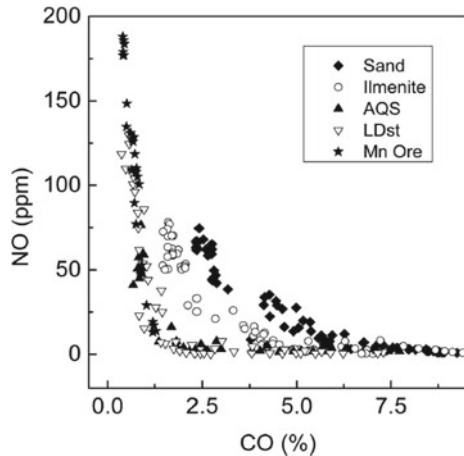
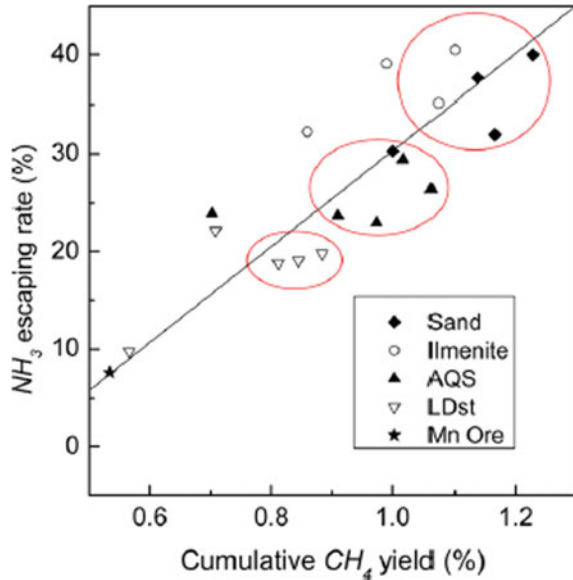


**Fig. 3.18** Effects of oxygen carriers on rates of release of volatiles and ammonia (reprinted from [5] with permission of American Chemical Society)

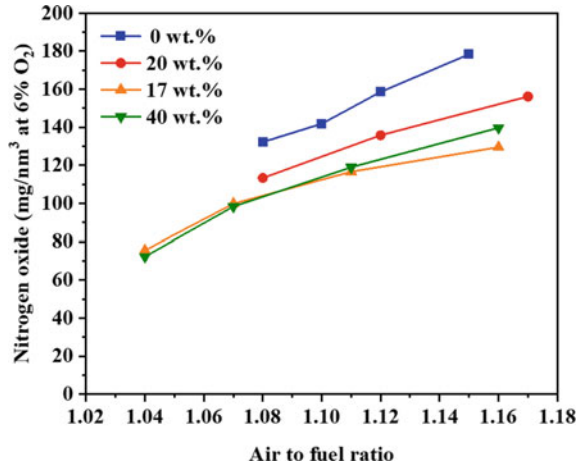


ilmenite at high temperature will cause the migration of iron to the particle surface and increase the active sites [29–31]. This suggests that the presence of ilmenite ore improves the catalytic reduction of NO [1]. However, an opposite result was obtained on the same boiler by Rydén et al. [9, 11] when manganese ore and steel slag were used as OCs (fuel: wood chips). Figure 3.20 shows that the NO emission increases with the increase of OC ratio in the bed inventory, while adding S or using regenerated bed materials reduces the NO emission. This can be explained by the consumption of reducing gas (such as H<sub>2</sub> and CO) by OCs, that results in more NO formation and emission. In addition, the presence of OC may catalyze the oxidation reaction to produce NO. The effects of S addition and regenerated bed material on the NO emission, however, have not been explained [9, 11]. All the results indicate that higher air–fuel ratio leads to higher NO emission, which is not beyond the expectation.

From an OCAC operation on a 115 MW<sub>th</sub> commercial CFB boiler with ilmenite ore as bed material (fuel: waste wood), Moldenhauer et al. [18] found that the NO<sub>x</sub> emissions and ammonia consumption were all slightly higher compared to the traditional operation with silica sand as bed materials. However, the NO concentration of these gases decreased with the increase of furnace temperature, which was unexpected. This may be because the reduction of excess air in the OCAC case led to a more reducing local atmosphere, thereby reducing NO emissions (Fig. 3.21).

In conclusion, the micromechanism of NO formation and emission during the OCAC process is not that clear, which makes it worthy of further investigation. The application of OCs in CFB boiler may impose either positive or negative effects on the NO emission depending on operation parameters such as fuel type, OC type, temperature, excess air, and the ratio of primary and secondary air, etc. The possible influence

**Fig. 3.19** Measured concentrations of NO (mg/nm<sup>3</sup>, at 6% O<sub>2</sub>) in the convection path at various OC concentrations in the bed (adapted from [1])



of OCAC on the NO emission in fluidized bed combustion can be divided into direct influence and indirect influence. Direct effects may include: (1) Active components such as Fe<sub>2</sub>O<sub>3</sub>, CuO and MnO<sub>2</sub>, etc., contained in the OC may be directly or catalytically oxidized through the nitrogen-containing gas components, such as NH<sub>3</sub> and HCN, to generate more NO<sub>x</sub>; (2) The reduced OC may directly or catalytically reduce nitrogen-containing gas components (HCN, NH<sub>3</sub> and NO<sub>x</sub>, etc.), resulting in a lower NO<sub>x</sub> emission. Indirect effects may include: (1) the application of OCAC can reduce the hot spots and improve the uniformity of temperature distribution in a furnace, which can reduce the NO formation; (2) the presence of OC makes the reduction zones smaller in the furnace, which will weaken the reduction of NO<sub>x</sub>; (3) Under OCAC operation, the physical property parameters (such as particle density, size and specific heat capacity) of the bed material are different from those found during operation with inert bed material. This will affect the heating of the fuel and may change the type and concentration of the nitrogen-containing gas components in the pyrolysis products.

### 3.2.2 SO<sub>x</sub> Emission and Desulfurization

At present, the effect of OCAC technology on the SO<sub>x</sub> emission characteristics under air combustion has not been deeply studied. This may be since most experimental studies have applied pure biomass or MSW as fuel, and the sulfur content in such fuels is very low. However, the SO<sub>x</sub> emission should be considered when burning fuels with high sulfur content, such as coal and petroleum coke.

When Vigoureaux et al. [16] performed OCAC combustion with ilmenite in the CUT 12 MW<sub>th</sub> CFB boiler, they added sulfur into the furnace during combustion and found that both the outer ash layer and the core contained sulfur. With an increase of



**Fig. 3.20** Measured concentrations of NO (mg/nm<sup>3</sup>, at 6% O<sub>2</sub>) in the convection path at various Mn concentrations in the bed (adapted from [9])

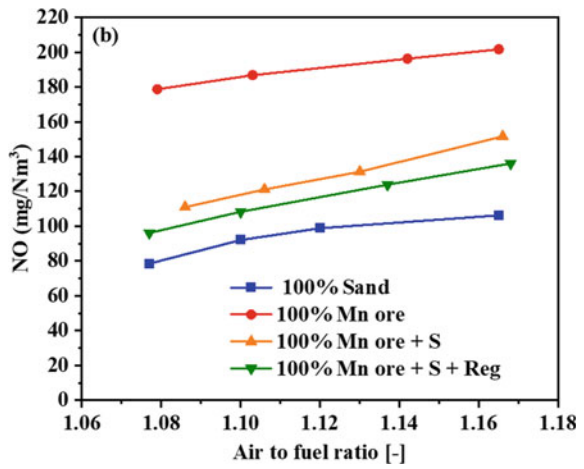
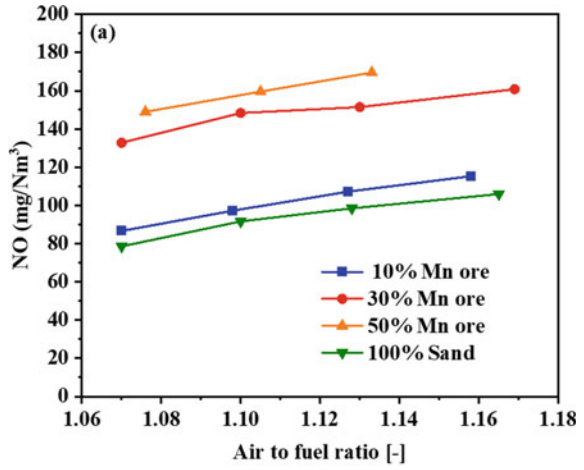
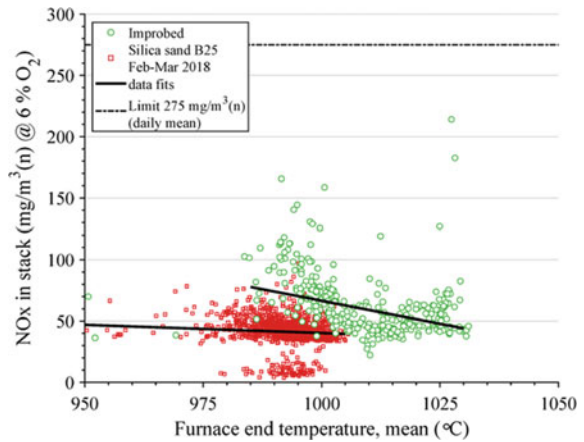


**Fig. 3.21** NO<sub>x</sub> concentration measured as dry-gas at 6% O<sub>2</sub> as a function of the temperature, the red and green circles represent silica sand case and OCAC case, respectively [18]



the test time, the potassium and sulfur contents in the ilmenite particles were gradually increased, which indicates that the application of OCAC technology may help to reduce SO<sub>x</sub> emissions. During normal CFB operation, limestone is injected into the furnace as a desulfurization sorbent. It decomposes into CaO and then captures SO<sub>2</sub> through the sulfation reaction [32]:



On the one hand, OCAC technology can make the temperature and oxygen distribution in the furnace more uniform, which promotes the desulfurization reaction. On the other hand, although it is difficult to directly oxidize SO<sub>2</sub> to SO<sub>3</sub>, it can be achieved through a catalytic reaction [33]. Existing studies [34, 35] have shown that metal oxides can be used as catalysts to oxidize SO<sub>2</sub>. One of the most widely known oxidation catalysts is Fe<sub>2</sub>O<sub>3</sub> [35]. Jørgensen et al. [34] experimentally studied the oxidation reaction of SO<sub>2</sub> to SO<sub>3</sub> in the temperature range of 873–1323 K under semi-dry and moist conditions, and evaluated the catalytic effects of quartz, alumina, and iron oxide on this reaction. They found that the homogeneous oxidation reaction between O<sub>2</sub> and SO<sub>2</sub> was slow. However, alumina and iron oxide could promote the SO<sub>2</sub> oxidation, and the iron oxide is a strong oxidation catalyst for the reaction between O<sub>2</sub> and SO<sub>2</sub>.

When the temperature is below 400 °C [36], SO<sub>3</sub> is highly reactive with water vapor to form H<sub>2</sub>SO<sub>4</sub> and can be completely transformed at around 200 °C [35]. The generated H<sub>2</sub>SO<sub>4</sub> is highly corrosive to the heated surface. Higher SO<sub>3</sub> concentration in the flue gas increases the acid dew point. If the desulfurization efficiency in the furnace is low, corrosion of the low-temperature heating surfaces, such as air preheaters may be enhanced. At present, there is no research on the characteristics of SO<sub>3</sub> emission under OCAC operation, but further research is needed. For high-sulfur fuels, the impact of OCAC on SO<sub>2</sub> and SO<sub>3</sub> emissions should be considered, because it is critical for the safe operation of downstream heat exchangers. The desired research includes: the potential impact of OC addition on the formation and emission of SO<sub>x</sub>, migration paths and desulfurization reactions. In addition, high concentrations of SO<sub>x</sub> may reversely affect the physicochemical characteristics of OCs, and this needs to be considered.

### 3.3 Ash-Related Issues

Solid fuels (such as coal and biomass) are usually containing a heterogeneous mixture of organic and inorganic matter [37, 38]. During the thermal conversion of fuel in a CFB system, the inorganic matter is mainly transferred from the fuel to the solid

residues, mainly ash, and may cause problems, such as agglomeration, ash deposit, fouling and corrosion of heat-transfer equipment [39, 40].

### 3.3.1 *Bed Agglomeration*

Bed agglomeration is caused by sintering of bed material may lead to defluidization. This can collapse the entire bed into a solid mass [41]. Consequently, bed agglomeration can cause unplanned shut down of a boiler. Inert bed material, such as silica sand or ashes, is most used for CFB boilers, and their agglomeration mechanism has been extensively studied [40]. The agglomeration mechanism is generally dominated by two regimes: melt-induced agglomeration (Fig. 3.22) and coat-induced agglomeration (Fig. 3.23) [42]. Melt-induced agglomeration is caused by the collision of large molten ash particle and bed material, where the molten ash acts as a “viscous glue” [43] bonding the latter into tough agglomerates. Scala and Chirone [44] pointed out that a char particle in the bed can create a local hot spot, which can enhance the adhesive potential of this “viscous glue” and intensify agglomeration. The coat-induced agglomeration is initiated by ash deposition on the surface of bed particles via the attachment of small ash particles, the condensation of vaporized alkali species, and/or the chemical reactions at the surface of bed particles. Then, the generated alkali-silicate (usually K-silicate) layer grows inwards after reaction with silicate species in the bed material, which causes the bed particles to possess two- or three-layer coatings [45, 46]. Lastly, the bed particles would experience a sintering and homogenizing process, resulting in partial melting, agglomeration, and defluidization [41].

In order to avoid bed agglomeration, the bed material needs to be repeatedly regenerated according to the fuel and bed material characteristics. Within the existing experimental studies of OCAC technology in 12 MW<sub>th</sub>, 75 MW<sub>th</sub> and 115 MW<sub>th</sub> boilers, bed agglomeration was not reported. The used OCs were ilmenite ore, manganese ore, and LD-slag, which possessed high melting points, and the operation time was relatively short in these studies. However, when OCs with lower melting points such as CuO was considered to be applied in OCAC, agglomeration must be carefully looked after. One solution is to frequently replace the bed material, which means the loss of OCs. Another solution is to use some supports to fabricate the OC particles and elevate their melting point. It should be noted that both ways can be costly [47].

### 3.3.2 *Ash-Layer Formation of OC*

Elements found in ash-layers mainly originate from the bed material and the fuel [48, 49]. As shown in Fig. 3.24, there are three growth modes that have been proposed from previous studies for the formation of ash-layer [41, 50]:

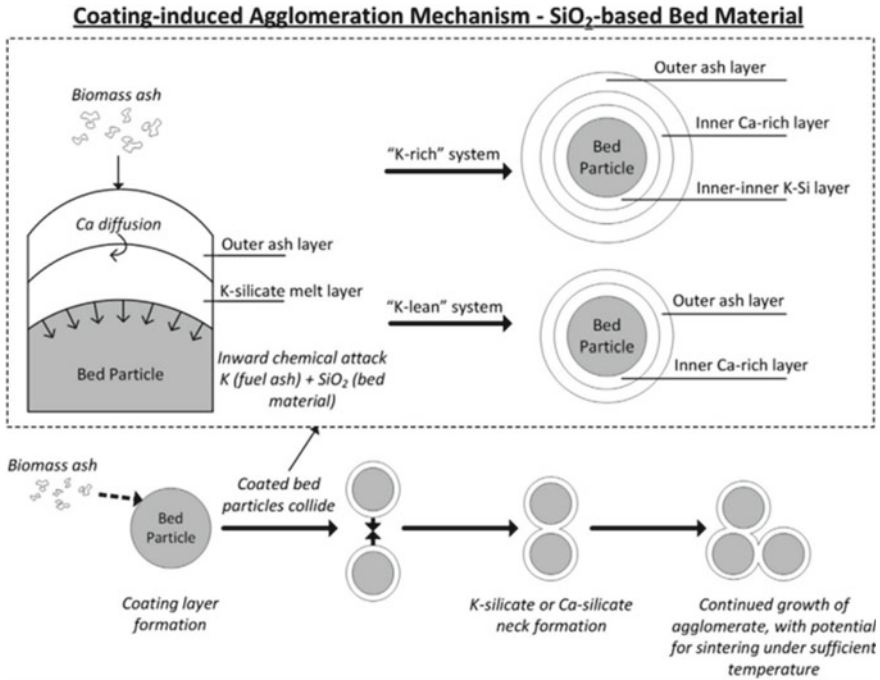


**Fig. 3.22** The schematic of coating-induced agglomeration mechanism (reprinted from [42] with permission of Elsevier)

- Mode (1): An ash-layer is attached to the inert bed particle and grows outward, while the elements contained in the ash-layer originate from the fuel;
- Mode (2): The initially formed ash-layer may react with the bed particles resulting in further inward growth;
- Mode (3): The ash layer grows both inward and outward.

Several research groups have investigated layer formation on bed materials during solid fuel combustion and found that the formation of an ash-layer usually follows the growth Mode (3) [45, 49, 51, 52], and the outer section of the ash-layer is more heterogeneous in elemental composition than the inner section. The heterogeneous outer layer grows outward on the surface of bed particles with a similar composition to fly ash. The less heterogeneous inner layer is often dominated by Ca and/or K, which can diffuse into the bed material and reciprocally react together [48, 49, 51, 53]. Most research on ash-bed material interaction focused on Si-based bed particles, while few studies have been centered on the interaction between OC and coal ash [54–56].

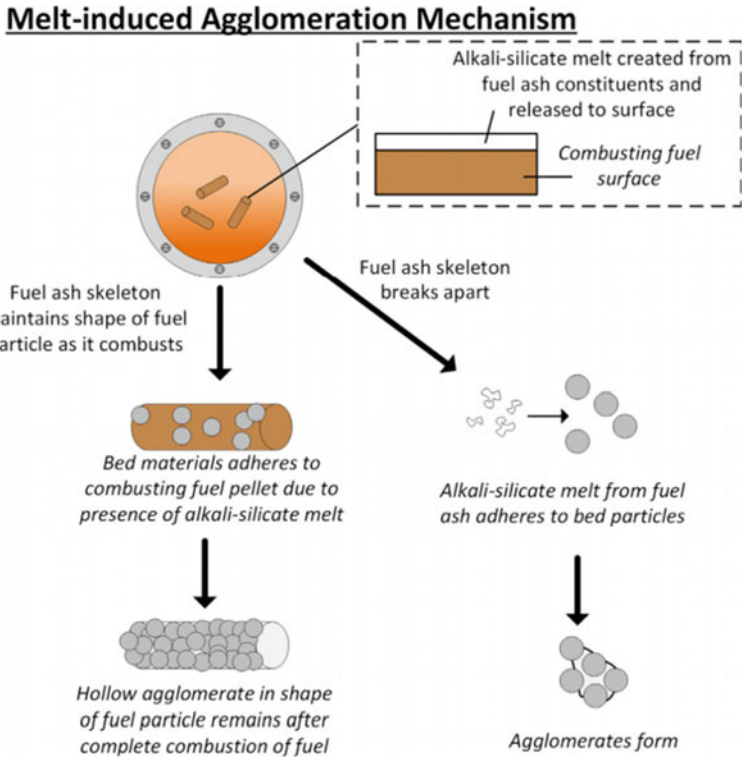


**Fig. 3.23** The schematic of melt-induced agglomeration mechanism (reprinted from [42] with permission of Elsevier)

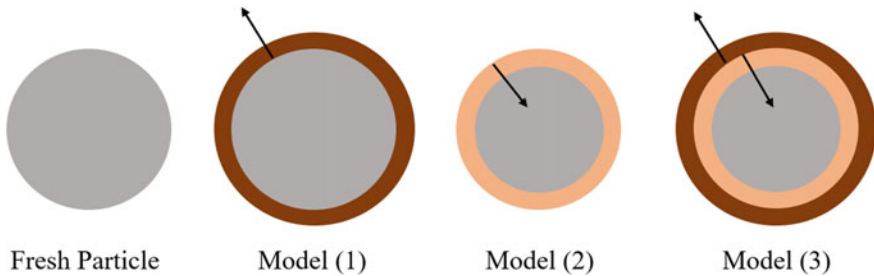


**Fig. 3.24** Illustration of the different mechanisms for ash layer formation on bed particles

#### 3.3.2.1 Ilmenite Ore as Bed Material

Corcoran et al. [8] have investigated the physical and chemical changes of ilmenite when it is used as OC during a typical OCAC process in the CUT 12 MW<sub>th</sub> CFB boiler. As shown in Fig. 3.25, the particle of ilmenite ore underwent an element

segregation with an iron moving to the surfaces and titanium enriched in the core. Such a phenomenon is quite like the observation in a CLC process when the ilmenite is subjected to redox cycles. Figure 3.26 showed the EDX line profiles of the outer parts of an ilmenite particles cross-section from sample II (24 h), a calcium-enriched double lamellar structure with iron layer surrounded by calcium was observed on the ilmenite particles. Interestingly, the potentially problematic element compound (potassium) was found to diffuse into the ilmenite particles to form a homogeneous compound, and the concentration of K in the particle increases sharply with time on stream. The XRD analysis shows that potassium titanium oxide (KTi<sub>8</sub>O<sub>16</sub>) was formed in the particle's core, which suggested the reaction between K and TiO<sub>2</sub>. In addition, a 72 h' leaching experiment was carried out with Sample II in Fig. 3.16 by deionized water to understand the leaching properties of potassium titanium oxide, the results as shown in Fig. 3.27. Figure 3.27 showed that the highest amount of K and Ca in the leachate were a very limited degree, namely, to less than 32 ppm (<1%) and 7 ppm (<0.2%), respectively. This indicates that the contents of water-leachable Ca and K were very limited. The water-leachable K might be derived from the unreacted K, and it became water-unleachable once forming KTi<sub>8</sub>O<sub>16</sub>.

Corcoran et al. [13, 41] studied the mechanisms of element migration and ash-layer growth on the ilmenite OC during the OCAC of biomass in the CUT 12 MW<sub>th</sub> CFB combustor. The fresh ilmenite included over 50 wt% of fine particles (<125 μm), less than 1 wt% of large-sized particles (250–355 μm). During the 364 h test, the irregular bed material was sampled. The resulting cumulative size distribution curve of the bed material is shown in Fig. 3.28. With the increase of time, the size of the particles increased significantly. For the fresh OCs, most of the particles are found to be in the size range of 90 – 180 μm, which increased to 125 – 250 μm after exposure. When the OC bed materials were used for 147 h, over 95 wt% of the particles were larger than 125 μm, and over 10 wt% of particles were above 250 μm. It should be emphasized that particles with diameter larger than 355 μm were found in all samples, regardless of exposure time. Only the sample exposed for more than 364 h shows a deviation from this trend. This deviation could have two reasons: (1) new material was added to the boiler to maintain the pressure drop over the bed; (2) a structural damage can occur after long exposure in the reactor [12]. In addition, agglomeration was not found in any bed sample.

Figure 3.29 shows images of the calcium and potassium elemental cross-sections of OC particles after different times of operation. Both Ca and K migrate to the interior of bed particles, and the K migrates much faster than Ca. Concurrently, Ca and other ash components (such as Si and P) accumulate on the surface of the bed particles forming an outwardly growing ash layer. No K was found in this layer (as shown in Fig. 3.30). In addition, the authors found that the particles became more porous as the time-on-stream increased, which might be due to the replacement of Fe within the Titanate complex by guest elements (such as K and Ca) from the ash-layer. Consequently, the increase of particle size for OC bed particles probably contributed to the growth of the ash-layer.

The reactivity of OC samples can be tested using a laboratory scale bubbling fluidized bed. In the tests, syngas was used as fuel and the oxygen transfer capacity

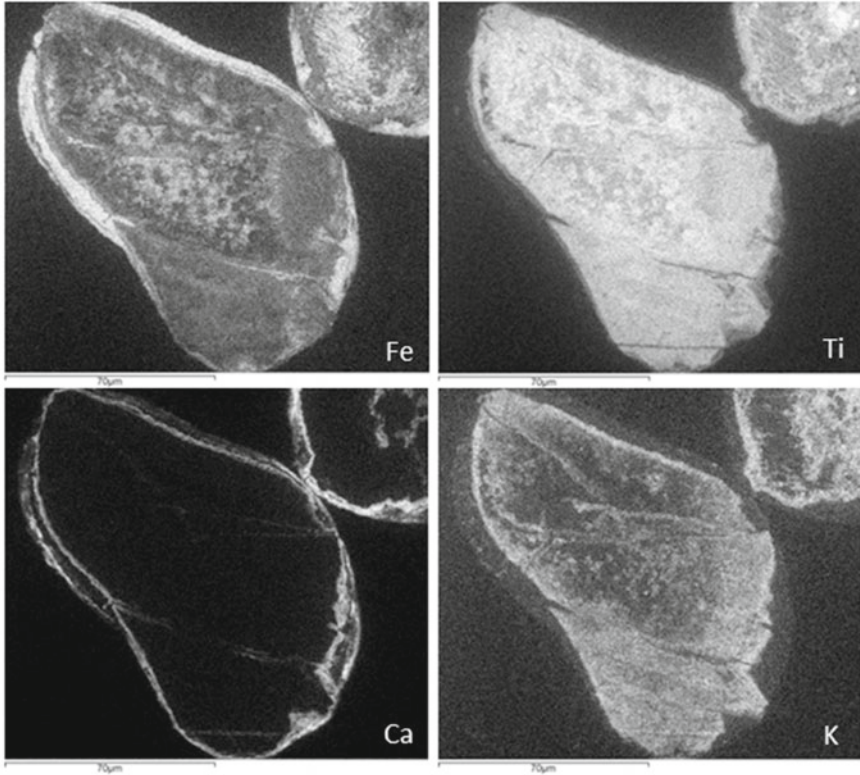


**Fig. 3.25** EDX maps of the distribution of iron, titanium, calcium, and potassium in the cross-section of an ilmenite particle from sample in 24 h, (Reprinted from [8] with permission of American Chemical Society)

of the OC was established by the oxidation rate of CO (also called  $\text{CO}_2$  yield). The  $\text{CO}_2$  yield of OCs with different exposure time from a 12  $\text{MW}_{\text{th}}$  CFB-boiler are summarized in Fig. 3.31. The relatively inert quartz sand was used as a reference. The fresh ilmenite ore shows a low initial  $\text{CO}_2$  yield, while that of used OC samples increases with exposure time, except for the OC after 322 h exposure, where the  $\text{CO}_2$  yield decreased slightly. This was because as the reaction time increases, ilmenite ore undergoes more redox cycles, more iron atoms migrate to the outer surface of the ilmenite particles to form a Fe-rich shell [57, 58]. At the same time, the pore structure of the oxygen carrier particles would develop [58], resulting in a high reactivity of OCs. These phenomena were also found in CLC technology. Furthermore, the decrease in reactivity of the sample with a longer test time (322 h) indicates that the ilmenite has a limited lifetime as an oxygen carrier, which is due to the reduction in the number of reactive sites. There are two possible reasons: (1) the ash layer covers the surface of the bed particles, and (2) the abrasion of the surface.

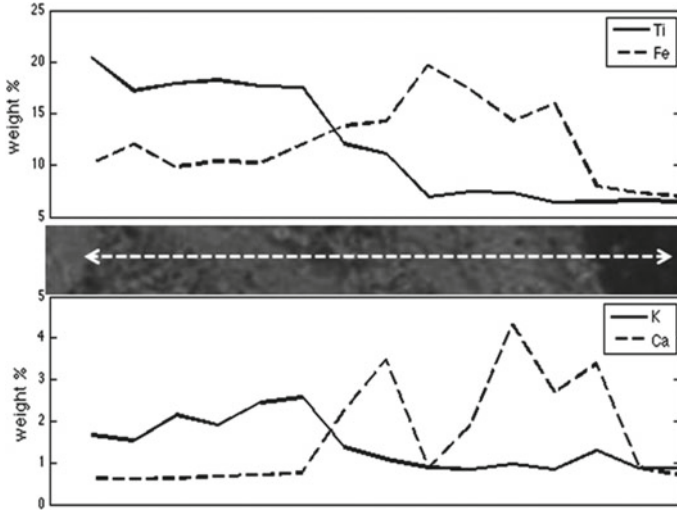


**Fig. 3.26** EDX line profiles of the outer parts of an ilmenite particles cross-section from sample II (24 h) (reprinted from [8] with permission of American Chemical Society)

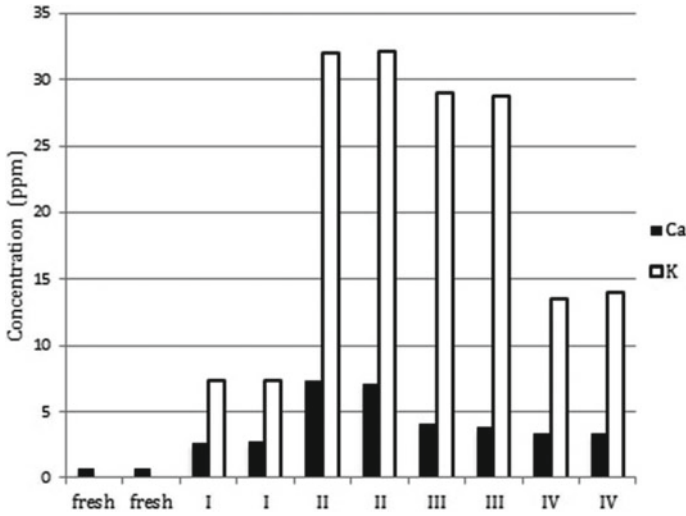


**Fig. 3.27** Elemental composition in leachates from fresh ilmenite as well as samples I (1 h), II (24 h), III (48 h), and IV (72 h) exposed in the CFB boiler (reprinted from [8] with permission of American Chemical Society)



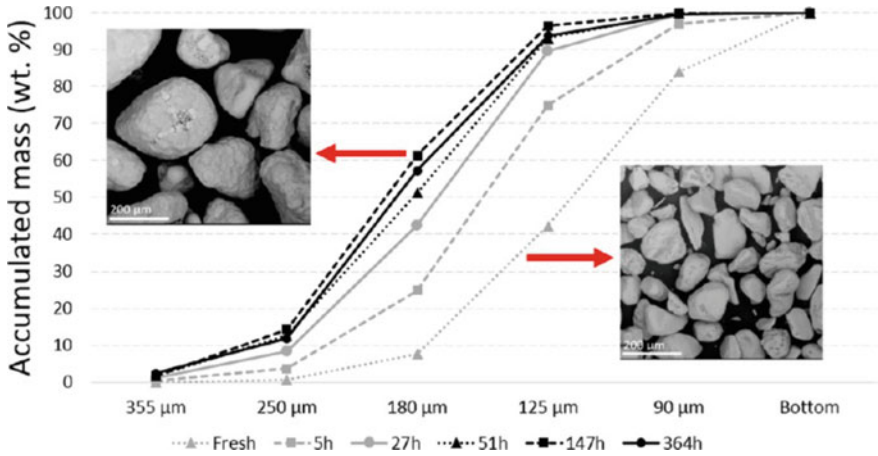


**Fig. 3.28** The size distribution curve of bed particles at different test times (reprinted from [13] with permission of American Chemical Society)

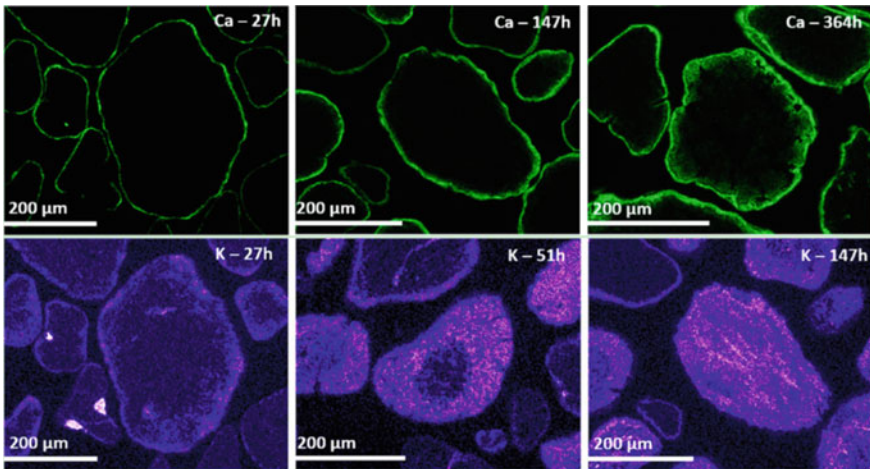


**Fig. 3.29** The distribution of Ca and K on the ilmenite ore particles [41]

Vigoureux et al. [16] investigated the accumulation of alkali metals and S on OC during the OCAC of wood with the addition of elementary S in the 12 MW<sub>th</sub> CFB boiler (as shown in Fig. 3.32). It was found that ilmenite as bed material can absorb not only Ca and K but also S. Besides, the absorption of S by aged ilmenite with an ash-layer is higher than that of a fresh one. This was because the aged ilmenite has higher contents of Ca and K, especially in the ash-layer, which could react with S [38]. Furthermore, the aged ilmenite exhibits a more developed pore structure with higher surface area, which facilitates the accumulation of S on and within the particles [58]. Therefore, when fresh ilmenite was used, S accumulated mainly in

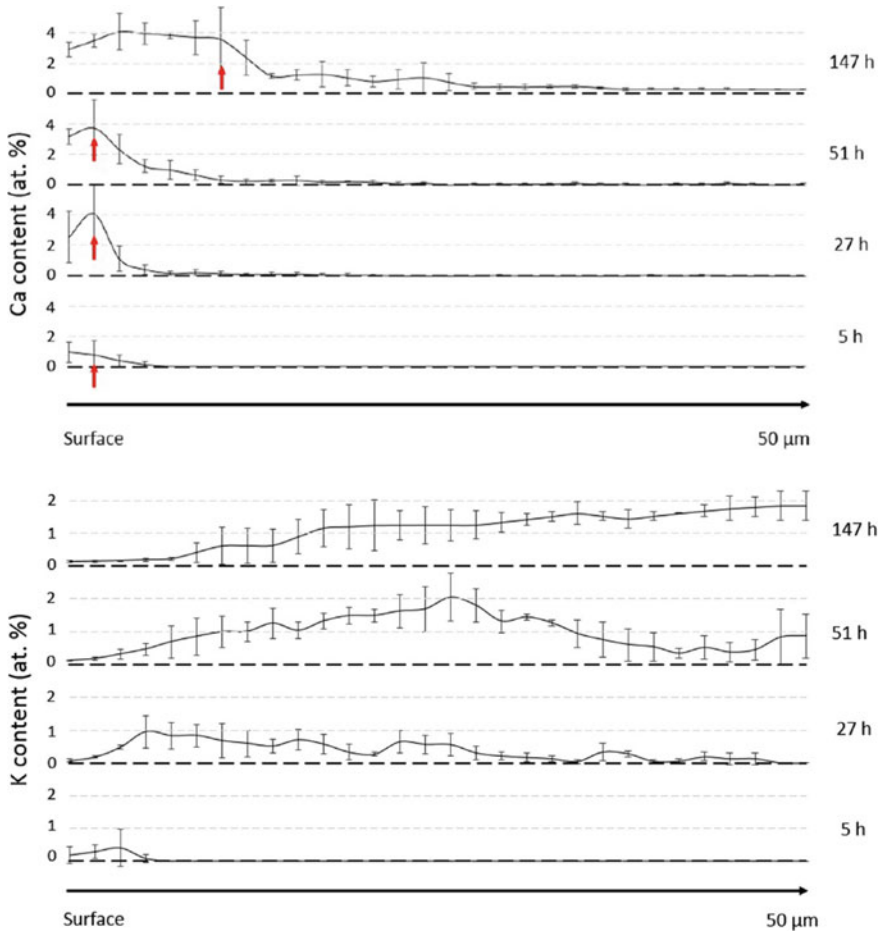
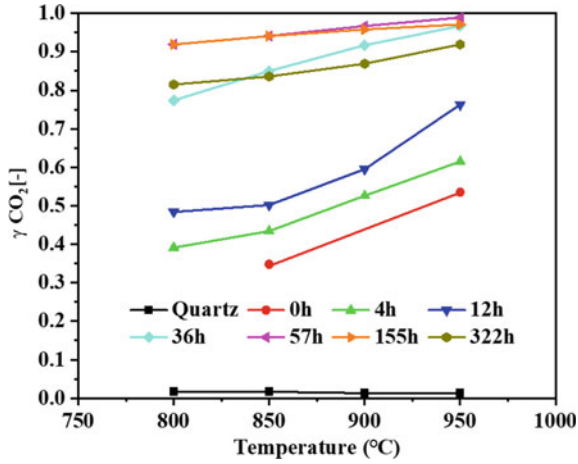


Fig. 3.30 Migration of Ca and K into the particle, the content is the weight percentages [41]

the ash-layer, while when aged ilmenite was used, S was found in the particle core. In addition, the quantitative analysis suggested that K<sub>2</sub>SO<sub>4</sub> may be formed.

### 3.3.2.2 Manganese Ore as Bed Material

Hanning et al. [14] investigated the interaction between biomass and manganese ore as a bed material in the same 12 MW<sub>th</sub> CFB boiler. No bed material was regenerated during the one-week experiment period. The concentration of different components in bed samples as a function of operational time are shown in Fig. 3.33, the results indicated that Si, Ca, K, and S elements accumulate on the bed material. The SEM–EDS results of the samples taken after 172 h of operation are shown in Fig. 3.34.



**Fig. 3.31** CO<sub>2</sub> yield of bed samples with different exposure time from bench scale experiments with syngas as fuel. Solid lines denote materials obtained from the 12MW<sub>th</sub> CFB-boiler, while dashed lines represent fresh materials (adapted from [59])

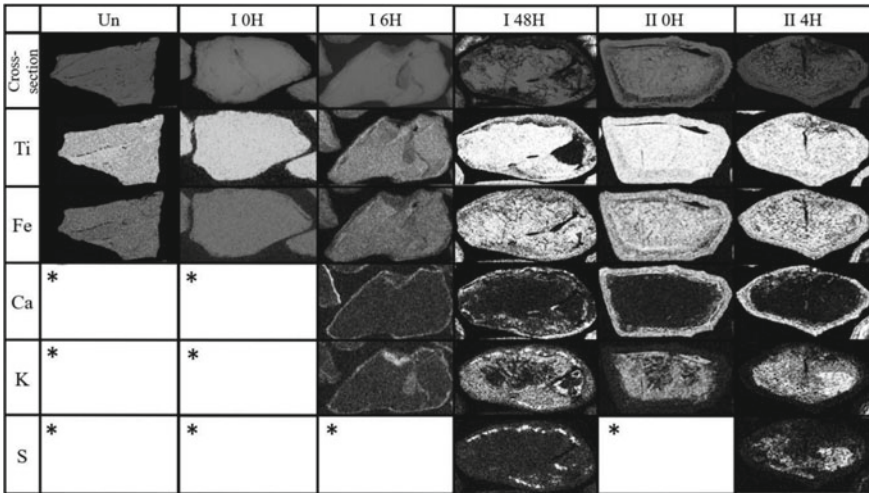


**Fig. 3.32** The element distribution of Ti, Fe, C, K and S on the cross-section of OC of ilmenite ore after the OCAC process. The “Un” means fresh ilmenite particle, I and II means using the fresh and used ilmenite particle as bed materials, respectively. The asterisk means undetectable (reprinted from [16] with permission of American Chemical Society)

The Si, Ca and K could be found on the OC particles, both inside and outside, while S was mainly in the outer ash-layer. The formation of an ash-layer on the particle surface leads to a significant increase of particle size, which continues with a prolonged OCAC operation. The fresh OC particle-size range was 100–400  $\mu\text{m}$ , with an average size of 200  $\mu\text{m}$ . After 172 h of exposure, a large number of bed particles in the sample were larger than 500  $\mu\text{m}$ . Despite the increase of the size of the OC particles, the bed material did not show any severe agglomeration during the one-week test. Interestingly, some hollow particles could be found after a 172-h operation. The elemental distribution of a hollow particle is shown in Fig. 3.35, showing that Ca and Si are enriched in shell of the hollow particle, while Si, K, Mn, Fe and S exist inside the particle. The study concluded that the formation of hollow particles is mainly due to the collision between ash and char, resulting in a char particle surrounded by an ash-layer. With the burn-out of char core, a hollow particle with a shell of ash-layer forms [43].

As shown by Fig. 3.36, the reactivity of the bed particles towards syngas decreases as the OCAC operation time increases. There are two possible reasons: (1) during the operation of the boiler, the structure of the bed particles may change, affecting their reactivity, such as the deactivation caused by accumulation of ash elements on the surface; (2) the ash elements, migrating into the particles, may react with the active components to form inactive substances.

With silica sand as bed material, it is usually necessary to regenerate the bed material regularly to avoid bed agglomeration, as mentioned above. However, a bed of manganese ore did not show any tendency of agglomeration, even if the boiler was operated at 870 °C for a whole week. This is because the manganese ore is not prone to ash melting, which is positive for the continued safe operation of the boiler. From another point of view, the concentration of alkali vapor in the flue gas may increase if less alkali is absorbed by the manganese ore, which may affect the combustion, fouling and corrosion inside the boiler. The fouling and corrosion behavior of the boiler with manganese ore as OC should be further investigated in detail.

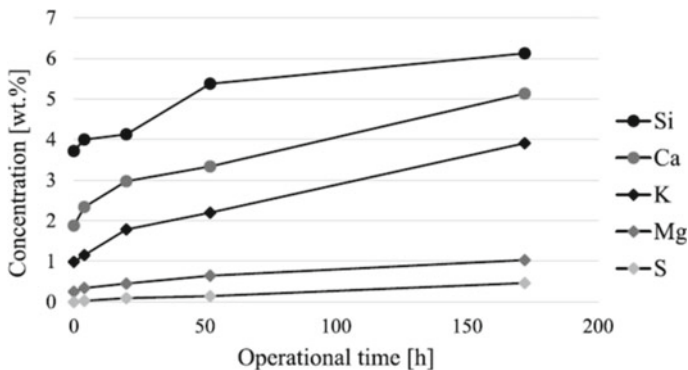


**Fig. 3.33** Concentration of different components in the fresh material and used bed samples as a function of operational time (reprinted from [14] with permission of Elsevier)

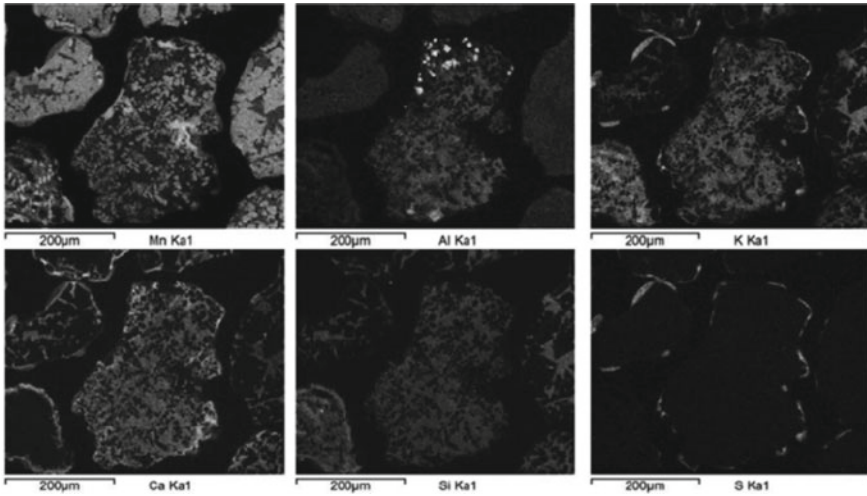


**Fig. 3.34** Elemental distribution of manganese, aluminium, potassium, calcium, silicon and sulphur in the sample taken after 172 h of operation (reprinted from [14] with permission of Elsevier)

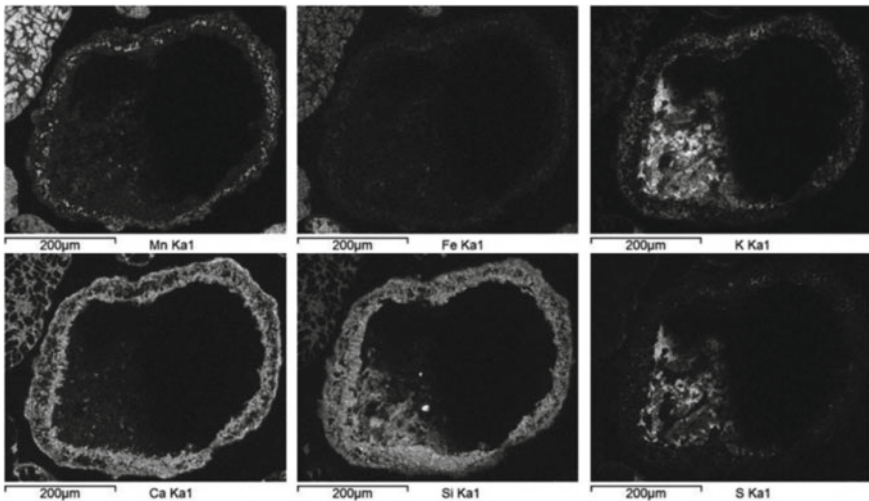
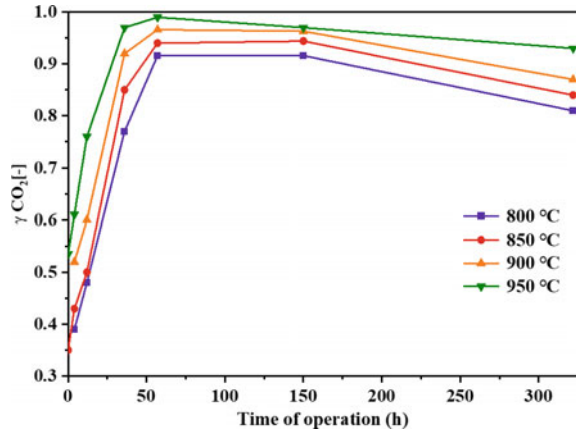


**Fig. 3.35** Elemental distribution of Mn, Fe, K, Ca, Si and S in the hollow particle from the sample taken after 172 h (reprinted from [14] with permission of Elsevier)

### 3.4 The Aging of Oxygen Carrier

In the general operation of a biomass-fired CFB boiler, the used bed material is partially and continuously replaced by fresh one to avoid agglomeration issues. As the residence time of the bed material increases, the physicochemical properties of

**Fig. 3.36** CO<sub>2</sub> yield of bed samples with different exposure time from the boiler. The conversion is tested with syngas (adapted from [59])



the bed material change to a certain extent. This process is called bed-material aging. Several phenomena cause aging in the thermal conversion of biomass, including the formation of an ash layer and of pores, cracks, and cavities [60–62].

Corcoran et al. [12, 13] evaluated the structural development and mechanical change of ilmenite OCs (rock- and sand-ilmenite) during long-term OCAC operation. They found that the cavities within particles and the cracks and clusters on the particle's surface developed with the exposure time (the SEM micrographs of ilmenite particles extracted from different exposure time are shown in Fig. 3.37 and Fig. 3.38). The study evaluated samples of fresh ilmenite and of the same OC collected after a certain period of operation in the CUT 12 MW<sub>th</sub> CFB boiler. During the operation, the sand-ilmenite generated several cavities. The cavity size increased, and more cavities emerged with longer operation time. The cavities were held together by an ash-layer before the particles were shattered into numerous pieces. The rock ilmenite particles first developed cracks, then the cracks extended inward, leading eventually to the splitting of the particle. The mechanical strength of both materials was weakened due to the development of cavities and cracks. The possible ways for particle degradation of sand and rock ilmenite particles are displayed in Fig. 3.39.

Combined with the attrition test, it was found that the mechanical resistance of both fresh ilmenite OC is similar, but that of sand is slightly higher. After the OCAC operation, the sand ilmenite particles became more prone to attrition, while its mechanical resistance did not change dramatically over time. The rock ilmenite was initially sensitive to mechanical stress, but it became more resistant over time [12].

Appropriate determination of bed regeneration frequency is the key to the economy of operation of OCAC. Higher regeneration frequency of bed material reduces the risk of agglomeration and ensures the mechanical strength and high reactivity of OCs but increases the cost of OC procurement. However, if the regeneration frequency of bed materials is too low, it will not only increase the risk of agglomeration, but also reduce the reactivity of OCs due to ash-related problems

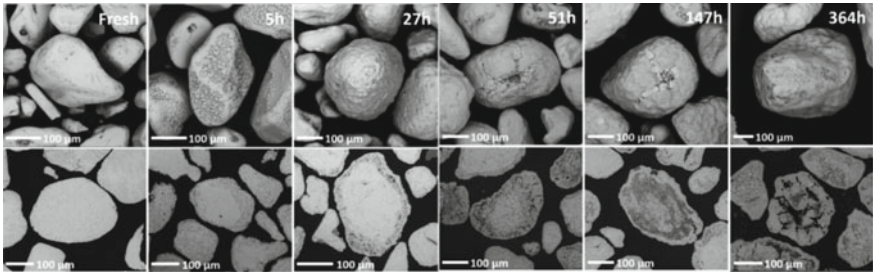


**Fig. 3.37** SEM images of ilmenite particles (0, 5, 27, 51, 147 and 364 h). The top row shows overviews of particles, and the bottom row shows the cross-sections of particles (reprinted from [13] with permission of American Chemical Society)

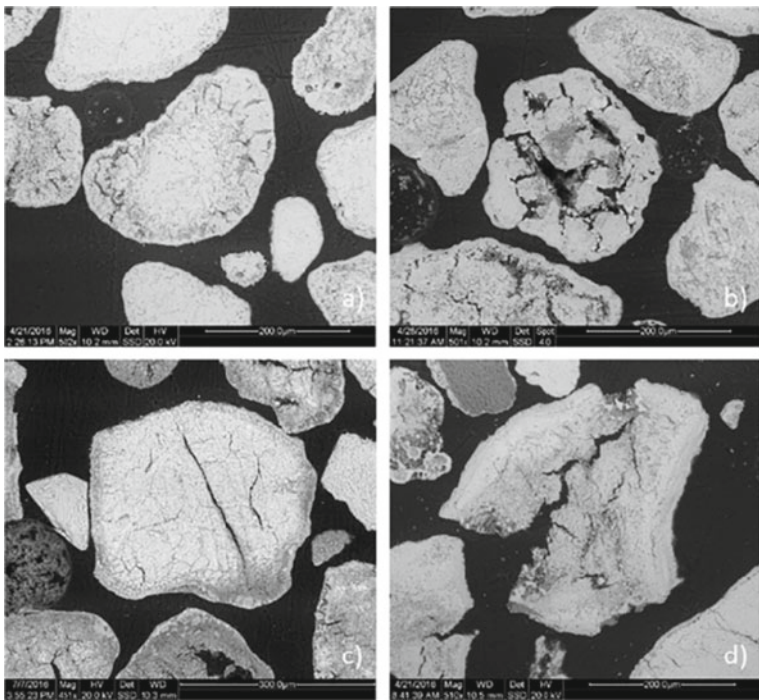


**Fig. 3.38** SEM micrographs of cross-section of ilmenite particles extracted after 2 and 15 days of exposure where **a** and **b** are sand ilmenite and **c** and **d** are rock ilmenite (reprinted from [12] with permission of Elsevier)

(especially using high-ash fuel). Moreover, mechanical crushing and elutriation may lead to the deficit of OC particles in the reactor, resulting in excessive renewal. The optimal regeneration frequency is determined by the fuel properties (volatile content,

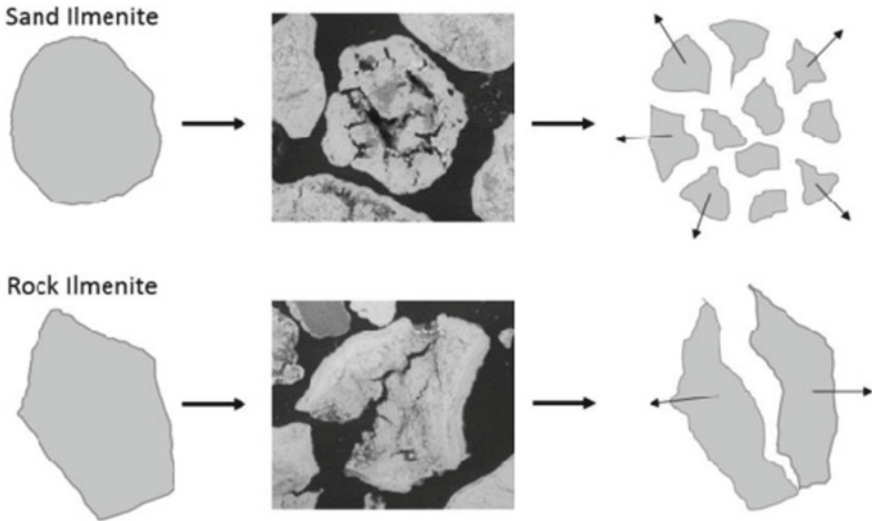


**Fig. 3.39** The schematic of possible ways for particle degradation of sand and rock ilmenite particles [41]

ash content and elemental composition) and the OC physicochemical characteristics (composition, reactivity, abrasion resistance and crushing characteristic), which should be considered comprehensively in OCAC applications.

### 3.5 Bed Material Recovery

To reduce the cost of OC, it is very important to recover and reuse OC from slag discharge. Moldenhauer et al. [18], Gyllén et al. [59] and Lind et al. [63] presented an idea of magnetic separation for ilmenite OCs in operating large-scale CFB boilers. The proposed magnetic separator consists of a belt stretched across two horizontal cylinders. It can be seen from Fig. 3.40 that the left cylinder comprises an electric drum, and the right cylinder includes four sections of powerful neodymium magnets. The pre-treated bed materials is fed evenly to the belt by a distributor. Due to inertial force, the trajectory non-magnetic material shows a parabola and falls in front of the separator, while the magnetic material will fall from the belt behind the magnetic drum due to the attraction of the magnetic drum. The magnetic separator has been used in both the 75 MW<sub>th</sub> and the 115 MW<sub>th</sub> CFB boilers. It should be noted that the bed material should be sieved to remove impurities, including nails and stones, before added to separator.

Moldenhauer et al. [18] investigated the effect of the ratio of ilmenite ore in the bed material by measuring its magnetic content and the feed rate of fresh ilmenite to the 115 MW<sub>th</sub> CFB boiler. In the first day, the feeding rate of fresh ilmenite was



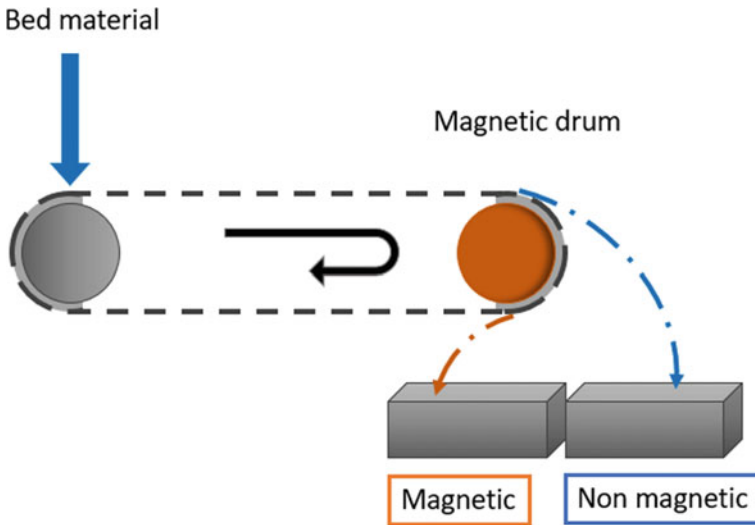


**Fig. 3.40** The schematic diagram of the roll belt magnetic separator (reprinted from [59] with permission of Elsevier)

set to 15 t/day, then the feed rate was increased to 25 t/day in the second day. On the third day, the feed rate was set to 15 t/day, where it was kept for about two weeks followed by three days at 8 t/day, two days at 4 t/day and finally a little more than four days at 2 t/day. During the transition back to silica-sand operation, the feed rate was set to the nominal value for silica-sand operation, i.e. 8 t/day.

The magnetic fraction in the bed ash and feeding rate of fresh ilmenite as shown in Fig. 3.41. It should be noted that the bed particles with a size over 710  $\mu\text{m}$  were discarded, which accounted for almost 6 wt% of the total bed inventory. The results showed that the magnetic content increased rapidly during the first 130 h, since a significant portion of the silica sand was gradually replaced by ilmenite ore. The magnetic susceptibility of the bed particles increases along with residence time. Interestingly, when the regeneration rate of bed material fell from 15 to 8 t/day, the magnetic fraction in the bed continued to increase. Even when the regeneration rate dropped from 8 to 2 t/day (approximately 0.72 kg/MWh), the magnetic fraction still rose. This indicates that the longer the residence time of ilmenite is in the furnace, the more magnetic it becomes. By testing the reactivity of the magnetic and non-magnetic fractions in a lab-scale bubbling bed with syngas as fuel, the results are plotted together with results from the Chalmers 12 MW<sub>th</sub> boiler for comparison, as shown in Fig. 3.42. The reactivity of the sample accepted by the separator was close to that of 303 h sample from 12 MW<sub>th</sub> CFB boiler, while the sample rejected by the separator has quite low reactivity. These results indicated that magnetic separation was a feasible way to recover the ilmenite ore from the boiler ash [59].

In addition, it is essential to note that the above OC recovery case was for biomass combustion, whose ash content is small. Therefore, bed material must always be

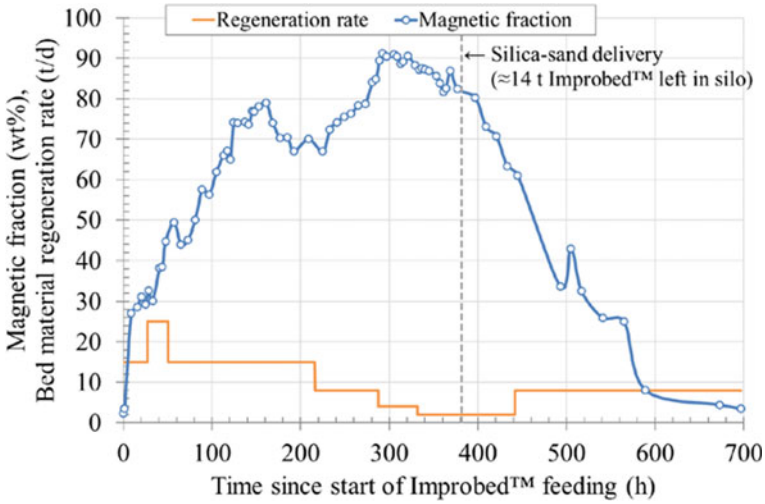
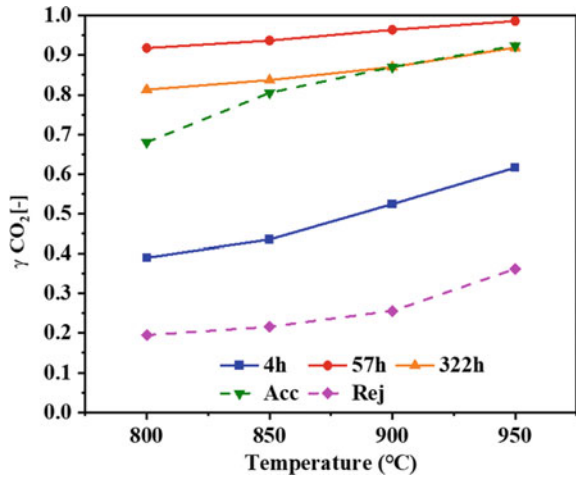


**Fig. 3.41** Measured magnetic fraction in the bed ash and feeding rate of fresh ilmenite to the furnace (reprinted from [14] with permission of Elsevier)

**Fig. 3.42** Conversion rate of syngas for different samples (adapted from [59])



added to the boiler, and the replaced bed material (OC) is easy to add and discharge which facilitates OC recovery. However, for boilers burning high ash fuels (such as coal), the bed inventory in the boiler is always more than sufficient, and bottom ash needs to be discharged continuously. Therefore, increasing the residence time of OC in CFB boiler and low-cost recovery of OC from the discharge of the bottom ash is the basis for OCAC application in the case of high-ash fuel. On the one hand, the residence time of OC in the boiler can be increased and the amount of OC in slag can be reduced by reducing the size of OC; on the other hand, combined with the

differences of magnetism, density and particle size between OC and ash, magnetic separation, pneumatic concentration, and sieving can be used to recover the OC from the ash discharge.

In addition, a separation procedure can combine the changes in the physicochemical characteristics of OC after being used in order to reduce the production costs of downstream companies providing them with better raw material. For example, after ilmenite ore has undergone multiple redox cycles, an iron-rich layer will be formed on the surface of the particles [29, 60]. The ilmenite ore particles are abraded for a long time before being discharged [41], which will move the Fe content to the ash and correspondingly increase the Ti concentration in the spent particles. High-concentration Ti-containing ore particles may benefit downstream industrial applications that facilitate the production of Ti-related products. Different schemes for the utilization of OC require comprehensive consideration of the complex factors in the furnace environment, such as fuel characteristics, physicochemical properties of OCs, impurities of OCs, potential downstream industries and their own processing. Therefore, the selection and low-cost utilization of OCs under different OCAC application scenarios require specific case analysis with contributions from diverse areas.

### 3.6 Characteristic Properties of OC

The selection of an OC is mainly determined by its reactivity, its price and whether it is suitable for long-term operation. General, important criteria for a good OC are as followed: (1) low production cost; (2) high reactivity with fuel and oxygen; (3) low fragmentation and attrition, as well as low tendency for agglomeration [64]. In the existing studies of OCAC, the selected OC is frequently ilmenite ore, manganese ore, and steel slag, of which ilmenite ore was used in most cases. Ilmenite ore is widely used by researchers due to its low price, acceptable reactivity, and good resistance to sintering and wear in fluidized beds [13, 29, 41, 59]. The disadvantages of manganese ore and steel slag are that they are easy to wear and have low reactivity.

In addition, the research on OC characteristics has accumulated a good knowledge in the CLC technology [65–68], which can provide a strong guarantee for the application of OCAC, including various natural ores and synthetic oxygen carriers. The choice of bed material needs to consider the reactivity of the OC and the mechanical properties (wear resistance), economy, and whether it will have other effects on the safe and efficient operation of the system. For the application of natural ore/synthetic materials with moderate reactivity but low cost, the product gas can also be regulated by controlling the addition amount of OC and adjusting the operation mode (such as adjusting the fluidization state). Overall, the bed material should be selected based on a comprehensive consideration of various characteristics of the material and the operating characteristics of the boiler, rather than a single characteristic such as reactivity, oxygen-carrying capacity and cost.

## References

1. Thunman H, Lind F, Breitholtz C, Berguerand N, Seemann M (2013) Using an oxygen-carrier as bed material for combustion of biomass in a 12-MWth circulating fluidized-bed boiler. *Fuel* 113:300–309
2. Chadeesingh DR, Hayhurst AN (2014) The combustion of a fuel-rich mixture of methane and air in a bubbling fluidised bed of silica sand at 700°C and also with particles of Fe<sub>2</sub>O<sub>3</sub> or Fe present. *Fuel* 127:169–177
3. Källén M, Rydén M, Lind F (2015) Improved performance in fluidised bed combustion by the use of manganese ore as active bed material. In: 22nd international conference on fluidized bed conversion, 14–17 June 2015
4. Pour N, Zhao D, Schwebel G, Leion H, Lind F, Thunman H (2014) Laboratory fluidized bed testing of ilmenite as bed material for oxygen carrier aided combustion (OCAC)
5. Wang P, Leion H, Yang H (2017) Oxygen-carrier-aided combustion in a bench-scale fluidized bed. *Energy Fuels* 31:6463–6471
6. Schneider T, Krumrein J, Müller D, Karl J (2021) Investigation of the oxygen supply and distribution in a bubbling fluidized bed by using natural ilmenite for oxygen carrier aided combustion. *Energy Fuels* 35:12352–12366
7. Garcia E, Liu H (2022) Ilmenite as alternative bed material for the combustion of coal and biomass blends in a fluidised bed combustor to improve combustion performance and reduce agglomeration tendency. *Energy* 239:121913
8. Corcoran A, Marinkovic J, Lind F, Thunman H, Knutsson P, Seemann M (2014) Ash properties of ilmenite used as bed material for combustion of biomass in a circulating fluidized bed boiler. *Energy Fuels* 28:7672–7679
9. Rydén M, Hanning M, Corcoran A, Lind F (2016) Oxygen carrier aided combustion (OCAC) of wood chips in a semi-commercial circulating fluidized bed boiler using manganese ore as bed material. *Appl Sci* 6:347
10. Lind F, Corcoran A, Thunman H (2017) Validation of the oxygen buffering ability of bed materials used for OCAC in a large scale CFB boiler. *Powder Technol* 316:462–468
11. Rydén M, Hanning M, Lind F (2018) Oxygen carrier aided combustion (OCAC) of wood chips in a 12 MWth circulating fluidized bed boiler using steel converter slag as bed material. *Applied Sciences* 8
12. Corcoran A, Knutsson P, Lind F, Thunman H (2018) Comparing the structural development of sand and rock ilmenite during long-term exposure in a biomass fired 12MWth CFB-boiler. *Fuel Process Technol* 171:39–44
13. Corcoran A, Knutsson P, Lind F, Thunman H (2018) Mechanism for migration and layer growth of biomass ash on ilmenite used for oxygen carrier aided combustion. *Energy Fuels* 32:8845–8856
14. Hanning M, Corcoran A, Lind F, Rydén M (2018) Biomass ash interactions with a manganese ore used as oxygen-carrying bed material in a 12 MWth CFB boiler. *Biomass Bioenerg* 119:179–190
15. Hildor F, Mattisson T, Leion H, Linderholm C, Rydén M (2019) Steel converter slag as an oxygen carrier in a 12 MWth CFB boiler—ash interaction and material evolution. *Int J Greenhouse Gas Control* 88:321–331
16. Vigoureux M, Knutsson P, Lind F (2020) Sulfur uptake during oxygen-carrier-aided combustion with ilmenite. *Energy Fuels* 34:7735–7742
17. Lind F, Corcoran A, Andersson B-Å, Thunman H (2017) 12,000 hours of operation with oxygen-carriers in industrially relevant scale. *VGB Power Tach*
18. Moldenhauer P, Corcoran A, Thunman H, Lind F (2018) A scale-up project for operating a 115 MWth biomass-fired CFB boiler with oxygen carriers as bed material. In: 5th international conference on chemical looping, Park City, Utah, USA
19. Hayhurst AN (1991) Does carbon monoxide burn inside a fluidized bed? A new model for the combustion of coal char particles in fluidized beds. *Combust Flame* 85:155–168

20. Żukowski W (2002) The pressure pulses generated by the combustion of natural gas in bubbling fluidized beds. *Combust Flame* 130:15–26
21. Chadeesingh DR, Hayhurst AN (2019) The combustion of mixtures of methane and air in bubbling fluidized beds of hot sand. In: Proceedings of the 19th international conference on fluidized bed combustion
22. Dennis JS, Hayhurst AN, Mackley IG (1982) The ignition and combustion of propane/air mixtures in a fluidised bed. *Symposium (International) on Combustion* 19:1205–1212
23. Kassman H, Båfver L, Åmand L-E (2010) The importance of SO<sub>2</sub> and SO<sub>3</sub> for sulphation of gaseous KCl—an experimental investigation in a biomass fired CFB boiler. *Combust Flame* 157:1649–1657
24. Lindau L, Skog E (2003) CO-Reduktion i FB-Panna via Dosering AV Elementärt Svavel; Värmeforsk Rapport 812; Värmeforsk: Stockholm, Sweden (in Swedish)
25. Kassman HA, Carlsson C, Björklund J, Strömberg U, Strömberg B (2005) Minskade Utsläpp av CO Och NOx Genom Dosering AV Ammoniumsulfat i Förbränningsrummet; Värmeforsk Rapport 908; Värmeforsk: Stockholm, Sweden (in Swedish)
26. Hayhurst AN, Lawrence AD (1997) The reduction of the nitrogen oxides NO and N<sub>2</sub>O to molecular nitrogen in the presence of iron, its oxides, and carbon monoxide in a hot fluidized bed. *Combust Flame* 110:351–365
27. Hayhurst AN, Ninomiya Y (1998) Kinetics of the conversion of NO to N<sub>2</sub> during the oxidation of iron particles by NO in a hot fluidised bed. *Chem Eng Sci* 53:1481–1489
28. Basu P (2013) Fluidized bed boilers: design and application
29. Cuadrat A, Abad A, Adánez J, de Diego LF, García-Labiano F, Gayán P (2012) Behavior of ilmenite as oxygen carrier in chemical-looping combustion. *Fuel Process Technol* 94:101–112
30. Rana S, Sun Z, Mehrani P, Hughes R, Macchi A (2019) Ilmenite oxidation kinetics for pressurized chemical looping combustion of natural gas. *Appl Energy* 238:747–759
31. Lasek JA (2014) Investigations of the reduction of NO to N<sub>2</sub> by reaction with Fe under fuel-rich and oxidative atmosphere. *Heat Mass Transf* 50:933–943
32. Anthony EJ, Granatstein DL (2001) Sulfation phenomena in fluidized bed combustion systems. *Prog Energy Combust Sci* 27:215–236
33. Belo LP, Elliott LK, Stanger RJ, Spörl R, Shah KV, Maier J et al (2014) High-temperature conversion of SO<sub>2</sub> to SO<sub>3</sub>: homogeneous experiments and catalytic effect of fly ash from air and oxy-fuel firing. *Energy Fuels* 28:7243–7251
34. Jørgensen TL, Livbjerg H, Glarborg P (2007) Homogeneous and heterogeneously catalyzed oxidation of SO<sub>2</sub>. *Chem Eng Sci* 62:4496–4499
35. Spörl R, Maier J, Scheffknecht G (2013) Sulphur oxide emissions from dust-fired oxy-fuel combustion of coal. *Energy Procedia*. 37:1435–1447
36. Fleig D, Alzueta MU, Normann F, Abián M, Andersson K, Johnsson F (2013) Measurement and modeling of sulfur trioxide formation in a flow reactor under post-flame conditions. *Combust Flame* 160:1142–1151
37. Anthony EJ (1995) Fluidized bed combustion of alternative solid fuels; status, successes and problems of the technology. *Prog Energy Combust Sci* 21:239–268
38. Vassilev SV, Baxter D, Andersen LK, Vassileva CG (2013) An overview of the composition and application of biomass ash. Part 1. Phase–mineral and chemical composition and classification. *Fuel* 105:40–76
39. Boström D, Skoglund N, Grimm A, Boman C, Öhman M, Broström M et al (2012) Ash transformation chemistry during combustion of biomass. *Energy Fuels* 26:85–93
40. Hupa M (2012) Ash-related issues in fluidized-bed combustion of biomasses: recent research highlights. *Energy Fuels* 26:4–14
41. Gyllén A (2019) Oxygen carrier aided combustion: implementation of oxygen carriers to existing industrial settings. Doctoral dissertation, Chalmers University of Technology
42. Morris JD, Daood SS, Chilton S, Nimmo W (2018) Mechanisms and mitigation of agglomeration during fluidized bed combustion of biomass: a review. *Fuel* 230:452–473
43. Chirone R, Miccio F, Scala F (2006) Mechanism and prediction of bed agglomeration during fluidized bed combustion of a biomass fuel: effect of the reactor scale. *Chem Eng J* 123:71–80

44. Scala F, Chirone R (2006) Characterization and early detection of bed agglomeration during the fluidized bed combustion of Olive Husk. *Energy Fuels* 20:120–132
45. Brus E, Öhman M, Nordin A (2005) Mechanisms of bed agglomeration during fluidized-bed combustion of biomass fuels. *Energy Fuels* 19:825–832
46. Öhman M, Pommer L, Nordin A (2005) Bed agglomeration characteristics and mechanisms during gasification and combustion of biomass fuels. *Energy Fuels* 19:1742–1748
47. Störner F, Lind F, Rydén M (2021) Oxygen carrier aided combustion in fluidized bed boilers in Sweden—review and future outlook with respect to affordable bed materials. *Appl Sci* 11(17):7935
48. Öhman M, Nordin A, Skrifvars B-J, Backman R, Hupa M (2000) Bed agglomeration characteristics during fluidized bed combustion of biomass fuels. *Energy Fuels* 14:169–178
49. Zeevenhoven-Onderwater M, Öhman M, Skrifvars B-J, Backman R, Nordin A, Hupa M (2006) Bed agglomeration characteristics of wood-derived fuels in FBC. *Energy Fuels* 20:818–824
50. Visser HJM, Kiel JHA, Veringa HJ (2004) The influence of fuel composition on agglomeration behaviour in fluidised-bed combustion. Delft: Energy research Centre of the Netherlands ECN
51. Kirnbauer F, Hofbauer H (2011) Investigations on bed material changes in a dual fluidized bed steam gasification plant in Güssing, Austria. *Energy Fuels* 25:3793–3798
52. Grimm A, Öhman M, Lindberg T, Fredriksson A, Boström D (2012) Bed agglomeration characteristics in fluidized-bed combustion of biomass fuels using olivine as bed material. *Energy Fuels* 26:4550–4559
53. Kuba M, He H, Kirnbauer F, Skoglund N, Boström D, Öhman M et al (2016) Mechanism of layer formation on olivine bed particles in industrial-scale dual fluid bed gasification of wood. *Energy Fuels* 30:7410–7418
54. Azis M, Leion H, Jerndal E, Steenari B-M, Mattisson T, Lyngfelt A (2013) The effect of bituminous and lignite ash on the performance of ilmenite as oxygen carrier in chemical-looping combustion. *Chem Eng Technol* 36:1460–1468
55. Bao J, Li Z, Cai N (2014) Interaction between iron-based oxygen carrier and four coal ashes during chemical looping combustion. *Appl Energy* 115:549–558
56. Dai J, Whitty KJ (2019) Predicting and alleviating coal ash-induced deactivation of CuO as an oxygen carrier for chemical looping with oxygen uncoupling. *Fuel* 241:1214–1222
57. Cuadrat A, Abad A, García-Labiano F, Gayán P, de Diego LF, Adánez J (2011) The use of ilmenite as oxygen-carrier in a 500Wth chemical-looping coal combustion unit. *Int J Greenhouse Gas Control* 5:1630–1642
58. Adánez J, Cuadrat A, Abad A, Gayán P, de Diego LF, García-Labiano F (2010) Ilmenite activation during consecutive redox cycles in chemical-looping combustion. *Energy Fuels* 24:1402–1413
59. Gyllén A, Knutsson P, Lind F, Thunman H (2020) Magnetic separation of ilmenite used as oxygen carrier during combustion of biomass and the effect of ash layer buildup on its activity and mechanical strength. *Fuel* 269:117470
60. He H, Skoglund N, Öhman M (2017) Time-dependent crack layer formation in quartz bed particles during fluidized bed combustion of woody biomass. *Energy Fuels* 31:1672–1677
61. Knutsson P, Linderholm C (2015) Characterization of ilmenite used as oxygen carrier in a 100kW chemical-looping combustor for solid fuels. *Appl Energy* 157:368–373
62. Mathekgä H, Oboirien B, North BC (2016) A review of oxy-fuel combustion in fluidized bed reactors. *Int J Energy Res* 40:878–902
63. Lind F, Israelsson M, Thunman H (2017) Magnetic separation for the recirculation of oxygen active bed materials when combusting municipal solid waste in large scale CFB boilers. In: *Proceedings of the clear water clean energy conference*
64. Lyngfelt A (2014) Chemical-looping combustion of solid fuels—status of development. *Appl Energy* 113:1869–1873
65. Adanez J, Abad A, Garcia-Labiano F, Gayan P, de Diego LF (2012) Progress in chemical-looping combustion and reforming technologies. *Prog Energy Combust Sci* 38:215–282
66. Zhao X, Zhou H, Sikarwar V, Zhao M, Park A, Fennell P, Shen L, Fan L (2017) Biomass-based chemical looping technologies: the good, the bad and the future. *Energy Environmental Science*. 10:1885–1910

67. Mattison T (2013) Materials for chemical-looping with oxygen uncoupling. *ISRN Chemical Engineering* 3:526375
68. Nandy A, Loha C, Gu S, Sarkar P, Karmakar M, Chatterjee P (2016) Present status and overview of chemical looping combustion technology. *Renew Sustain Energy Rev* 59:597–619

**Open Access** This chapter is licensed under the terms of the Creative Commons Attribution 4.0 International License (<http://creativecommons.org/licenses/by/4.0/>), which permits use, sharing, adaptation, distribution and reproduction in any medium or format, as long as you give appropriate credit to the original author(s) and the source, provide a link to the Creative Commons license and indicate if changes were made.

The images or other third party material in this chapter are included in the chapter's Creative Commons license, unless indicated otherwise in a credit line to the material. If material is not included in the chapter's Creative Commons license and your intended use is not permitted by statutory regulation or exceeds the permitted use, you will need to obtain permission directly from the copyright holder.



# Chapter 4

## OCAC Technology in Oxy-Fuel Combustion for Carbon Capture



Oxy-fuel combustion is regarded as one of the most promising carbon capture and storage (CCS) technologies to mitigate the climate change, which has been widely studied and demonstrated in academia and industry [1–3]. In the oxy-fuel process, a mixture of recycled flue gas and pure O<sub>2</sub> obtained from an air separation unit (ASU) is introduced into the combustion chamber to replace air as oxidant gas. Therefore, high concentration of CO<sub>2</sub> can be obtained in flue gas, which is suitable for the subsequent carbon storage and utilization, the schematic diagram of oxy-fuel combustion system is shown in Fig. 4.1. It also has other advantages, such as low NO<sub>x</sub> emission, easy scale-up, and applicability in existing power plant [4, 5].

However, the intensive energy consumption associated with the ASU is the bottleneck limiting its further commercialization [2, 6]. The systematic analysis through process simulation has shown that the energy consumption of ASU is about 61.5 MW<sub>th</sub>, accounting for ~15.9% energy of a 388 MW<sub>th</sub> coal-firing oxy-fuel boiler (as shown in Fig. 4.2) [7]. As stated in the earlier sections, the OCAC process has a proven advantage of burning fuel at lower oxygen-fuel ratio compared to conventional FBCs. In addition, because the recirculation brings oxygen to the furnace adding to the new oxygen from outside, the oxy-fuel boiler using flue-gas recirculation may have a very low over-all oxygen excess. There is an overall oxygen stoichiometric factor and an internal oxygen stoichiometric factor, the latter is always larger than the overall factor [8]. Therefore, the combination of oxy-fuel combustion and the OCAC technology, i.e. oxygen-carrier-aided oxy-fuel combustion (oxy-fuel-OCAC), can be expected to improve the utilization of O<sub>2</sub>, leading to less energy consumption from the ASU.

At present, the only oxy-fuel-OCAC studies were carried out by the fluidized-bed conversion and gasification (FBC&G) group from CanmetENERGY in a 50 kW<sub>th</sub> CFB combustor (Fig. 4.3) [9–11]. Different factors including the type of fuels (coal, biomass and natural gas), the bed materials (quartz sand, olivine sand, ilmenite ore or their mixture), O<sub>2</sub> concentration in flue gas (2, 5 and 8%), the bed temperature (800, 850 and 900 °C) and Ca/S ratio (0 and 2) have been systematically analyzed in both bubbling and circulating fluidizing modes (Tables 4.1 and 4.2).



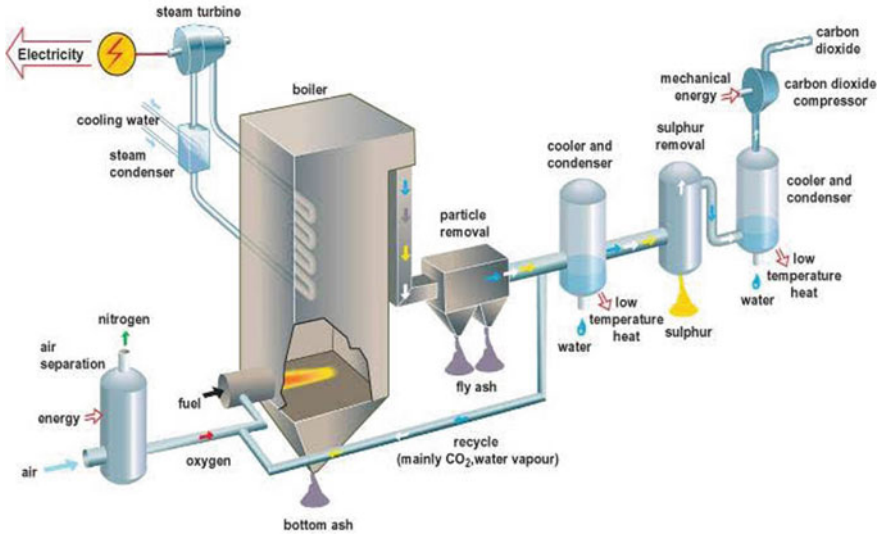


Fig. 4.1 Schematic of the oxy-fuel combustion

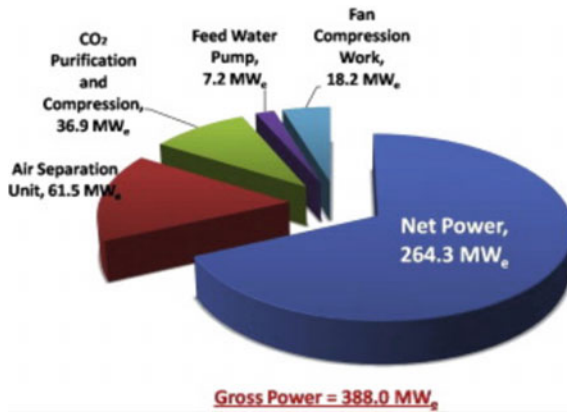
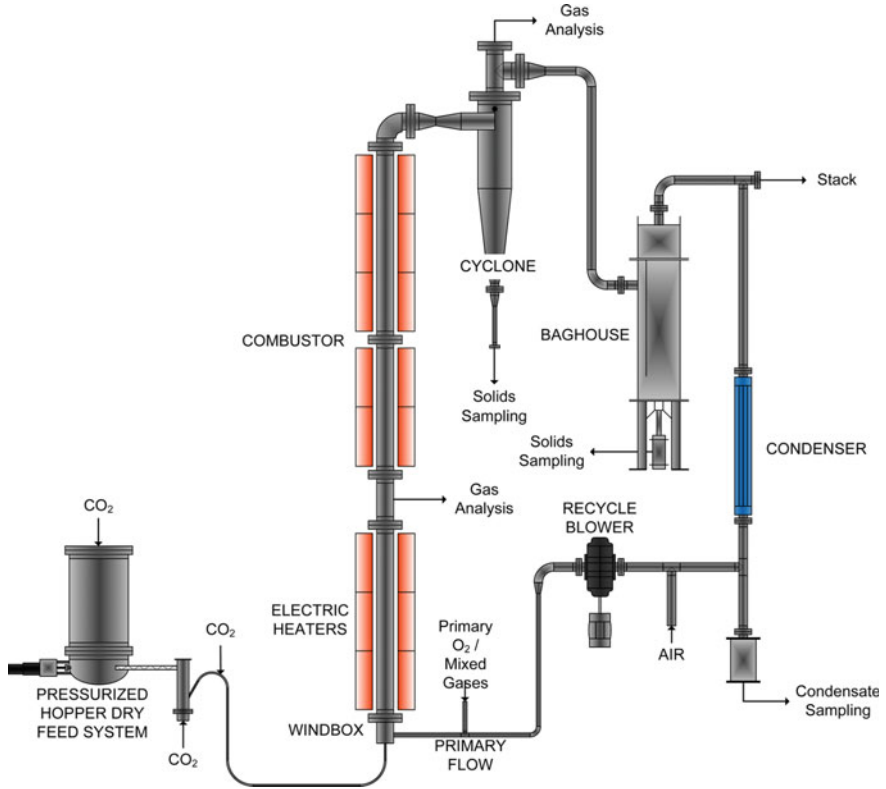


Fig. 4.2 Net power and parasitic power demand of the oxy-fuel power cycle (reprinted from [7] with permission of Elsevier)

### 4.1 Combustion Performance

The typical temperature profiles when burning coal with different bed are shown in Fig. 4.4. The research results of oxy-fuel-OCAC show that the fluctuation of reactor temperature profile using ilmenite ore as the bed material was less than that using quartz sand [9], suggesting that oxy-fuel-OCAC was beneficial to obtain an evenly distributed furnace temperature. The unburned species (CO and C<sub>x</sub>H<sub>y</sub>) emissions



**Fig. 4.3** Schematic of the 50 kW<sub>th</sub> Oxy-FBC of CanmetENERGY (reprinted from [9] with permission of American Chemical Society)

**Table 4.1** Test matrix (adapted from [9])

Test ID	Solid fuel	Bed material	Limestone coinjection	Temperature (°C)	O <sub>2</sub> in flue gas, dry basis, vol.%
1	Highvale	Quartz	N	850	1-3, 4-6, 7-9
2	Highvale	Ilmenite	N	850	1-3, 4-6, 7-9
3	Highvale	Spent Mix (1:1)	N	850	1-3, 4-6, 7-9
4	Polar River	Spent Mix (1:1)	Y	800, 850, 900	1-3, 4-6
5	Polar River	Ilmenite	Y	800, 850, 900	1-3, 4-6
6	Polar River	Quartz	Y	800, 850, 900	1-3, 4-6
7	Polar River	Fresh Mix (1:1)	Y	800, 850, 900	1-3, 4-6

**Table 4.2** Operating parameters (adapted from [9])

	Ilmenite	Sand	Mix (1:1)
Size range, $\mu\text{m}$	643 (425–869)	706 (600–1040)	676 (425–1040)
Density, $\text{kg/m}^3$	4330	2445	3388
Umf, m/s	0.37	0.36	0.36
U/Umf	6.76	6.67	6.67
Temperature ( $^{\circ}\text{C}$ )		800, 850, 900	
Combustion mode		Oxy-fired	
O <sub>2</sub> in flue gas, vol.%		2, 5, 8	
Pulv. Coal size, micron		~ 70	
Feul feed rate, kg/h		4.6–6.1	
Recycled flue gas, kmol/h		0.48–0.62	
Pure O <sub>2</sub> , kmol/h		0.22–0.25	
Sorbent		KK Karson Limestone	
Ca/S		2 (with Polar River only)	

were significantly reduced by replacing the quartz sand with the ilmenite ore. Using ilmenite ore as bed material to replace the quartz sand, the CO concentration in the flue gas was reduced by 30% when burning Highvale coal and 13% for Poplar River coal, and the hydrocarbons, i.e. CH<sub>4</sub> and C<sub>2</sub>H<sub>4</sub>, measured above the bed were also reduced by almost 50% for both coals [9]. By measuring the unburned species at the top of the bed and cyclone, it was found that the improvement on combustion was even more pronounced in the dense phase than that in the dilute phase using OCAC, in particular under conditions with low O<sub>2</sub> in flue gas or low bed temperature (as shown in Fig. 4.5). When bed material was switched from quartz sand to ilmenite ore, at the case of 2.5% O<sub>2</sub> in the flue gas, a 50% reduction of CO concentration occurred at the top of the bed. If the O<sub>2</sub> in the flue gas was increased to 5%, the reduction in CO concentration was 40%, and finally, there was almost no observed reduction of CO concentration when O<sub>2</sub> in the flue gas was 8%. This is because the reaction rate of CO with gaseous oxygen is much faster than that with the OCs. Therefore, gaseous O<sub>2</sub> tends to be the control factor in the overall rate of CO conversion in the high O<sub>2</sub> concentration case. Similar conclusion was also drawn from the oxy-fuel-OCAC experiments using natural gas and biomass as the fuels [11].

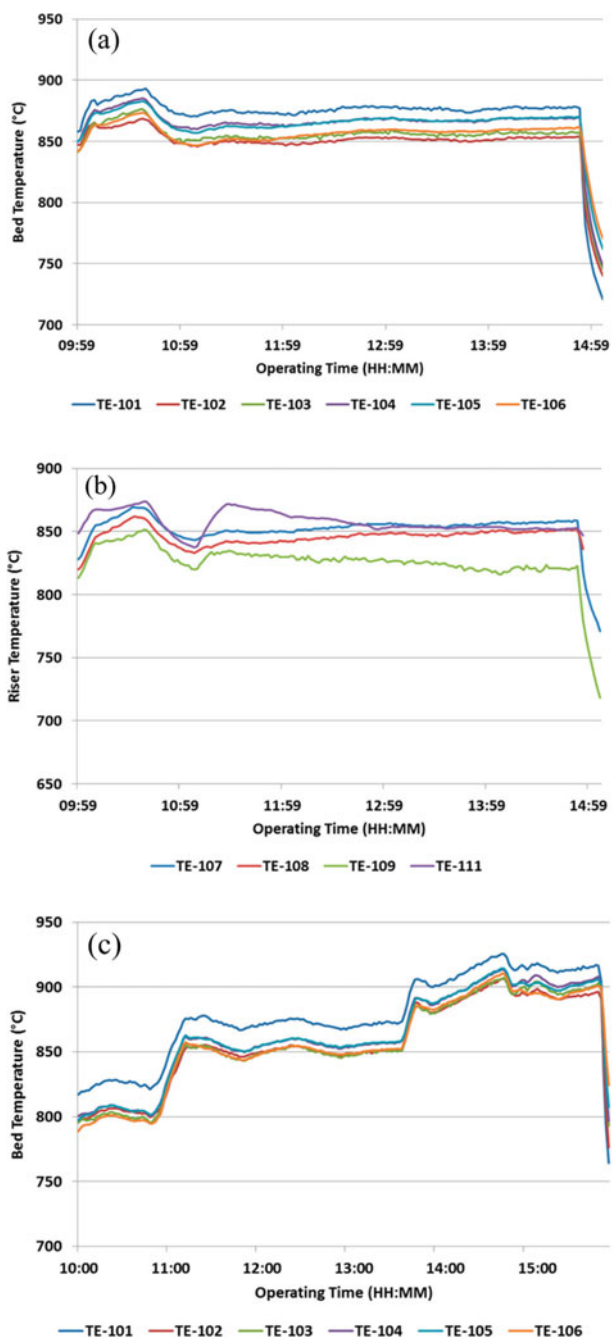
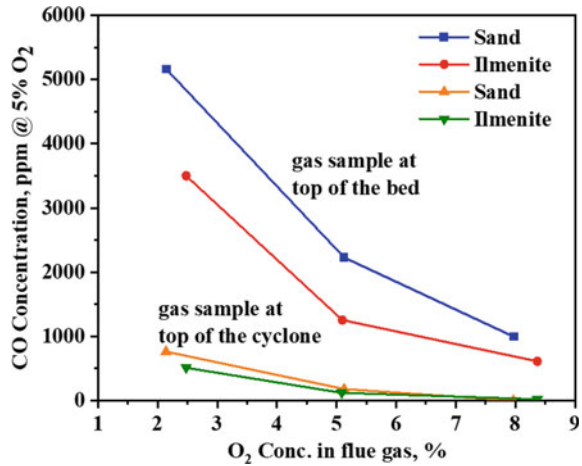


**Fig. 4.4** Temperature profiles when burning coal with different bed: **a** in the bed (sand bed, highvale coal), **b** in the riser (sand bed, Highvale coal) and **c** in the bed (ilmenite bed, Poplar River coal) (reprinted from [9] with permission of American Chemical Society)

**Fig. 4.5** CO emission from burning Highvale coal (adapted from [9])



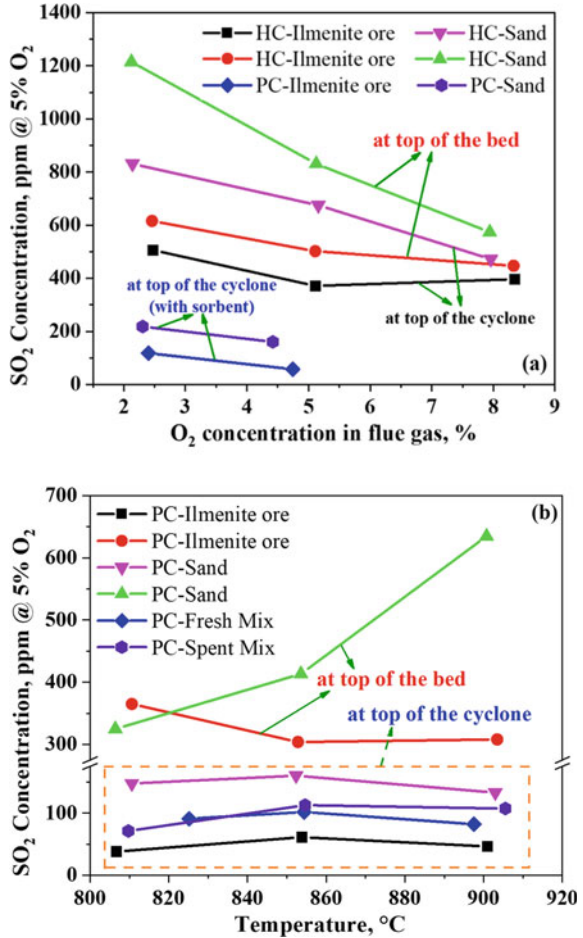
## 4.2 Emissions

### 4.2.1 SO<sub>2</sub> Emission and Desulfurization

Figure 4.6 shows the SO<sub>2</sub> emissions in the different operation conditions of oxy-fuel-OCAC. When the quartz sand as bed material was replaced by ilmenite ore, the SO<sub>2</sub> concentration at the top of the bed and cyclone both always became lower, regardless of the bed temperature, the exhaust oxygen concentration, and the use of a desulfurizer [10]. Under the condition of low exhaust oxygen concentration, the inhibition effect of ilmenite ore on the SO<sub>2</sub> emission was more significant. When the bed materials were all ilmenite ores, the SO<sub>2</sub> emission was reduced by more than 60% at different bed temperatures compared to the usage of quartz sand as bed material. Under the same mixing ratio (1:1) of quartz sand and ilmenite ore, the fresh ilmenite ore was more beneficial to the reduction of the SO<sub>2</sub> emission than the used one. When desulfurizer was introduced during the OC aided oxy-fuel combustion process, the process with ilmenite ore as bed material also obtained a lower SO<sub>2</sub> emission in comparison to the case of quartz sand.

The existing study [10] only gave the variation rules of SO<sub>2</sub> emissions in OCAC conditions, but the potential mechanisms of SO<sub>2</sub> emission and desulfurization in oxy-fuel-OCAC was not clear. Combining with the mechanisms of SO<sub>2</sub> reduction proposed in Ref. [10], it may be speculated that the low SO<sub>2</sub> emissions in oxy-fuel-OCAC process depend on three factors. Firstly, the ash-related components on the surface of and inside the OC particles can absorb sulfur [12], thereby reducing the SO<sub>2</sub> emission. Secondly, the addition of OCs leads to more uniformly distributed bed temperature and oxygen concentration, which may potentially reduce the absorption of SO<sub>2</sub>. Finally, more uniform oxygen distribution can promote direct desulfurization and indirect desulfurization according to Reactions 3.3 and 3.4, thus improving the

**Fig. 4.6** SO<sub>2</sub> emissions in different operating condition. HC and PC are Highvale coal and Poplar River coal (adapted from [10])

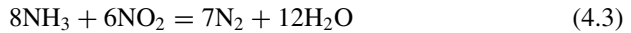
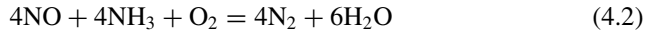
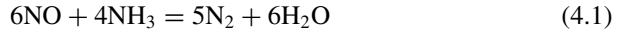


desulfurization efficiency and reducing the SO<sub>2</sub> emission. Further investigations in this subject are highly desired to validate these hypotheses.

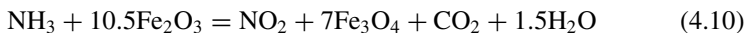
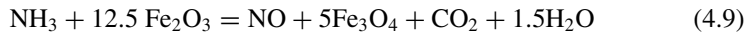
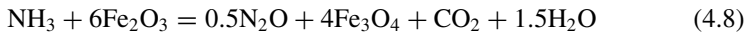
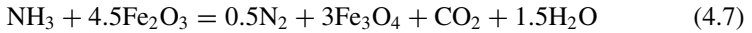
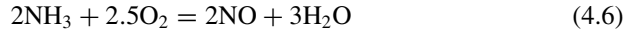
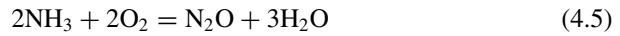
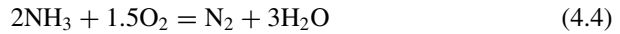
### 4.2.2 NO<sub>x</sub> and N<sub>2</sub>O Emission

Lu et al. [10] investigated the NO<sub>x</sub> and N<sub>2</sub>O emissions in oxy-fuel combustion in the presence of OCAC in the plant of Fig. 4.7. They found that the NO<sub>x</sub> concentration increased significantly at different measured locations at various temperatures and exhaust oxygen concentrations. They assumed that the CO and hydrocarbons concentrations in the boiler decreased in the OCAC condition, which will weaken the reduction of NO<sub>x</sub> through gas-phase reaction. Meanwhile, OC may reduce the

concentration of ammonia (from the volatiles) in the dense-phase zone, thus reducing the reduction of  $\text{NO}_x$  by  $\text{NH}_3$  in the recirculated flue gas (via Reactions 4.1–4.3), resulting in a higher  $\text{NO}_x$  emission. Lu et al. [10] measured the composition of flue gas and found that the exhaust  $\text{NH}_3$  concentration was reduced for oxy-fuel-OCAC compared to the case of using quartz sands as bed materials [13, 14].



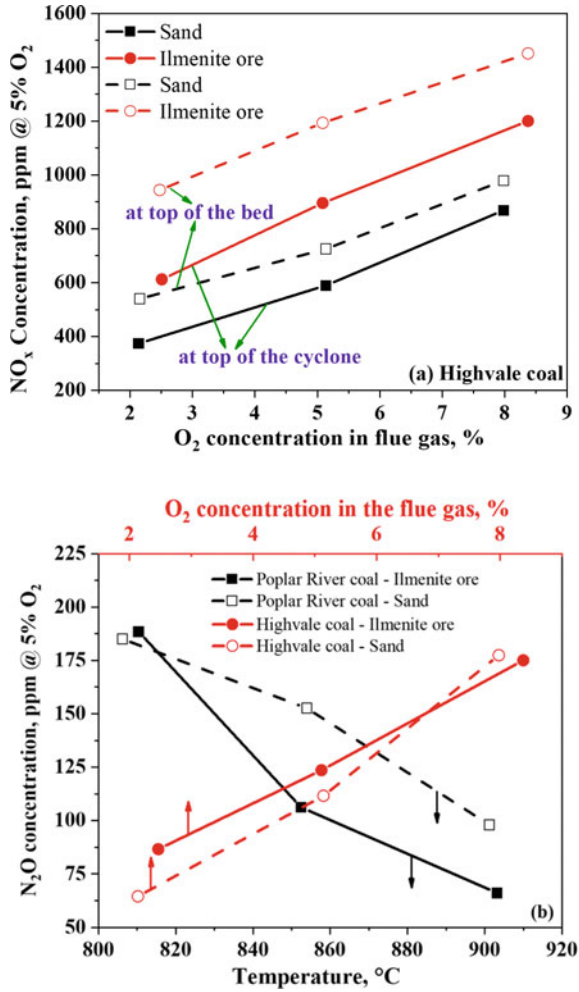
On the other hand,  $\text{NH}_3$  not only can participate in the Reactions 4.1–4.3 in CFB boilers, but it also may be oxidized by  $\text{O}_2$  and OCs, resulting in a high  $\text{NO}_x$  emission. Taking iron-based OC as an example, the possible reactions are as suggested as follows [15–19]:



Several studies [15–19] have also shown that OCs can oxidize HCN, another typical  $\text{NO}_x$  precursor, into  $\text{N}_2$ ,  $\text{N}_2\text{O}$ ,  $\text{NO}$  and  $\text{NO}_2$  (4.4–4.10). Therefore, more uniform oxygen distribution under oxy-fuel-OCAC operation may reduce the formation of  $\text{NH}_3$  and HCN, which in turn promote the generation of  $\text{NO}_x$ .

No matter whether OCs or inert silica sand were used as bed materials, the  $\text{N}_2\text{O}$  emission always decreased with the increase of bed temperature, while it increased with the increase of exhaust oxygen concentration. At high exhaust  $\text{O}_2$  concentration and low bed temperature,  $\text{N}_2\text{O}$  emission is slightly lower in the case of oxy-fuel-OCAC than that of using quartz sand, and vice versa [10]. It should be noted that

**Fig. 4.7**  $\text{NO}_x$  and  $\text{N}_2\text{O}$  emissions in different operating conditions. **a**  $\text{NO}$  emission from Highvale coal at constant temperature. **b**  $\text{N}_2\text{O}$  from Highvale and Poplar River coals at constant  $\text{O}_2$  in the stack (adapted from [10])



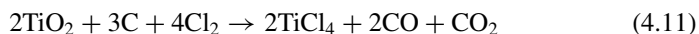
the  $\text{N}_2\text{O}$  concentration was measured and the difference in  $\text{N}_2\text{O}$  emissions were very small between the two bed-material cases.

Since  $\text{N}_2\text{O}$  can be decomposed at high temperature, the main parameter affecting  $\text{N}_2\text{O}$  emission under oxy-fuel-OCAC process during FBC is still dominated by temperature [10]. Although higher temperature can reduce  $\text{N}_2\text{O}$  emissions, it will also enhance the generation of  $\text{NO}_x$  and reduce the desulfurization efficiency of the boiler. Thus, it is hard to simultaneously reduce  $\text{N}_2\text{O}$  and  $\text{NO}_x$  emissions via variation of the combustion temperature [20–22]. In addition, compared with quartz sand as bed material, the oxy-fuel-OCAC enables to operate the boiler at a lower excess air, i.e. exit  $\text{O}_2$  concentration, which is also expected to make the boiler achieve lower  $\text{N}_2\text{O}$  emissions.



### 4.2.3 Condensate Liquid Analysis

Lu et al. [10] also analyzed the liquid discharged from the front cooling of the recycle blower, the analysis results are shown in Table 4.3. It was found that all the samples were acidic with pH values ranging from 2.32 to 2.62. The pH value of the aqueous condensate from the oxy-fuel-OCAC case was slightly higher than that from using silica sand, which may help to alleviate the corrosion of the heat-exchanger surface. The main components in the aqueous condensate were sulfate (180 mg/L to 270 mg/L) and chlorides (9.6–50.7 mg/L) accounting for approximately 90 wt% of dissolved species, with the coexistence of fluorides and bromines (<0.5 mg/L). There is no obvious change in the content of the sulfate condensate between conventional combustion and oxy-fuel-OCAC. However, the concentration of the chlorides in the condensate varies significantly between the two cases. The aqueous condensate generated from the oxy-fuel-OCAC case was reduced by more than 50% compared to that from conventional combustion. This might be due to the reaction between  $\text{Cl}_2$  and  $\text{TiO}_2$  following the reaction [23]:



Reaction 4.11 is a part of the process for producing  $\text{TiO}_2$  from ilmenite by using chlorine as the oxidant [24]. This process is typically performed in a fluidized bed at 900–1000 °C, and coke needs to be added to the bed inventory to generate a reducing atmosphere, which is very close to the dense-bed environment during fluidized-bed combustion. The product,  $\text{TiCl}_4$ , is a hazardous volatile gas pollutant, whose boiling point is 136 °C. Whether the OCAC technology using ilmenite ore as bed material causes an emission of  $\text{TiCl}_4$  into the atmosphere or not needs to be further evaluated by specific experiments.

The effect of the chlorine content on the corrosion and ash deposition of the boiler's heat exchanger tubes is particularly significant [25, 26]. In severe cases, it

**Table 4.3** Condensate analysis (adapted from [9])

Sample ID		Test #1	Test #2	Test #3	Test #4	Test #5	Test #6
Coal		Highvale	Highvale	Highvale	Polar river	Polar river	Polar river
Bed material		Sand	Ilmenite	Mix (1:1)	Mix (1:1)	Sand	Ilmenite
Parameter	Method				mg/L		
Sulfate	In-house	270	240	250	190	180	220
Chloride	In-house	38.5	18.0	50.7	22.9	20.9	9.6
Fluoride	In-house	0.31	0.23	0.35	0.17	0.11	0.15
Bromine	In-house	0.18	0.24	0.48	0.20	0.13	0.15
pH	–	2.32	2.62	2.36	2.44	2.44	2.52

may cause an unplanned shutdown of the boiler. Although it is known that the oxy-fuel-OCAC technology using ilmenite ore as bed material can significantly reduce the emission of chlorides, many aspects need to be further clarified. The generation of potentially harmful substances should be investigated in detail. In addition, OC-based bed materials other than ilmenite ore should be screened to find the best option to achieve low chloride emission. Nevertheless, control of Cl emission could be a key feature of oxy-fuel-OCAC technology, especially for burning fuels with high chlorine content, such as MSW.

### 4.3 Bed Material Analysis

Hughes et al. [9] have analyzed the OC bed materials (ilmenite ore) by *in-situ* sampling the bed particles followed by XRD characterization, the analysis results are shown in Table 4.4. It was found that the crystallinity of the used ilmenite ore was about 30–36% after oxy-fuel-OCAC, far lower than that in the original material (65–75%). The used ilmenite ore may have better reactivity, as the amorphous-phase species in the ilmenite ore are usually more reactive [27, 28]. In addition, under the operating conditions of low exhaust O<sub>2</sub> concentration and bed temperature, higher concentrations of FeTiO<sub>3</sub> and FeO were found in the bed material, which were the reduced phases of Fe<sub>2</sub>TiO<sub>5</sub> and Fe<sub>2</sub>O<sub>3</sub>, respectively. It suggests that the OC-based bed material indeed participates in the redox reactions during the oxy-fuel-OCAC process, especially at low temperature and exhaust O<sub>2</sub> concentration.

**Table 4.4** XRD analysis of bed samples (adapted from [9])

Sample ID		Test#1	Test#2	Test#3	Test#4
Coal		Highvale	Highvale	Poplar River	Poplar River
Bed temperature	°C	858	862	807	901
O <sub>2</sub> in flue gas	%	2.5	5.0	4.7	5.3
Chemical compound			% Chemical compound		
Pseudobrookite, syn	TiFe <sub>2</sub> O <sub>5</sub>	1.1	16.8	3.7	16.0
Rutile, syn	TiO <sub>2</sub>	1.5	0.8	1.2	1.0
Hematite, syn	Fe <sub>2</sub> O <sub>3</sub>	3.0	8.4	2.2	5.6
Ilmenite, syn	Fe TiO <sub>3</sub>	23.8	7.1	19.1	7.0
Gehlenite, syn	Ca <sub>2</sub> (Al(AlSi)O <sub>7</sub> )			1.1	2.2
Magnesioferrite, syn	MgFe <sub>2</sub> O <sub>4</sub>	3.6	2.8	2.1	1.7
Crystalline (%)		32.9	36.0	29.5	33.5
Amorphous (%)		67.1	64.0	70.5	66.5

The tested coal in the above-mentioned studies contains a high concentration of Na [9]. A high content of Na in the ash is likely to cause problems related to bed agglomeration and fouling downstream [29, 30]. However, no Na-related compounds were found in the solid samples from the bed, which indicates the potential for Na release to the downstream. During the experiments, no hot spots and defluidization were found in the bed. After SEM analysis, it was found that the bed material did not show any signs of agglomeration. This indicates that the OCAC technology has a good applicability in burning high Na-content coal, and that there is no agglomeration problem or Na-induced deactivation of the oxygen carrier. This is beneficial for burning high-sodium coal. The Na-based salts have an important influence on the formation of atmospheric particulate matter (PM) and the formation of ash deposits on the heat-exchanger surface. The effect of the OCAC technology on the PM formation, ash deposition and corrosion is still unclear, which is worthy a detailed investigation.

## References

1. Chen L, Yong SZ, Ghoniem AF (2012) Oxy-fuel combustion of pulverized coal: characterization, fundamentals, stabilization and CFD modeling. *Prog Energy Combust Sci* 38(2):156–214
2. Toftegaard MB, Brix J, Jensen PA, Glarborg P, Jensen AD (2010) Oxy-fuel combustion of solid fuels. *Prog Energy Combust Sci* 36:581–625
3. Buhre BJP, Elliott LK, Sheng CD, Gupta RP, Wall TF (2005) Oxy-fuel combustion technology for coal-fired power generation. *Prog Energy Combust Sci* 31:283–307
4. Duan L, Sun H, Zhao C, Zhou W, Chen X (2014) Coal combustion characteristics on an oxy-fuel circulating fluidized bed combustor with warm flue gas recycle. *Fuel* 127:47–51
5. Kunze C, Spliethoff H (2012) Assessment of oxy-fuel, pre- and post-combustion-based carbon capture for future IGCC plants. *Appl Energy* 94:109–116
6. Escudero AI, Espatolero S, Romeo LM, Lara Y, Paufigue C, Lesort A-L et al (2016) Minimization of CO<sub>2</sub> capture energy penalty in second generation oxy-fuel power plants. *Appl Therm Eng* 103:274–281
7. Hong J, Chaudhry G, Brisson JG, Field R, Gazzino M, Ghoniem AF (2009) Analysis of oxy-fuel combustion power cycle utilizing a pressurized coal combustor. *Energy* 34:1332–1340
8. Leckner B, Gómez-Barea A (2014) Oxy-fuel combustion in circulating fluidized bed boilers. *Appl Energy* 125:308–318
9. Hughes R, Lu D, Symonds RT (2017) Improvement of Oxy-FBC using oxygen carriers: concept and combustion performance. *Energy Fuels* 31:10101–10115
10. Lu D (2018) Enhancement combustion performance and emission control in Oxy-FBC using oxygen carriers. In: 76th IEA-FBC meeting, Seoul, Korea, 13 May 2018
11. Loscertales M, Lu D, Li L, Hughes R (2020) Investigation of OCAC using Canadian ilmenite ore in a circulating fluidized bed combustor. In: 13th international conference on fluidized bed technology (CFB-13), Vancouver, Canada, 11–15 May 2020
12. Vigoureux M, Knutsson P, Lind F (2020) Sulfur uptake during oxygen-carrier-aided combustion with ilmenite. *Energy Fuels* 34:7735–7742
13. Lyon RK, Benn D (1979) Kinetics of the NO–NH<sub>3</sub>–O<sub>2</sub> reaction. *Symposium (International) on Combustion* 17:601–610
14. Mahmoudi S, Baeyens J, Seville JPK (2010) NO<sub>x</sub> formation and selective non-catalytic reduction (SNCR) in a fluidized bed combustor of biomass. *Biomass Bioenerg* 34:1393–1409
15. Song T, Shen L, Xiao J, Chen D, Gu H, Zhang S (2012) Nitrogen transfer of fuel-N in chemical looping combustion. *Combust Flame* 159:1286–1295

16. Song T, Guo W, Shen L (2015) Fuel nitrogen conversion in chemical looping with oxygen uncoupling of coal with a CuO-based oxygen carrier. *Energy Fuels* 29:3820–3832
17. Hayashi J-I, Kusakabe K, Morooka S, Nielsen M, Furimsky E (1995) Role of iron catalyst impregnated by solvent swelling method in pyrolytic removal of coal nitrogen. *Energy Fuels* 9:1028–1034
18. Ohtsuka Y, Mori H, Nonaka K, Watanabe T, Asami K (1993) Selective conversion of coal nitrogen to N<sub>2</sub> with iron. *Energy Fuels* 7:1095–1096
19. Ohtsuka Y, Furimsky E (1995) Effect of ultrafine iron and mineral matter on conversion of nitrogen and carbon during pyrolysis and gasification of coal. *Energy Fuels* 9:141–147
20. Hayhurst AN, Lawrence AD (1992) Emissions of nitrous oxide from combustion sources. *Prog Energy Combust Sci* 18:529–552
21. Shen BX, Mi T, Liu DC, Feng B, Yao Q, Winter F (2003) N<sub>2</sub>O emission under fluidized bed combustion condition. *Fuel Process Technol* 84:13–21
22. Hou X, Zhang H, Yang S, Lyu J, Yue G (2008) N<sub>2</sub>O decomposition over the circulating ashes from coal-fired CFB boilers. *Chem Eng J* 140:43–51
23. Gázquez MJ, Bolívar J, García-Tenorio R, Vaca GF (2014) A review of the production cycle of titanium dioxide pigment. *Mater Sci Appl* 05:441–458
24. McNulty GS (2011) Production of titanium dioxide. Plenary lecture NORM V international conference, vol 2007. Sevilla, 19–22 March 2007, pp 169–188
25. Nielsen HP, Frandsen FJ, Dam-Johansen K, Baxter LL (2000) The implications of chlorine-associated corrosion on the operation of biomass-fired boilers. *Prog Energy Combust Sci* 26:283–298
26. Wang Y, Ma H, Liang Z, Chen H, Zhao Q, Jin X (2016) Experimental study on dew point corrosion characteristics of the heating surface in a 65 t/h biomass-fired circulating fluidized bed boiler. *Appl Therm Eng* 96:76–82
27. Masumoto T, Hashimoto K, Komiyama H (1986) Catalytic properties of amorphous alloys. In: Amorphous metals and semiconductors, pp 431–434
28. Indra A, Menezes PW, Sahraie NR, Bergmann A, Das C, Tallarida M, Schmeisser D, Strasser P, Driess M (2014) Unification of catalytic water oxidation and oxygen reduction reactions: amorphous beat crystalline cobalt iron oxides. *J Am Chem Soc* 136:17530–17536
29. Morris JD, Daood SS, Chilton S, Nimmo W (2018) Mechanisms and mitigation of agglomeration during fluidized bed combustion of biomass: a review. *Fuel* 230:452–473
30. Chen S, Yu R, Soomro A, Xiang W (2019) Thermodynamic assessment and optimization of a pressurized fluidized bed oxy-fuel combustion power plant with CO<sub>2</sub> capture. *Energy* 175:445–455

**Open Access** This chapter is licensed under the terms of the Creative Commons Attribution 4.0 International License (<http://creativecommons.org/licenses/by/4.0/>), which permits use, sharing, adaptation, distribution and reproduction in any medium or format, as long as you give appropriate credit to the original author(s) and the source, provide a link to the Creative Commons license and indicate if changes were made.

The images or other third party material in this chapter are included in the chapter's Creative Commons license, unless indicated otherwise in a credit line to the material. If material is not included in the chapter's Creative Commons license and your intended use is not permitted by statutory regulation or exceeds the permitted use, you will need to obtain permission directly from the copyright holder.



# Chapter 5

## Oxygen Carrier Aided Gasification (OCAG)



Gasification is regarded as an effective clean utilization technology of solid fuel (especially for coal, biomass and solid waste), which can convert the chemical energy of solid fuel into gaseous fuel [1–4]. However, the primary gas products contain not only the essential gas products (such as CO, H<sub>2</sub>, CO<sub>2</sub>, CH<sub>4</sub> and light hydrocarbons), but also an unacceptable amount of condensable hydrocarbons, which are often referred to as tars. The tars will begin to condense at 350 °C [5], and will cause operational problems such as blockage of downstream equipment during gasification.

Tars are included in a comprehensive classification of complex mixtures of hydrocarbons from 1 to 5-ring aromatic compounds, oxygen and sulfur-containing hydrocarbons [1, 4]. The presence of tar components preclude raw gas from being used directly as fuel for gas turbines and internal combustion engines, or as a chemical feedstock. Consequently, the primary gas after gasification needs to be upgraded to gaseous products suitable for combustion and chemical applications. At present, a large number of research and review papers [3, 6–10] have been published in the field of tar removal and gas product regulation, among which the primary and secondary techniques associated with catalytic tar reforming are considered as one of the most promising hot gas cleaning methods. The primary tar cleaning has been included in the existing gasification process through the catalytic bed material to promote tars cracking, and the secondary tar cleaning needs to be carried out on the fixed bed or fluidized bed downstream of the gasifier. These can significantly reduce tar content and improve the flexibility of process optimization and gas regulation [1, 8, 10–12]. However, the activity of catalysts generally declines over time, as they will be poisoned by prolonged exposure to an atmosphere containing elements such as sulfur, chlorine and alkali metals (which are all present to varying degrees in the raw gas) [10]. In addition, under the condition of high tar content, carbon deposition may form on the surface of catalyst, which leads to the deactivation of catalyst [10, 13, 14].

## 5.1 The Proposed of Technical Routes

In 2011, Fredrik et al. [15, 16] proposed a new technique route for secondary catalytic tar cleaning (as shown in Fig. 5.1), which is performed in a dual fluidized bed reactor system that simultaneously removes carbon deposits on the catalyst surfaces, even at high tar contents. The new process can be applied to all types of biomass gasifiers, regardless of whether the gasifier technique includes primary measures for tar reduction or not.

The system in Fig. 5.1 consists of two reactors and two loop seals. The two reactor, one is regenerator reactor, also referred to as the air reactor (AR), the fluidizing agent is air; another is reformer reactor, also called the fuel reactor (FR), which is fluidized by the raw gas. The two loop seals are fluidized with inert gas or steam to ensure the circulation of the OC and prevent cross contamination of the gases in different reactor. In the FR, the metal oxide ( $Me_xO_y$ ) as an oxygen supplier, catalyst and heat carrier for partial oxidation reaction and reforming reactions of the tar components.

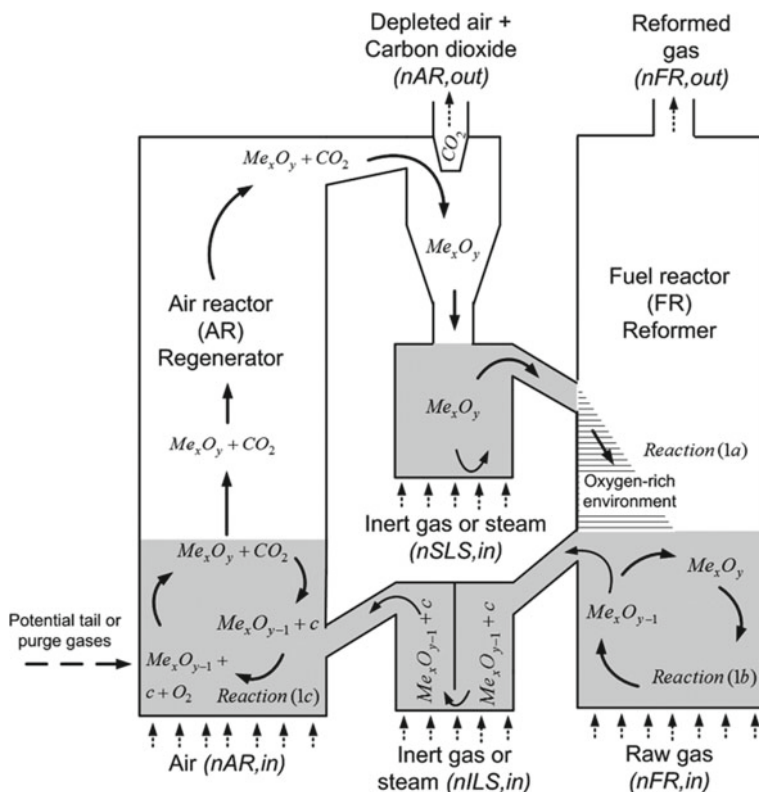
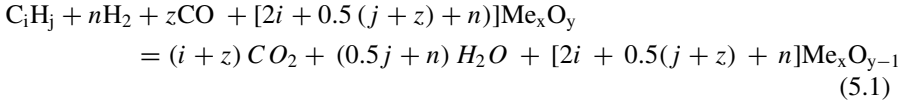
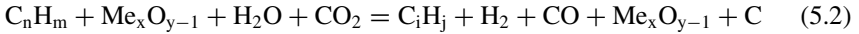


**Fig. 5.1** New concept for secondary upgrading of biomass producer gas (reprinted from [16] with permission of American Chemical Society)

The part or all of the  $\text{Me}_x\text{O}_y$  is reduced to  $\text{Me}_x\text{O}_{y-1}$  by hydrocarbons ( $\text{C}_i\text{H}_j$ ),  $\text{H}_2$ , and  $\text{CO}$  [16]:



The  $\text{Me}_x\text{O}_{y-1}$  in the bed acts as a catalyst for reforming the tars ( $\text{C}_n\text{H}_m$ ) in the presence of reforming media (such as  $\text{H}_2\text{O}$  and  $\text{CO}_2$  in the raw gas), the reactions can be simplified as [16]:



In addition to the desired tar-reforming reaction, the carbon generated by the additional carbonization reaction will be deposited on the surface of OC particles. While the  $\text{Me}_x\text{O}_{y-1}$  moves into AR,  $\text{Me}_x\text{O}_{y-1}$  will be oxidized to  $\text{Me}_x\text{O}_y$ , and the carbon on the surface of OC particles will be eliminated by oxidation. Both of these reactions are exothermic. At this point, OC particles as a heat carrier will bring heat to FR for the catalytic cracking of tar components. The regeneration of oxygen carriers and oxygen transport can effectively remove the tar, which also provides the possibility for the development of new catalytic bed materials. This technology can achieve many advantages: (1) even using natural oxygen carrier ore as the bed material can still significantly reduce the tar content in the product gas. (2) the deactivation of catalyst caused by carbon deposition is avoided and the reaction efficiency of the system is improved; (3) widened the selectivity of OC or catalyst, natural ore or synthetic catalyst can be selected according to product gas demand, providing the possibility to reduce catalyst cost; (4) more flexible product gas regulation capacity; (5) the tar cleaning system can be thermally integrated with the gasifier outlet temperature, which leads to minimal heat losses.

Vienna University of Technology [17–21] has proposed a dual fluidized bed (DFB) gasification technology (the basic principle is shown in Fig. 5.2) to reduce the tar in product gas, and designed and built a 100 kW<sub>th</sub> pilot plant (the schematic diagram is shown in Fig. 5.3). Gasification reaction (in a bubbling bed) and combustion process (in fast fluidized bed) take place in separate reactors, which are thermally connected by a circulating bed material. The fuel is fed into the gasification reactor to react with the gasification agent to form product gas, and the residual char is transported to the combustion reactor along with the bottom bed material. The char is burned in an air reactor and releases heat to heat the bed materials, then hot bed material is captured by the separator and returned to the gasification reactor to provide heat for the gasification reaction (endothermic) [21]. The two reactors produce two different flows: product gas and conventional flue gas. In this technology route, the bed material is used to transfer heat, and when the catalyst is added to the bed material, it can significantly promote the cracking of tars while avoiding the carbon deposition problem of the catalyst.

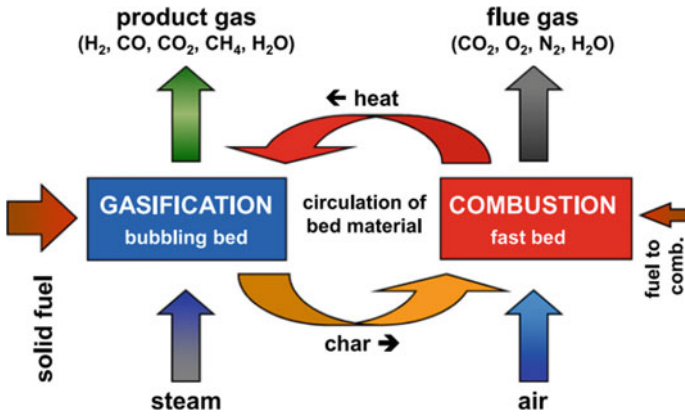


**Fig. 5.2** The schematic diagram of the DFB gasification technology (reprinted from [21] with permission of Elsevier)

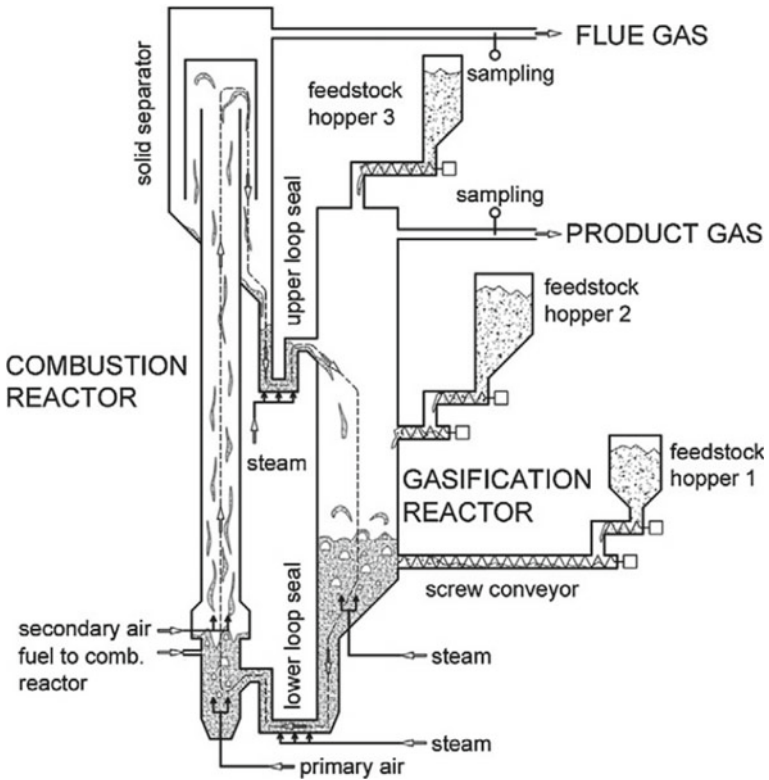


**Fig. 5.3** The schematic diagram of Vienna University of Technology's 100 kW<sub>th</sub> pilot plant (reprinted from [21] with permission of Elsevier)



The oxygen carrier particles of natural ores (such as ilmenite ore and manganese ore) not only can transport oxygen, but also contain various metal elements that can be used as catalysts for tar cracking. Therefore, introduce the OCs to complete or partial replace inert bed materials may not only provide a cheap catalyst for the technology, but also complete the transfer of oxygen between the two reactors. It should be noted that the activity of OC ore as a catalyst may be significantly lower than that of synthetic catalysts, but synthetic catalysts in operation are generally expensive and the proportion of catalyst added in the bed is generally low, while the addition of OC ore can be up to 100%. Increasing the concentration of OC ore may make up for the relatively poor catalytic activity. Therefore, the diversity of the selection of bed material combination provides enterprises with the possibility of efficient and low-cost operation, which greatly improve the flexibility of operation.

## 5.2 Gasification/Reforming Characteristics

### 5.2.1 OC Aided Tar Reforming

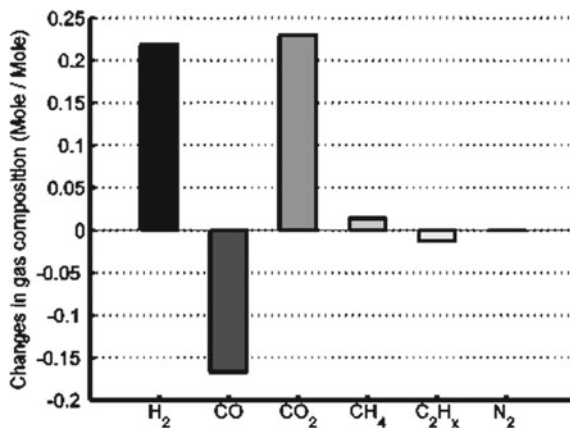
Lind et al. [15] used ilmenite ( $\text{FeTiO}_3$ ) as the bed material to perform reforming experiments on the raw gas produced by the biomass gasifier, and found that oxygen can be continuously transported by the ilmenite in the system, and verified that the tar-cleaning concept can be achieved. The results show that when the tar content in the produced gas is about  $30 \text{ gtar/Nm}^3$ , the gas residence time of 0.4–0.5 s reduces the total amount of tar by 35% at  $800^\circ\text{C}$  (the tar compositions in raw gas and reformed gas downstream of the CLR-system are shown in Table 5.1). Branched tars and phenol were largely converted to pure aromatic compounds. Ilmenite shows high activity in the water–gas shift reaction (WGSR), the  $\text{H}_2/\text{CO}$  ratio increases from about 0.7 at the reactor inlet to about 3 at the reactor outlet, while a decrease in light hydrocarbons is observed, and the methane content downstream of the reactor system slightly increased (as shown in Fig. 5.4). In addition, carbon deposits on ilmenite were continuously removed by oxidation to  $\text{CO}_2$ . During the operation, inactivation of ilmenite or interference with oxygen transfer was not observed. After that, Lind et al. [16] compared the effects of two kinds of metal oxides, natural ore (ilmenite ore) and synthetic catalyst ( $\text{NiO}/\text{Al}_2\text{O}_3$ ), on the upgrading of gasification product gas at operating temperature from  $700$  to  $880^\circ\text{C}$ . The results showed that both materials have activity against tar decomposition and increase the yield of hydrogen, and the removal of tar and the generation of hydrogen were significantly enhanced with increasing temperature. Although the tar loading in the feed gas is as high as  $30 \text{ gtar/Nm}^3$ , all phenolic compounds and most monocyclic branched tar are decomposed by two catalysts at  $800^\circ\text{C}$ . Based on the calculation of tar to reformed gas, the tar removal efficiency with  $\text{NiO}/\text{Al}_2\text{O}_3$  catalyst and ilmenite ore as bed material were 95% ( $880^\circ\text{C}$ ) and 60% ( $850^\circ\text{C}$ ), respectively (as shown in Fig. 5.5). In addition, the  $\text{NiO}/\text{Al}_2\text{O}_3$  catalyst has rather high activity for tar removal already

at 700 °C. For the ilmenite catalyst, compared to the increase in conversion when the temperature increased from 750 to 800° C, the total tar removal increased by 4 times as the temperature increased from 800 to 850 °C. In general, ilmenite ore have lower activity as tar-cleaning catalysts than NiO/AL<sub>2</sub>O<sub>3</sub> catalysts. Analysis of the effluent stream from the regeneration reactor found that the carbon deposits had been removed from the catalyst, and no deactivation due to coke deposition was detected during the 8-h operation of the system. However, in the above studies, it was found that OC's strong ability to transfer oxygen would lead to a decrease in cool gas yield, which could be adjusted by selecting the appropriate oxygen carrier and adding amount.

**Table 5.1** Compositions in raw gas and reformed gas downstream of the CLR-system (adapted from [15])

Compound	Reference (gasifier) (g <sub>tar</sub> /Nm <sup>3</sup> gas)	Ilmenite 800 °C (g <sub>tar</sub> /Nm <sup>3</sup> gas)	Compound	Reference (gasifier) (g <sub>tar</sub> /Nm <sup>3</sup> gas)	Ilmenite 800 °C (g <sub>tar</sub> /Nm <sup>3</sup> gas)
Phenol	0.98	0.01	2-methylnaphthalene	1.10	0.06
o-cresol	0.03	n.d	1-methylnaphthalene	0.70	0.03
m-cresol	0.15	n.d	Biphenyl	0.47	0.84
p-cresol	0.04	n.d	Acenaphthylene	2.03	0.37
Benzene	0.65	1.90	Acenaphthene	0.13	0.01
Toluene	0.71	0.17	Fluorene	0.65	0.09
m/p-xylene	0.14	n.d	Phenanthrene	1.66	1.45
o-xylene	1.06	0.16	Anthracene	0.29	0.18
Indan	0.05	0.17	Fluorantene	0.41	0.45
Indene	2.94	0.05	Pyrene	0.46	0.42
Naphthalene	7.53	10.77	Unknowns	5.54	0.92
			Total tar	27.70	18.04

**Fig. 5.4** Changes in gas composition between reformed gas and raw gas (reprinted from [15] with permission of American Chemical Society)



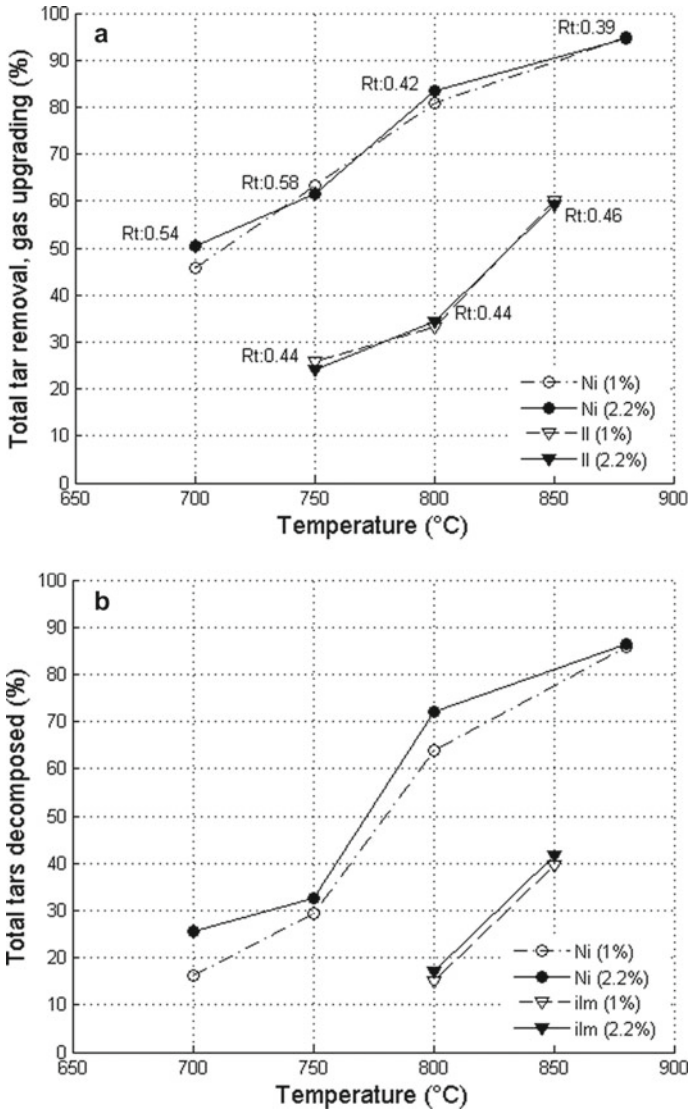
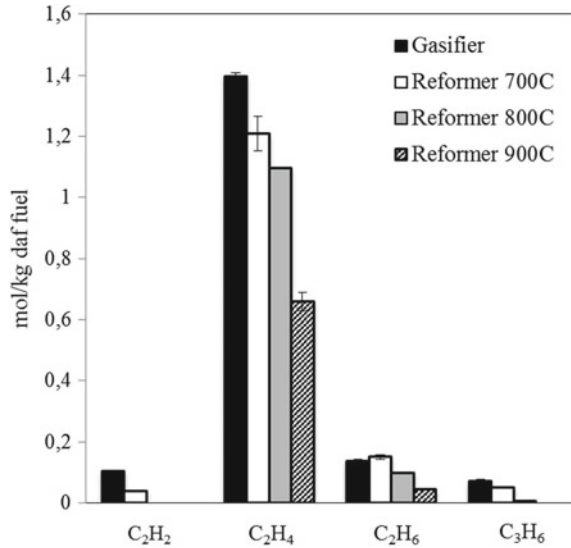


**Fig. 5.5** **a** Percentages of total tar removal in gas upgrading for NiO/Al<sub>2</sub>O<sub>3</sub> and ilmenite (1.0% and 2.2% O<sub>2</sub>), **b** Percentages of total tars decomposed by NiO/Al<sub>2</sub>O<sub>3</sub> and ilmenite (1.0% and 2.2% O<sub>2</sub>) (reprinted from [16] with permission of American Chemical Society)

Berguerand et al. [22] evaluated the upgrading effect of alkali-feldspar [(K, Na)AlSi<sub>3</sub>O<sub>8</sub>] ore as the bed material on gasification product gas in a single bubbling bed reactor. The results indicated that the catalytic cracking capacity of alkali-feldspar ore is higher than that of fresh olivine. Even at low temperature, alkali-feldspar ore can eliminate most of C<sub>2</sub>H<sub>2</sub> and C<sub>3</sub>H<sub>6</sub> (the most problematic compounds in

**Fig. 5.6** Molar yields of permanent gases for the dry raw and reformed gases (reprinted from [22] with permission of Elsevier)



fuel synthesis), and improve the water–gas shift reaction (as shown in Fig. 5.6). However, alkali-feldspar ore as bed material not only cannot reduce the methane concentration in the gas, but also can form methane. Alkali-feldspar ore exhibit a remarkable tar selectivity, which resulted in the reformed gas having exclusively pure ring-compounds. Moreover, the alkali-feldspar ore shows good mechanical properties and is suitable for fluidized bed, and displayed neither bed agglomeration nor loss of activity in a longer reducing periods, despite there was a carbon deposit (which can be easy to oxidized to CO<sub>2</sub>). Furthermore, because (1) even high sulfur content (>100 ppm) in raw gas, the catalytic activity towards hydrocarbon reforming of alkali-feldspar ore is still unaffected; (2) alkali-feldspar ore has a really low oxygen capacity, it is a promising material and very suitable for the application of this technical.

### 5.2.2 OC Aided Gasification

Koppatz et al. [23] investigated the steam gasification behavior of biomass in a 100 kW<sub>th</sub> dual fluidized bed (DFB) reactor system by using olivine and silica sand as bed material. The experimental results found that there is a significant difference in the activity of silica sand and olivine. The application of different bed materials will cause significant change in composition of the product gas, the relevant results as shown in Fig. 5.7. The volume percentages of H<sub>2</sub>, CO, and CO<sub>2</sub> changed by about 5%, 10%, and 10%, respectively. Olivine is thought to increase the product gas yield and H<sub>2</sub> yield by promoting the CO shift reaction. In addition, it was also found that the application of olivine can change the yield and composition of tar.

Compared with silica sand as bed material, the GC/MS detectable tar and grav. detectable tars yield of product gas in olivine case were reduced by about 35% and 60% respectively. By analyzing the condensable hydrocarbons (see Table 5.2), the result of tar groups distribution at 850 °C as shown in Table 5.3. It can be found that the relative fractions of primary, secondary and tertiary tars are not shifted, and 40–45% (olivine) and 31–33% (silica sand) of naphthalene was found in GC/MS tar complex. This is because under olivine condition, the higher hydrocarbons can be rapidly catalyzed to decompose and lead to the formation of Class IV tars, while silica sand has no catalytic effect on this process.

**Fig. 5.7** Gas composition (main components) versus different solid inventories (reprinted from [23] with permission of Elsevier)

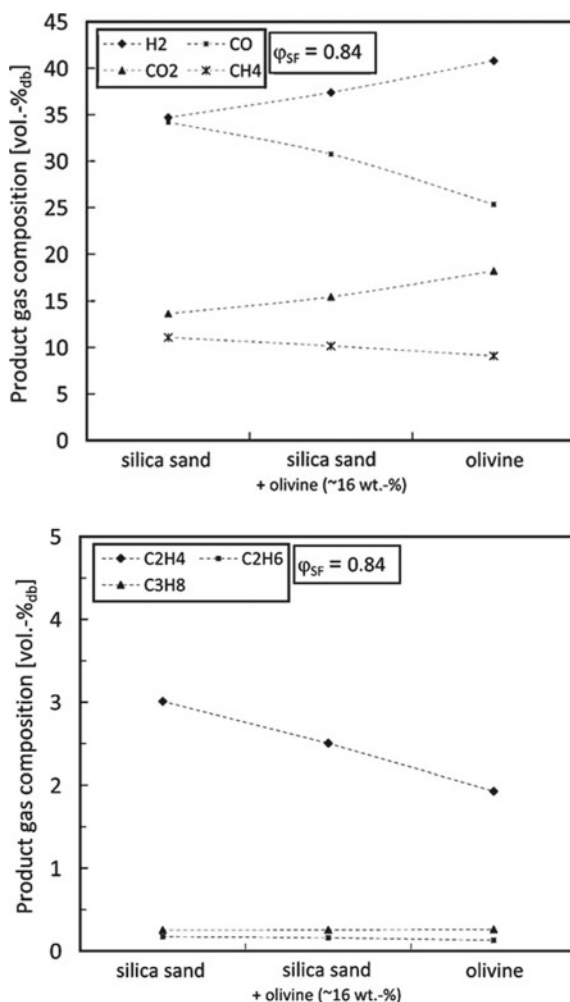


**Table 5.2** Detected GC/MS species and grouping according to ECN and Milne et al. classification (adapted from [24–26])

GC/MS species	ECN class	Milned <sup>a</sup>	GC/MS species	ECN class	Milned <sup>a</sup>
Phenol	Class II	p/s	Acenaphtene	Class IV	t
2-Methylphenol	(heterocyclic aromatic)	p/s	Anthracene	(light PAH, 2,3 ring)	t
4-Methylphenol		p/s	Phenanthrene		t
Benzofuran		s	Dibenzofuran		s
1H-indene		s/t	Fluorene		t
Isoeugenol		p	Fluoranthene		t
Isoquinoline		s	4,5-Methylphenanthrene		s
Quinoline		s	9-Methylanthracene		t
Styrene	Class III	s/t	Pyrene	Class V	t
Mesitylene	(1 ring aromatic)	t	Benzo(a)anthracene	(heavy PAH, > 3 ring)	t
Phenylacetylene		t	Chrysene		t
Naphthalene	Class IV	s/t	Benzo(b)fluoranthene		t
2-Methylnaphthalene	(light PAH, 2,3 ring)	s	Benzo(k)fluoranthene		t
1-Methylnaphthalene		s	Benzo(ghi)perylene		t
Biphenyl		s	Benzo(a)pyrene		t
Acenaphthylene		t	Indeno[1,2,3]pyren		t

<sup>a</sup>Classification: p, primary; s, secondary; t, tertiary

**Table 5.3** Distribution of tar groups at a temperature of 850 °C (adapted from [23])

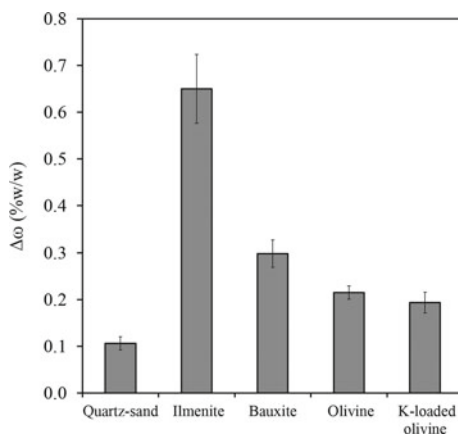
Classification/group	Unit	Olivine	Silica sand
Primary	[wt%]	1–5	3–5
Secondary	[wt%]	6–10	8–9
Tertiary	[wt%]	87–93	85–86
Class II	[wt%]	15–22	23–27
Class III	[wt%]	4–5	6–7
Class IV	[wt%]	70–76	62–66
Class V	[wt%]	<4	2–4

Larsson et al. [26], Marinkovic et al. [27] and Vilches et al. [28] have used different kinds of bed material (ilmenite, olivine, bauxite, quartz sand) in the Chalmers University of Technology's 2–4 MW<sub>th</sub> dual fluidized bed biomass gasifier system to decrease the yield of tar. Larsson et al. [26] found that adding 12% ilmenite in the bed could reduce the tar yield by about 50% (mass), but the proportion of heavy tars in gas was increased, which may increase the dew point of the tar mixture. The transport of oxygen resulted in a decrease in the chemical efficiency of the gasifier and the calorific value of the product gas. Compared with the case of 100% silica sand as the bed material, the cold gas efficiency in ilmenite (12%) case decreased by about 10%, and the calorific value of the gas decreased from about 17 MJ/Nm<sup>3</sup> (sand case) to 12.5 MJ/Nm<sup>3</sup> (12% ilmenite case). In addition, the effect of adding ilmenite is highly dependent on the gasifier's operating conditions. With the increase of fluidizing velocity, the promotion of ilmenite on WGSR was enhanced due to the improvement of gas–solid mixing, while the tar-cracking reaction was weakened and the levels of heavy components was increased. Overall, ilmenite as a bed material seems promising to reduce the tar yield in gasifier, but oxygen delivery levels need to be limited. Marinkovic et al. [27] using olivine as a bed material to continuously run the gasifier for 9 days, the results showed that a gradual decrease in tar content was observed from the second day of operation (the bed material first showed signs of activation), and the tar yield on the fourth day was 30% lower than the first day. The activated olivine significantly increased the production of H<sub>2</sub> with a maximum H<sub>2</sub>/CO ratio of 1.7. Obviously, in order to maximize the use of activated olivine as bed material to improve the gasification process, the activation process of olivine should be fully understood. Although the olivine has been widely used and studied, there is still uncertainty about the nature of its driving force for activation. In addition, the study also pointed out that the proportion of inorganics (from the ash of fuel) in the system also has a decisive influence on the final product gas composition and concentration, which will be discussed in detail in Sect. 5.4. Vilches et al. [28] evaluated the performance of four bed materials (olivine, bauxite, quartz sand and ilmenite) in the biomass gasifier, and found that all of the three activity bed material have tar cracking abilities. After one week of operation and exposure to biomass ash, the activities of bauxite and olivine to crack tars were further increased, both materials had catalytic effect on the WGSR, and bauxite shows a stronger ability to increase char conversion than olivine. Additionally, under the same operation, the oxygen carrying capacity of the four bed materials is as follows: quartz-sand < olivine < bauxite < ilmenite, as shown in Fig. 5.8. Interestingly, although the content of Fe in bauxite is lower than that in olivine, bauxite has higher oxygen transport capacity than olivine. This can be partially attributed to the ash load of bed material.

### 5.3 Screening of Bed Materials

Keller et al. [29] carried out screening study of up to 12 bed materials in a bubbling FB reactor with the aim of evaluating a serious of bed materials for tar-cracking

**Fig. 5.8** Oxygen transport capacity of different bed materials after one week of operation, the steam-to-fuel ratios was 0.8 (reprinted from [28] with permission of American Chemical Society)



process. The bed materials were based on the transition metals Mn, Fe, Cu, and Ni, and three of which were natural ores and other nine were synthetic materials. The bubbling bed was a small scale batch-feeding reactor, where allowed the bed materials can be exposed to reforming and regeneration conditions alternately. The conversion of ethylene from outlet of reactor was used as an indicator for the suitability of the bed materials for tar-cracking conversion. The results showed that the natural material bauxite and the synthetic materials  $\text{NiO}/\alpha\text{-Al}_2\text{O}_3$ ,  $\text{CuO}/\text{MgAl}_2\text{O}_4$ , and  $\text{La}_{0.8}\text{Sr}_{0.2}\text{FeO}_3/\gamma\text{-Al}_2\text{O}_3$  all exhibit high ethylene conversion rates (as shown in Fig. 5.9), and these materials have a broad application prospect in OC assisted gasification/reforming technology. The above results only indicate the catalytic reactivity sequence of the materials, but do not mean that the materials with low reactivity cannot be used in fluidized bed gasification reactors. Because the choice of catalytic bed material not only needs to consider the reactivity of the bed material, but also needs to consider the mechanical properties (wear resistance), economy and whether will have other effects on the safe and efficient operation of the system.

## 5.4 Ash-Related Effects

Kirnbauer et al. [30] studied the long-term changes to the bed material during regular production in a commercial DFB gasification system, the results showed that the elemental composition of the used bed material had a significant increase in calcium and potassium concentration (as shown in Fig. 5.10), two calcium-rich layer formatted on the bed material (as shown in Fig. 5.11), the inner layer consists mainly of calcium silicates while the outer layer has a similar composition to fine ash (as shown in Fig. 5.12 and Table 5.4). The formation of calcium-rich layers is attributed to the high calcium content of wood ash and to the addition of calcium-rich additives to improve the catalytic properties of tar-cracking. Then, Kirnbauer et al. [31]



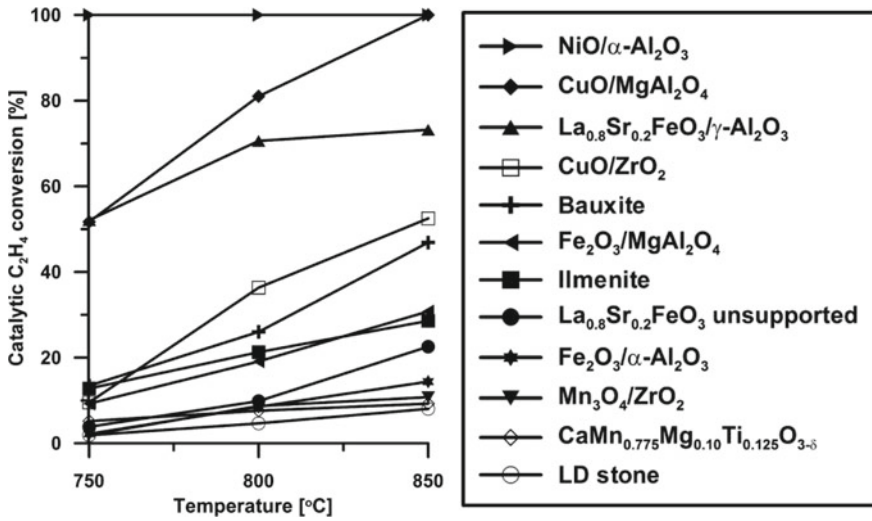
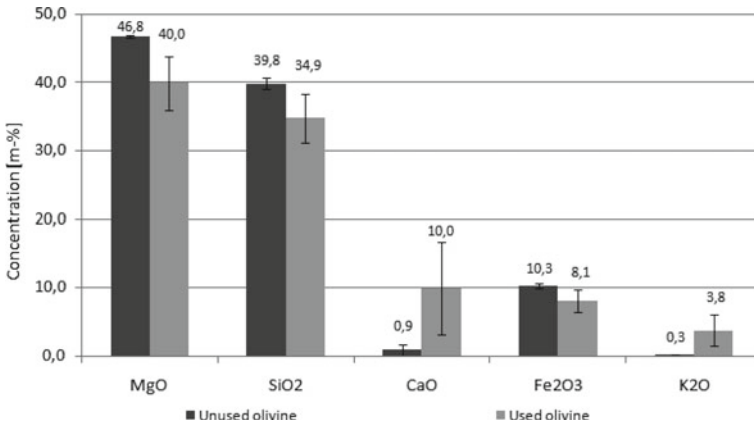


Fig. 5.9 Catalytic ethylene conversion ( $\gamma_{C_2H_4, catalytic}$ ) as a function of operating temperature for different kinds of bed materials (reprinted from [29] with permission of American Chemical Society)

investigated the difference between used olivine (from an industrial-scale plant) and fresh olivine on the gasification properties. The tests were carried out under same operations in a 100 kW<sub>th</sub> pilot plant at the Vienna University of Technology. The results showed that the used bed material can increase the H<sub>2</sub> and CO<sub>2</sub> in the product gas, and the corresponding CO concentration was decreased. Moreover, the used bed material can also enhance the WGSR (Exothermic reaction), thereby reducing the energy requirement for gasification. During the test of the used olivine case, the tar content (detected by GC–MS) was reduced by about 80%, and the analysis of the tar showed fewer components. Furthermore, the results obtained from the used olivine as bed material in the pilot plant of 100 kW<sub>th</sub> were very consistent with the results of the 8 MW<sub>th</sub> industrial plant of Gussing, Austria, and confirming the good scale-up performance from 100 kW to industrial-scale plants.

The enrichment of inorganic materials in the fuel bed has an important effect on the activity of olivine and the entire reaction process. Marinkovic et al. [27] examine the effect of S and SiO<sub>2</sub> on the activity of olivine, S and SiO<sub>2</sub> sand were added to the fuel reactor, respectively, and it was found that the addition of S had a positive effect on the cracking of tars in the gasification product gas, while the addition of SiO<sub>2</sub> had a negative effect on the cracking of tars. This is because the K in the ash of biomass is present in the bed material in the form of leachable. Then the K salts react with S in the combustion reactor to form K<sub>2</sub>SO<sub>4</sub> and migrate to the gasifier. In the reducing atmosphere of the gasifier, K<sub>2</sub>SO<sub>4</sub> can be converted into KOH or K<sub>2</sub>CO<sub>3</sub>, which have catalytic activity for gasification process. The addition of SiO<sub>2</sub> will form inactive potassium silicate with K, which will inhibit the catalytic effect of K on the gasification process, and cannot be attributed to the dilution effect of SiO<sub>2</sub>



**Fig. 5.10** XRF analysis result of unused and used olivine (reprinted from [30] with permission of American Chemical Society)

**Fig. 5.11** SEM images of used olivine (reprinted from [30] with permission of American Chemical Society)

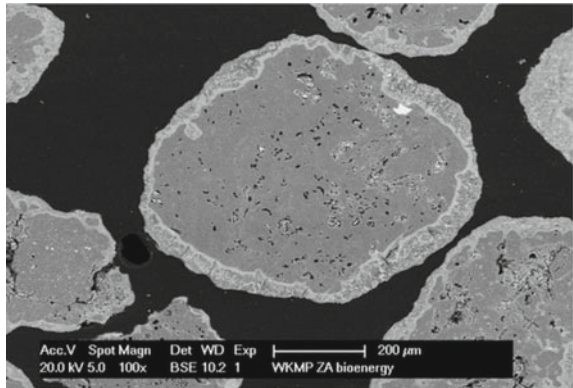


**Fig. 5.12** SEM of inner (1) and outer (2) layers of used olivine (reprinted from [30] with permission of American Chemical Society)

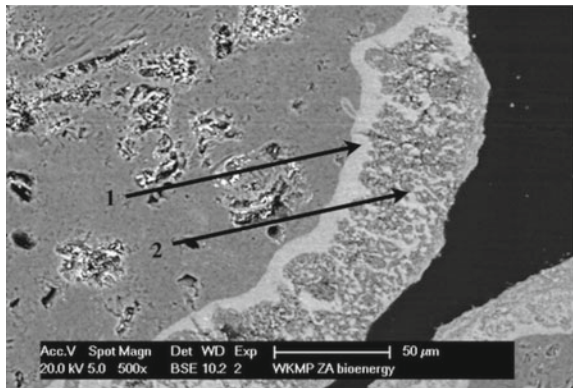


**Table 5.4** The EDS results of unused and used olivine (adapted from [30])

Element	Unused olivine	Used olivine		
	Particle inside (wt%)	Particle inside (wt%)	Inner layer (wt%)	Outer layer (wt%)
C	NA <sup>a</sup>	NA	5.3	9.8
O	15.2	14.2	12.9	13.7
Mg	37.4	30.3	8.6	18.5
Al	0.1	0.7	0.1	0.1
Si	35.5	32.2	17.3	15.4
P	NA	0.0	NA	0.3
K	NA	8.5	2.6	3.2
Ca	NA	1.8	46.5	33.5
Cr	NA	NA	2.7	0.4
Mn	NA	0.0	0.9	1.2
Fe	11.8	12.5	3.0	3.7

<sup>a</sup>Not applicable

particles on the olivine bed material. In addition, the results also proved that the K is a vital active ingredient that promotes the gasification process. Vilches et al. [32] investigated the ability of ash-coated olivine to catalyze the gasification of biomass char in a lab-scale reactor, the olivine bed material has been pre-activated by the addition of S and  $K_2CO_3$  in Chalmers DFB gasifier. The ash layer of olivine can catalyze the steam-char gasification by transferring catalytic potassium (presumably as gaseous KOH) to the char particles. The EDS line-scanning analysis (as shown in Fig. 5.13) of cross-sections of char sample can verify this transfer mechanism. When 40% of ash-coated olivine was used as bed material, higher concentration of K, Ca, S can be found in char (especially near the surface of particle).

In general, the alkali metal substances (especially K) in the biomass ash attached to the surface of the bed material particles have a promoting effect on biomass DFB gasification, including WGSR, char gasification and tar cracking processes. However, high alkali metal of ash-layer on the surface of bed material is often linked to bed agglomeration problems. Moreover, the high alkali metal content in fuels also can cause various ash-related problems during biomass combustion in FB boilers, such as fouling, corrosion and bed agglomeration [33]. When catalytic bed materials and catalytic additives are added to gasifier to reduce the tar yield, the ash characteristics and thermal characteristics may be different from those of combustion reactor, so the ash characteristics and its impact on downstream equipment need to be comprehensive considered.

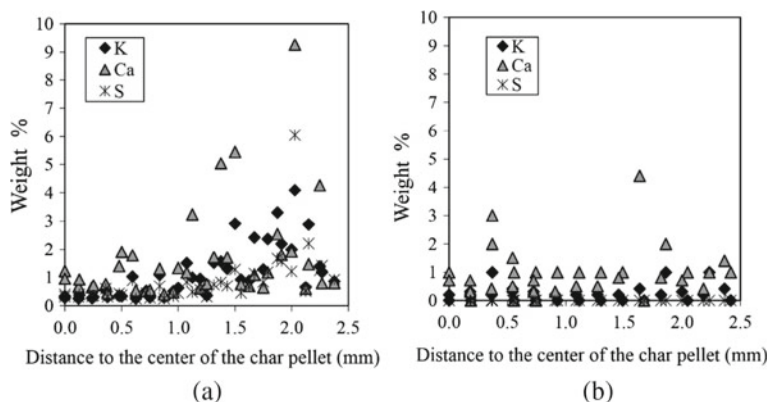


**Fig. 5.13** The EDS analysis of the concentration of K, Ca, and S in the cross-section of char, **a** 40% of ash-coated olivine as bed material; **b** 40% of untreated olivine as bed material (reprinted from [32] with permission of Elsevier)

## References

1. Devi L, Ptasinski KJ, Janssen F (2003) A review of the primary measures for tar elimination in biomass gasification processes. *Biomass Bioenergy* 24(2):125–140
2. Taralas G, Kontominas MG, Kakatsios X (2003) Modeling the thermal destruction of toluene ( $C_7H_8$ ) as tar-related species for fuel gas cleanup. *Energy Fuels* 17(2):329–337
3. Pfeifer C, Hofbauer H (2008) Development of catalytic tar decomposition downstream from a dual fluidized bed biomass steam gasifier. *Powder Technol* 180(1–2):9–16
4. Li CS, Suzuki K (2009) Tar property, analysis, reforming mechanism and model for biomass gasification—an overview. *Renew Sustain Energy Rev* 13(3):594–604
5. Bergman P, van Paasen S, Boerrigter H (2002) The novel “OLGA” technology for complete tar removal from biomass producer gas. In: *Pyrolysis and gasification of biomass and waste, expert meeting*, 30 Strasbourg, France
6. Delgado J, Aznar MP, Corella J (1997) Biomass gasification with steam in fluidized bed: effectiveness of CaO, MgO, and CaOMgO for hot raw gas cleaning. *Ind Eng Chem Res* 36(5):1535–1543
7. Bangala DN, Abatzoglou N, Martin JP, Chornet E (1997) Catalytic gas conditioning: application to biomass and waste gasification. *Ind Eng Chem Res* 36:4184–4192
8. Caballero MA, Corella J, Aznar MP, Gil J (2000) Biomass gasification with air in fluidized bed. Hot gas cleanup with selected commercial and fullsize nickel-based catalysts. *Ind Eng Chem Res* 39(5):1143–1154
9. Rapagna S, Jand N, Kiennemann A, Foscolo PU (2000) Steamgasification of biomass in a fluidised-bed of olivine particles. *Biomass Bioenergy* 19(3):187–197
10. Dayton D (2002) A review of the literature on catalytic biomass tar destruction, TP-510-32815, NREL
11. Uddin MA, Tsuda H, Wu SJ, Sasaoka E (2008) Catalytic decomposition of biomass tars with iron oxide catalysts. *Fuel* 87(4–5):451–459
12. Olivares A, Aznar MP, Caballero MA, Gil J, Frances E, Corella J (1997) Biomass gasification: produced gas upgrading by in-bed use of dolomite. *Ind Eng Chem Res* 36(12):5220–5226
13. Miyazawa T, Kimura T, Nishikawa J, Kado S, Kunimori K, Tomishige K (2006) Catalytic performance of supported Ni catalysts in partial oxidation and steam reforming of tar derived from the pyrolysis of wood biomass. *Catal Today* 115(1–4):254–262

14. Seemann MC, Schildhauer TJ, Biollaz S, Stucki S, Wokaun A (2006) The regenerative effect of catalyst fluidization under methanation conditions. *Appl Catal A* 313(1):14–21
15. Lind F, Seemann M, Thunman H (2011) Continuous catalytic tar reforming of biomass derived raw gas with simultaneous catalyst regeneration. *Ind Eng Chem Res* 50(20):11553–11562
16. Lind F, Berguerand N, Seemann M, Thunman H (2013) Ilmenite and nickel as catalysts for upgrading of raw gas derived from biomass gasification. *Energy Fuels* 27(2):997–1007
17. Hofbauer H, Rauch R, Loeffler G, Kaiser S, Fercher E, Tremmel H (2002) Proceedings of the 12th European conference on biomass and bioenergy, Amsterdam
18. Bolhar-Nordenkamp M, Hofbauer H, Bosch K, Rauch R, Aichernig C (2003) Proceedings of the international conference on biomass utilisation (Kirtikara K, ed), vol 1. Phuket, Thailand, pp 567–572
19. Pfeifer C, Rauch R, Hofbauer H (2004) In-bed catalytic tar reduction in a dual fluidized bed biomass steam gasifier. *Ind Eng Chem Res* 43(7):1634–1640
20. Pfeifer C, Rauch R, Hofbauer H, Świerczyński D, Courson C, Kiennemann A (2004) Hydrogen-rich gas production with a Ni-catalyst in a dual fluidized bed biomass gasifier, Na
21. Wilk V, Hofbauer H (2013) Conversion of mixed plastic wastes in a dual fluidized bed steam gasifier. *Fuel* 107:787–799
22. Berguerand N, Marinkovic J, Vilches TB, Thunman H (2016) Use of alkali-feldspar as bed material for upgrading a biomass-derived producer gas from a gasifier. *Chem Eng J* 295:80–91
23. Koppatz S, Pfeifer C, Hofbauer H (2011) Comparison of the performance behaviour of silica sand and olivine in a dual fluidised bed reactor system for steam gasification of biomass at pilot plant scale. *Chem Eng J* 175:468–483
24. Van Paasen S, Kiel J (2004) Tar formation in a fluidised-bed gasifier: impact of fuel properties and operating conditions. Energy Research Centre of the Netherlands ECN
25. Milne TA, Evans RJ, Abatzoglou N (1998) Biomass gasifier “Tars”: their nature, formation, and conversion (No. NREL/TP-570-25357; ON: DE00003726). National Renewable Energy Laboratory, Golden, CO (US)
26. Larsson A, Israelsson M, Lind F, Seemann M, Thunman H (2014) Using ilmenite to reduce the tar yield in a dual fluidized bed gasification system. *Energy Fuels* 28(4):2632–2644
27. Marinkovic J, Thunman H, Knutsson P, Seemann M (2015) Characteristics of olivine as a bed material in an indirect biomass gasifier. *Chem Eng J* 279:555–566
28. Berdugo Vilches T, Marinkovic J, Seemann M, Thunman H (2016) Comparing active bed materials in a dual fluidized bed biomass gasifier: olivine, bauxite, quartz-sand, and ilmenite. *Energy Fuels* 30(6):4848–4857
29. Keller M, Leion H, Mattisson T, Thunman H (2014) Investigation of natural and synthetic bed materials for their utilization in chemical looping reforming for tar elimination in biomass-derived gasification. *Energy Fuels* 28(6):3833–3840
30. Kimbauer F, Hermann H (2011) Investigations on bed material changes in a dual fluidized bed steam gasification plant in Gussing, Austria. *Energy Fuels* 25(8):3793–3798
31. Kimbauer F, Wilk V, Kitzler H, Kern S, Hofbauer H (2012) The positive effects of bed material coating on tar reduction in a dual fluidized bed gasifier. *Fuel* 95:553–562
32. Vilches T, Maric J, Knutsson P, Rosenfeld DC, Thunman H, Seemann M (2018) Bed material as a catalyst for char gasification: the case of ash-coated olivine activated by K and S addition. *Fuel* 224:85–93
33. Valmari T, Lind T, Kauppinen E, Sfiris G, Nilsson K, Maenhaut W (1999) Field study on ash behavior during circulating fluidized-bed combustion of biomass. 1. Ash formation. *Energy Fuels* 13(2):379–389

**Open Access** This chapter is licensed under the terms of the Creative Commons Attribution 4.0 International License (<http://creativecommons.org/licenses/by/4.0/>), which permits use, sharing, adaptation, distribution and reproduction in any medium or format, as long as you give appropriate credit to the original author(s) and the source, provide a link to the Creative Commons license and indicate if changes were made.

The images or other third party material in this chapter are included in the chapter's Creative Commons license, unless indicated otherwise in a credit line to the material. If material is not included in the chapter's Creative Commons license and your intended use is not permitted by statutory regulation or exceeds the permitted use, you will need to obtain permission directly from the copyright holder.



# Chapter 6

## New Concepts for OCAC in Other Applications



### 6.1 OCAC with Pressurized Oxy-Fuel Combustion

#### 6.1.1 Pressurized Oxy-Fuel Combustion

Pressurized oxy-fuel combustion (POFC) can be deemed as a second generation oxy-fuel combustion technology, the schematic diagram of POFC is shown in Fig. 6.1. In the conventional oxy-fuel combustion, the ASU, combustor, and CO<sub>2</sub> purification unit (CPU) are operated at around 0.6 MPa, 0.1 MPa and 8.0 MPa, separately [1, 2]. Compared to oxy-fuel combustion, POFC can dramatically reduce the energy loss caused by the pressure swing of the system. In addition, operation at elevated pressure reduces the boiler size [3], avoids air ingress, reduce the cost of CPU [4], improve the combustion efficiency [5, 6], lower the emission of pollutants [7–10], enhance heat transfer and gas–solid mixing characteristics [11, 12], improve the latent heat recovery of steam from flue gas [13], and so on. Many results from process simulation show that the net efficiency of power generation by the oxy-fuel combustion system can be improved by 1~5% with the increase of pressure [1, 14–17]. Gopan et al. [18] analyzed the fractional pressurized oxygen combustion system, and the results showed that the system efficiency loss caused by carbon capture could be reduced by 6% of the energy supplied (the comparison of net plant efficiencies for various cases is shown in Fig. 6.2). Therefore, POFC is expected to be a competitive CO<sub>2</sub> capture technology for coal-fired power plants.

Two modes for POFC have been proposed: oxy-fuel pressurized pulverized-coal combustion (oxy-PPCC) and oxy-fuel pressurized fluidized-bed combustion (oxy-PFBC). To date, the PFBC technology has been considered as a more mature choice, which has been widely used in the energy and chemical industries [19]. Furthermore, employing FBC technology in the POFC system can combine all the advantages of the two technologies.

Despite its advantages, the application of POFC technology is still facing many challenges. Compared with atmospheric oxy-fuel combustion, pressurized combustion systems place higher requirements on equipment and operation. For example,

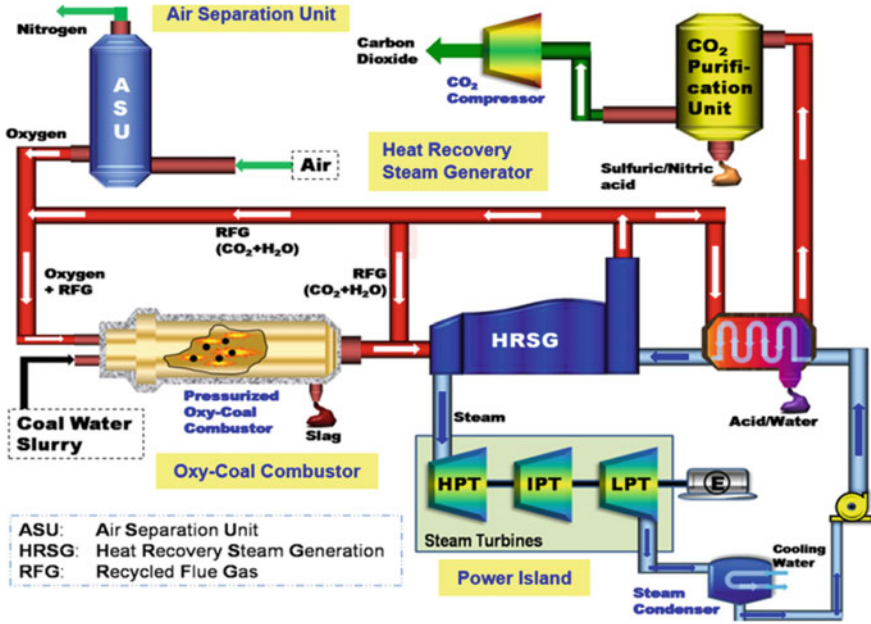


Fig. 6.1 The schematic diagram of pressurized oxy-fuel combustion

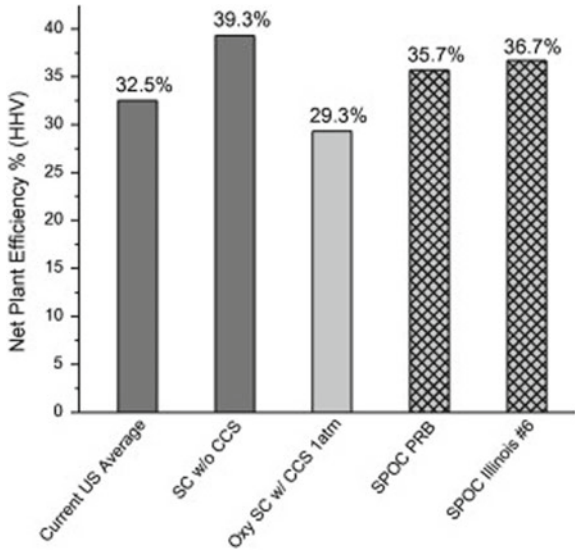


Fig. 6.2 The comparison of net plant efficiencies for various cases, SC: supercritical; SPOC: staged pressurized oxy-combustion; Both SPOC cases are supercritical (reprinted from [18] with permission of Elsevier)



although the mixing and mass transfer characteristics of a pressurized FB boiler are better than those of the atmospheric one [11, 20, 21], the locally uneven mixing of fuel and oxygen is still inevitable, although the smaller size of a pressurized reactor makes mixing between fuel and oxygen easier than at atmospheric pressure. This will bring a series of problems: (1) Unburnt combustible gases (CO, hydrocarbons, H<sub>2</sub>S and NH<sub>3</sub>, etc.) may damage the oxide layer (for corrosion resistance) on the surface of the heat exchanger [22] and may also cause an explosion of the downstream equipment [23]. Since pressurization can accelerate the corrosion rate and increase the deflagration/explosion hazard, these potential risks in a pressurized system are significantly higher than in an atmospheric pressure system; (2) Incomplete combustion not only reduces the boiler efficiency but also significantly increases the power consumption of CPU [24]; (3) To eliminate local oxygen deficiency, large combustion equipment need to increase the number of injection points of fuel and oxygen, which not only increases the equipment costs and system complexity, but also negatively affect the cost and reliability of operation [25, 26]. Therefore, there is a trade-off between technical and economic performance based on the ability of the system to transfer sufficient oxygen to complete combustion throughout the combustion region. In combustion technology, the sudden increase and decrease (or even interruption) of oxidant or fuel supplies cause the fuel to burn in a region with insufficient O<sub>2</sub> or excessive O<sub>2</sub>, which brings great safety risks. When anoxic combustion occurs, a sufficient proportion of combustible gases in the flue gas may explode in downstream equipment, causing catastrophic damage to the system [27]. However, if the fuel burns at excessive oxygen concentration, a high temperature (even up to 2000 °C) can be generated. This not only brings the risk of equipment damage (such as high-temperature tube bursting) but also increases the pollutant emissions (such as NO<sub>x</sub>) and increases the cost of deoxygenation in the CPU module. The above-mentioned drawbacks will be more significant in a pressurized atmosphere. Therefore, the improvement of the controllability of the oxygen-fuel ratio in the combustion system is of great significance to optimize the pressurized oxy-fuel combustion system.

### ***6.1.2 Oxygen-Carrier-Aided Oxy-PFBC Process***

A potential configuration of an oxy-PFBC system incorporating OCAC technology was proposed by the researchers from CanmetENERGY [25, 28–30], as shown in Fig. 6.3. The main innovation is to replace the inert bed material with OC material partially or completely. The OC not only improves oxygen uniformity in the boiler but it also provides a property of oxygen buffering to improve the operation safety, which will effectively alleviate the problems associated with fluidized bed POFC technology described in Sect. 6.1.1.

An important difference between an OC aided POFC and an OC aided oxy-fuel combustion system is the operating pressure. At atmospheric pressure, the reaction rate (for reduction and possibly oxidation) for many OCs with fuels is relatively

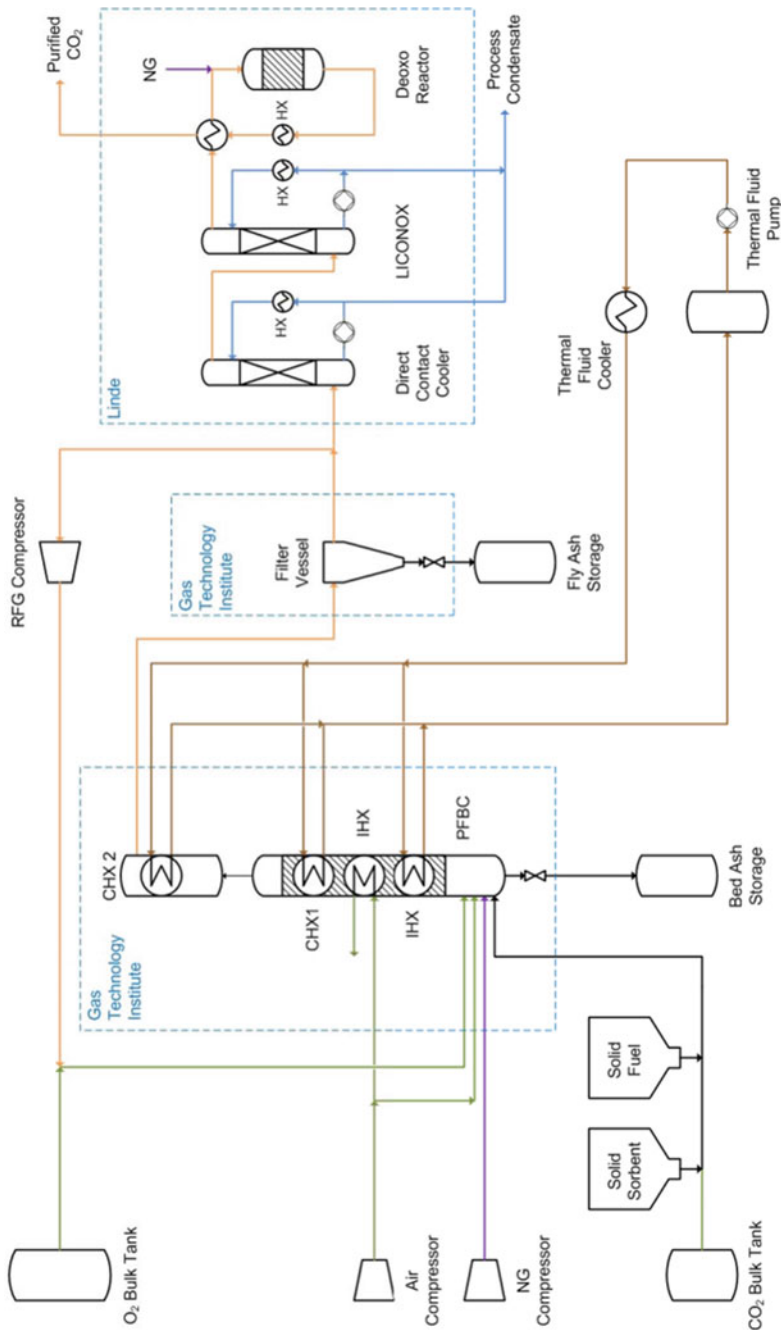
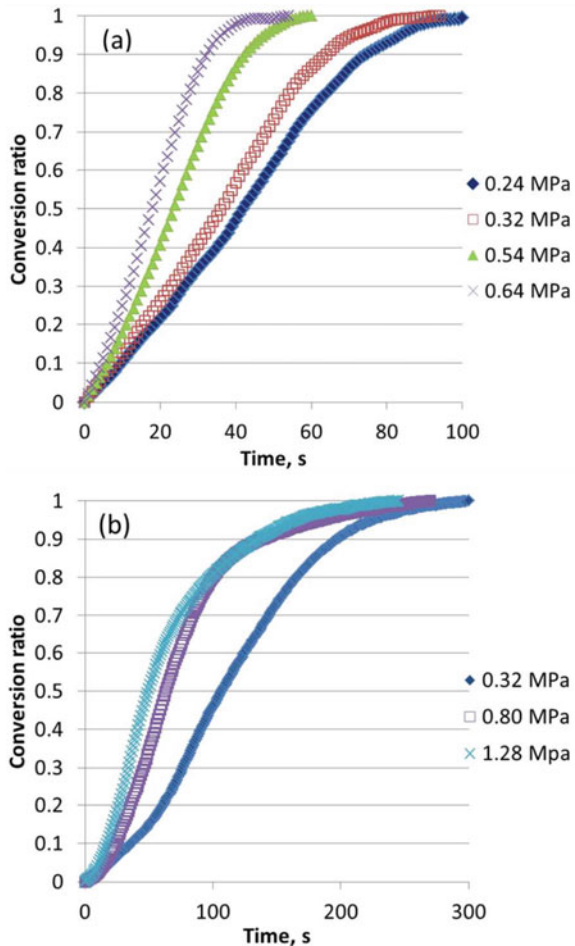


Fig. 6.3 Oxygen carrier assisted Oxy-PFBC process flow diagram [28, 29]

low [31]. Many studies [32–36] have proven that the reaction rate is a function of the partial pressure of the reactants. Increasing the partial pressure of reactants can improve the reaction rate of an OC. Taking ilmenite ore as an example, Fig. 6.4 shows its reduction rate measured by a pressurized TGA at different pressures. Regardless of whether  $\text{CH}_4$  or  $\text{CO}$  was used as the reduction gas, the reduction rate of the OC increases significantly with the increase of the operating pressure. Therefore, it is expected that the introduction of OCAC in POFC can achieve more significant auxiliary effects than OC-assisted atmospheric oxy-fuel combustion. This may lead to higher oxygen utilization efficiency, which also means lower cost of oxygen production (in the ASU) and deoxidation (in the flue gas).

In POFC, fuel and desulfurization adsorbent are usually carried by the high-pressure gas and injected into the bottom of the bed, where the drying, devolatilization and char combustion processes occur in sequence. The conveying gas velocity,

**Fig. 6.4** Reduction of ilmenite ore at various pressures: **a**  $\text{CH}_4$  partial pressure; **b**  $\text{CO}$  partial pressure (reprinted from [34] with permission of American Chemical Society)



location and quantity of injection points should be determined according to the load and hydrodynamic characteristics of the boiler. The conveying gas is typically purified  $\text{CO}_2$  that is generated from the CPU. The high-pressure  $\text{O}_2$  is mixed with the recycled flue gas (mainly composed of  $\text{CO}_2$  and  $\text{H}_2\text{O}$ ) and then injected into the wind box and subsequently into the combustion chamber through the distributor. The premixing of pure  $\text{O}_2$  and recycled flue gas is to avoid local hot points caused by locally high  $\text{O}_2$  concentration, thereby avoiding agglomeration of bed material and damage of the equipment.

The feed system of the pressurized combustion/gasification unit usually adopts pneumatic conveying or pump conveying [3], which inevitably causes fluctuations in the fuel feed. The unstable ratio of fuel to oxygen affects the combustion efficiency and operating safety. In general, to ensure combustion efficiency, the oxygen supply will be increased, which increases the cost of oxygen production and deoxidization [1, 36–38]. Moreover, in extreme conditions, if fuel or even oxygen interruption occurs during the operation, it will lead to disastrous results. The introduction of OCAC may greatly alleviate the threat of this problem because OC not only improves oxygen uniformity but it also provides oxygen buffering [39]. When the fluctuation of fuel and oxygen occurs, OCs can maintain the low combustible content and low oxygen concentration in the flue gas at through oxygen absorption and release. Take ilmenite ore (60.9 wt% hematite) as an example, the maximum theoretical oxygen transfer capacity is 9.9 wt%, which means that there is potentially 60.8 g of oxygen available in every kg of bed that can be provided to fuel combustion. Even in extreme cases of fuel and oxygen disruption, the buffering capacity of OC providing operators with valuable operating time, which can greatly improve the economy and safety of boiler operations. This exciting feature of OCAC has been demonstrated in atmospheric combustion [39] and can be also expected applicable in a POFC system. The elevated pressure only affects the OC's redox rate while maintaining its ability in oxygen transportation [34].

The OC aided oxy-fuel combustion can significantly improve the desulfurization efficiency [40], and the POFC technology can reduce  $\text{SO}_2$  emission [10]. Hence, the combination of OC aided oxy-PFBC technology is expected to achieve a further reduction of the  $\text{SO}_2$  emission compared to the former two technologies. It should be noted that the increase of operating pressure will enhance the partial pressure of  $\text{CO}_2$ , thus strongly inhibiting the decomposition of  $\text{CaCO}_3$  and weakening the indirect desulfurization reaction. Meanwhile, the direct desulfurization reaction will be significantly improved, since the increase of partial pressure of  $\text{SO}_2$  facilitates the diffusion of  $\text{SO}_2$  into the pores of desulfurized particles and promotes the desulfurization reaction. However, these conclusions were obtained when inert bed material was used, and the  $\text{SO}_x$  emission under OCAC conditions need to be further studied. In addition, the presence of  $\text{Fe}_2\text{O}_3$  at high pressure may also promote the oxidation of  $\text{SO}_2$  [41, 42], and the produced  $\text{SO}_3$  may intensify the corrosion of equipment. Therefore, the mechanism of sulfur conversion under the OC aided POFC conditions needs to be further studied.

Although the OCAC technology applied in oxy-fuel combustion increases the  $\text{NO}_x$  emission [40], it has been confirmed that the POFC can effectively reduce the

$\text{NO}_x$  emission [7, 8, 10, 43]. So, OC aided POFC is expected to achieve lower  $\text{NO}_x$  emission than OC aided oxygen-fuel combustion while gaining all the advantages of OCAC technology. In addition, both OCAC technology and pressurized oxy-fuel combustion can reduce unburnt matter in the flue gas [9, 44], which lowers the emission of soot related PM [45, 46]. Therefore, the combination of the two technologies has the potential to yield a significant advantage in PM control.

### ***6.1.3 The Potential Advantages of OC Aided POFC***

Although research on the new route—OC aided oxy-PFBC technology has not been carried out yet, according to the summary and analysis of the research progress related to pressurized oxy-fuel combustion and OCAC in air and oxy-fuel combustion, the new technology route can be summarized in the following potential advantages:

- (1) The existence of OCs in the bed materials can not only improve the combustion efficiency but also improves the stability and safety of operation, which is particularly valuable for pressurized combustion systems;
- (2) An appropriate OC as the bed material may absorb alkali metals and alkaline earth metals (such as K and Ca). This can slow down the ash deposition process on heat-transfer surfaces and it can reduce PM emissions;
- (3) This technology leads to the reduction of  $\text{SO}_2$  emissions and the possible increase of desulfurization efficiency due to the more uniform oxygen distribution;
- (4) The pressurized boiler has a high volumetric heat load and heat-transfer coefficient, thus, the boiler size and heat-transfer surface can be greatly reduced compared to those in an atmospheric boiler, which may further reduce the capital cost of the facility;
- (5) The combustion process can be conducted at a stoichiometric ratio closer to 1, which can significantly improve the utilization ratio of oxygen and reduce the energy consumption of ASU and CPU modules, and improve the system efficiency;
- (6) The pressurized system can not only avoid the significant increase in CPU energy consumption caused by air ingress, but it can also mitigate the pressure swing of the system;
- (7) The inherently low  $\text{NO}_x$  emission characteristics in pressurized oxy-fuel combustion may be equally effective for OC-aided POFC;
- (8) High pressure raises the dew point of steam and facilitates the recovery of the latent heat of steam from flue gas.

## 6.2 OCAC Coupled with Staged Conversion of Fuel

### 6.2.1 *Staged Conversion of Fuel*

$\text{NO}_x$  is one of the important culprits causing acid rain, smog, and other environmental problems. The main source of  $\text{NO}_x$  emission is the combustion of various fuels, where the contribution from power plants and industrial boilers is essential. Therefore, in recent decades, the  $\text{NO}_x$  emission has attracted a great attention with strict restriction measures because of emission limitations introduced in various countries. The CFB boilers, which are usually operated at 800–900 °C mainly generate fuel-type  $\text{NO}_x$  with no thermal  $\text{NO}_x$  produced due to the low combustion temperature. Thus, they show low  $\text{NO}_x$  emission compared to pulverized-coal boilers [47, 48]. Traditional CFB boilers can achieve an  $\text{NO}_x$  concentration as low as  $\sim 200 \text{ mg/Nm}^3$ , which is still not low enough to meet the increasingly stringent environmental protection requirements (below  $50 \text{ mg/Nm}^3$  in China) [49].

At present, researchers are devoted to developing technologies for further reduction of the  $\text{NO}_x$  emission. The factors that affect the  $\text{NO}_x$  emissions from CFB boilers are the combustion temperature, excess air coefficient, the ratio of primary and secondary air, air staging, flue-gas recycling, Ca/S molar ratio, etc. [50–54]. Optimizing these parameters controls  $\text{NO}_x$  emissions to a certain extent, but it is normally not enough to make the emission reach ultra-low levels. Therefore, most CFB boilers have introduced SNCR or even SCR accessory equipment to control  $\text{NO}_x$  emissions [55, 56], thereby increasing the cost of investment and the complexity of operation. Besides, ammonia slip from SNCR/SCR equipment is almost inevitable, bringing a series of problems including the blockage of air pre-heater and secondary pollution. Therefore, it is highly desired to establish a safe, stable, and efficient process to lower the  $\text{NO}_x$  emission, designed for a CFB boiler.

Decoupling the combustion technology of solid fuel (a kind of staged conversion of fuel) has been proven as a high-efficiency combustion technology with low  $\text{NO}_x$  emissions [57, 58]. In this process, the solid fuel is firstly pyrolyzed or gasified to produce a highly reducing product gas and coal char, which are then burned in a separate combustion boiler. Since the  $\text{NO}_x$  generated from the devolatilization stage can be mostly reduced to  $\text{N}_2$  by the product gas, this technology will greatly reduce  $\text{NO}_x$  emissions during the whole fuel conversion process. For some fuels with high volatile content, the  $\text{NO}_x$  originating from volatiles in a conventional combustion process is high, so this technology has a significant advantage in reducing  $\text{NO}_x$  for high volatile fuels.

### 6.2.2 *OCAC Coupled with Staged Conversion of Fuel*

The semi-industrial and industrial scale OCAC tests show that the addition of OC increases the  $\text{NO}_x$  emission, resulting in the injection of an excess of ammonia

into the deNO<sub>x</sub> equipment [59–61]. It can be assumed that the presence of OC makes the oxygen distribution more uniform, and as a result the reductive zone and the concentration of reductive gases (CO, H<sub>2</sub>, and C<sub>i</sub>H<sub>j</sub>) are significantly reduced. Therefore, the NO<sub>x</sub> reduction in the boiler is weakened. By combining OCAC with staged combustion of fuel, the advantages of the two technologies can be achieved, resulting in high efficiency and lower NO<sub>x</sub>.

Figure 6.5 is a schematic diagram of a proposed process (coal combustion is taken as an example). Both the gasification and the combustion reactor are CFBs. The coal is first added to the gasifier for air gasification. A portion of the char particles separated by the cyclone is recycled to the gasifier to continue the gasification, and the remainder is sent to the dense phase of the combustor for combustion. The product gas of the gasification is injected into different locations of the combustor. The flue gas of the combustor is partially circulated back to the wind box and mixed with air as secondary air. The combustion boiler uses OC as bed materials. This process has the following advantages: (1) The strong reduction of product gas reduces the NO<sub>x</sub> to N<sub>2</sub> in the gasifier, which will greatly reduce the conversion ratio of fuel N to NO<sub>x</sub>; (2) The introduction of circulating flue gas can further reduce the emission of NO<sub>x</sub>. On the one hand, the introduction of circulating flue gas can reduce the oxygen concentration of the secondary air, thereby reducing the temperature of the char particles [62] and reducing the conversion of char-N to NO<sub>x</sub>; on the other hand, when the circulating flue gas passes through the dense phase, the NO<sub>x</sub> from flue gas can be reduced on the surface of char particles; (3) The introduction of OC as bed material obtains all the technical advantages of OCAC technology, as described in Sects. 6.2 and 6.3.

The use of staged combustion of fuel and flue-gas circulation should significantly reduce NO<sub>x</sub> emissions without SNCR and SCR, so the new process—OCAC coupled with staged combustion is expected to become a competitive, efficient, and low-pollution combustion process. In addition, if the primary and secondary air in Fig. 6.5 are adjusted to O<sub>2</sub>/CO<sub>2</sub> or O<sub>2</sub>/H<sub>2</sub>O, it also applies to oxy-fuel combustion, which simultaneously achieves efficient CO<sub>2</sub> capture and low NO<sub>x</sub> emission. However, the process in Fig. 6.5 is just an example, OCAC technology can also control NO<sub>x</sub> emissions through a combination of staged air combustion, optimizing air distribution, separators, and adjusting the fluidization state, and so on.

### 6.3 OCAC Application Beyond Fluidized Bed

To date, the existing applications of OCAC technology are all carried out in FB reactors. It is expected that the unique ability of OCAC technology of oxygen transfer and buffering can also be applied in other kind of reactors in complementing the poor gas–solid mixing, such as rotary kilns, grate furnaces, and fixed-bed reactors. In the following part, the possible assistance provided by OCAC for rotary-kiln combustion will be introduced.

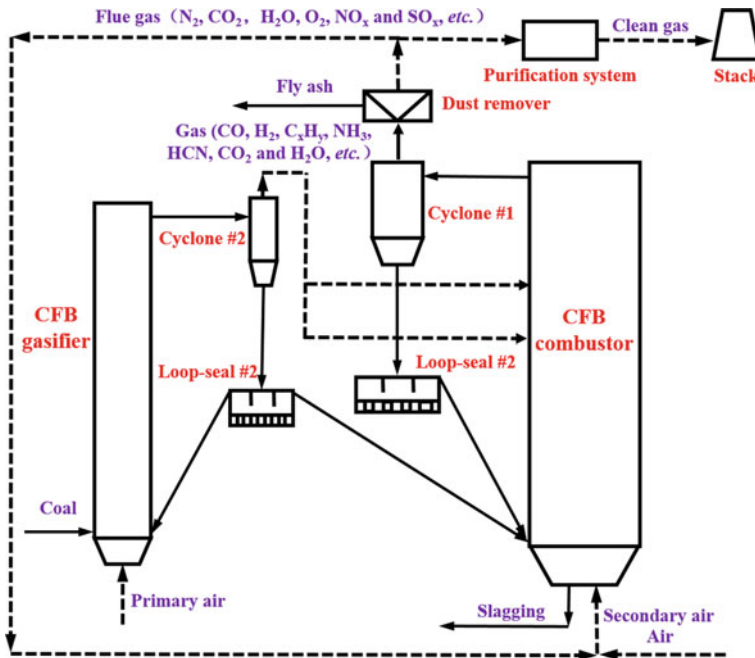


Fig. 6.5 The schematic diagram of the OCAC coupling with staged combustion

Rotary-kiln incinerators have been widely used for the incineration of various gaseous, liquid, or solid wastes, such as hazardous wastes, sludge and MSW [63–65]. The schematic diagram of typical rotary kiln incinerator system is shown in Fig. 6.6 The benefits lie in the drastic volume reduction of wastes and the substantial heat energy recovery from the exhaust gas. The harmless treatment of hazardous wastes is an important principle of this process, that is, the emission control of residual substances (such as CO and dioxins) in the exhaust gas from combustion is very important. The complete destruction of hazardous waste depends on a variety of factors [66, 67]: (1) the residence time of wastes in the incinerator and secondary combustion chamber (SCC), i.e. time; (2) the temperature distribution in the reactor, i.e. temperature; (3) the mixing of air and wastes, i.e. turbulence; (4) the oxygen concentration of the flue gas at the outlet; and so on. Factors 1–3 are called “The 3T”, considered decisive for a combustion process [66]. The residence time of materials in the reactor affects the combustion efficiency, the burning rate, and the decomposition of dioxin. A longer residence time of materials can bring a higher combustion efficiency, and a more thorough decomposition of precursors of dioxin. The combustion temperature is important for a rotary-kiln incinerator. Generally, low combustion temperature can cause insufficient combustion. In addition, from the perspective of the decomposition of the precursors to dioxines, the temperature should not be lower than 850 °C. With the increase of temperature, the reaction rate of the fuel increases, and this shortens the residence time of the fuel in the furnace, thereby



reducing the equipment volume and investment. However, the high temperature not only accelerates the corrosion rate of the furnace structure and promotes ash melting and agglomeration in the furnace but also increases the formation of  $\text{NO}_x$  [68]. The turbulence inside the kiln is an appropriate index for the mixing of fuel and oxygen. Enough turbulence ensures the effective utilization of oxygen and the burnout of fuel. If the turbulence is low, more air should be introduced to the chamber to ensure burnout. However, excessive air brings more violent disturbance and leads to more dust in the flue gas, resulting in a high heat loss and a low combustion efficiency [69].

The rotary-kiln incinerator has the advantages of simple equipment, reliable operation, wide fuel applicability, and low investment, etc. But it cannot be ignored that it also has the characteristics of poor gas–solid mixing and insufficient heat and mass transfer, which affects the system efficiency and pollutant emissions. In addition, the type of wastes is complex and mostly appears in the form of mixtures. It is difficult to characterize the physical, chemical, and thermal properties of the feed materials. This leads to very complex material transportation, transfer, and chemical reactions in the kiln [68]. Therefore, large fluctuations usually occur in the incineration process, such as fluctuations in oxygen and CO concentration, and temperature distribution. The combustion fluctuations in the incinerator are difficult to control, and that not only causes problems, such as low combustion efficiency, high CO emission, and slagging at the end of the kiln, but it also causes higher emissions ( $\text{NO}_x$ ,  $\text{SO}_x$  and dioxin) [66].

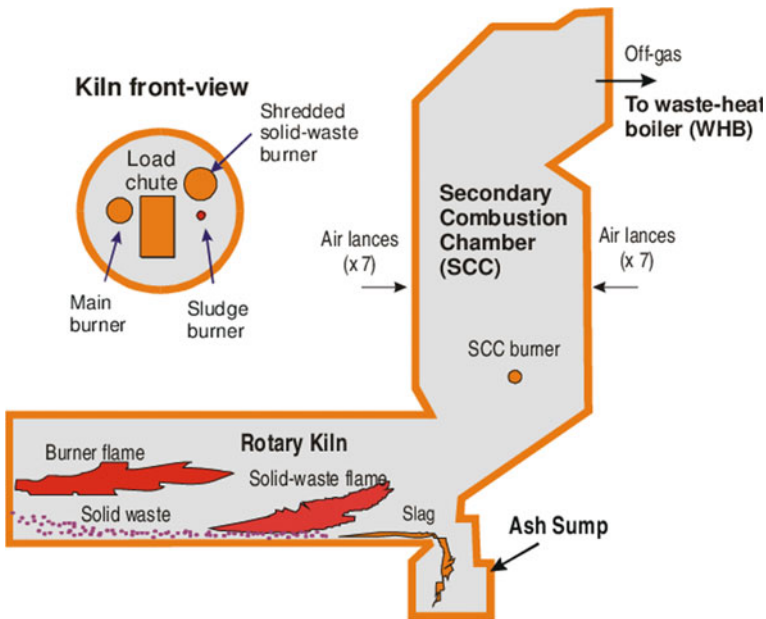


Fig. 6.6 The schematic diagram of the rotary kiln incinerator system for solid waste [70]

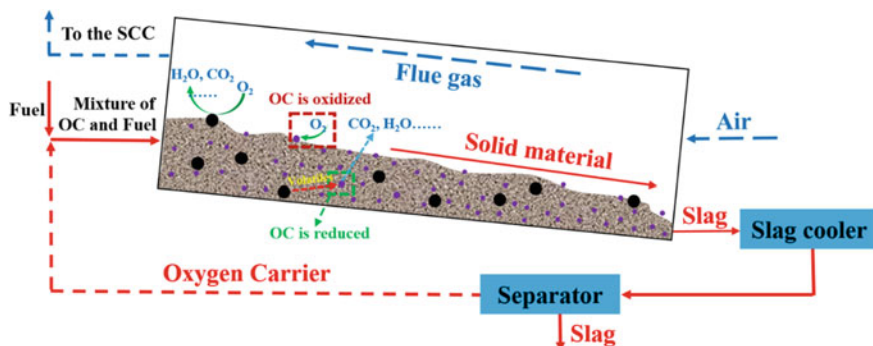


Fig. 6.7 The schematic of a potential rotary kiln incinerator coupling with OCAC

A potential design of a rotary-kiln incinerator coupled with OCAC is shown in Fig. 6.7. The mixture of OC and fuel is fed into the rotary-kiln incinerator. When the OC moves to the surface of the bed material, the OC fully contacts with  $O_2$  and oxidizes. When the OC moves inside the material, the surrounding is hypoxic, and the oxygen from the OC will be consumed by the fuel. This process achieves the oxygen transfer from an oxidizing area to an anoxic one, which may improve the uniformity of oxygen and temperature in the incinerator. The OC is finally discharged from the kiln tail together with ash and slag. After the solid mixture passes through the separation unit, OC will be recovered and recycled. With the above design, the following advantages are expected: (1) A good mixing of oxygen and fuel in time and space can be obtained in the main combustion chamber of the rotary kiln, which improves the utilization of oxygen, ensures the full combustion of fuel, and enhances the combustion efficiency; (2) The addition of OC can improve the uniformity of oxygen and temperature distribution in the main combustion chamber, resulting in lower emissions of  $CO$ ,  $NO_x$ ,  $SO_x$  and hydrocarbons. It can alleviate the problem that the emission of flue gas is unstable and frequently exceeds the emission standard in the existing rotary-kiln incineration. As a result, flue-gas treatment becomes easier and the equipment investment and operating cost are reduced; (3) A more uniform temperature also reduces the corrosion of the chamber structure and extends the service life; (4) This process has the characteristics of a simple system, compact structure, and easy scale-up, and the application prospect is broad. The OCAC technology not only can be directly applied to the existing rotary kiln device without changing the system, but also can be used in the design of new rotary-kiln incinerator.

## 6.4 Multi-functional OCAC

OCAC technology excels in transporting the oxygen species from oxygen-enriched locations to the oxygen-deficient areas within a fluidized-bed combustor, resulting in

an even oxygen distribution throughout the dense phase. The oxygen transportation performed by the OCs may reduce the local reducing areas in a furnace, and further reduce the reactive species that are essential for  $\text{NO}_x$  reduction. In such a situation, the denitration reaction rate should be fast enough to achieve an ideal performance. It is widely accepted that various transition metals can catalyze the denitration reaction, and almost all the OC materials are composed of transition metal oxides. Therefore, it provides an opportunity to introduce the process of catalytic denitration inside a fluidized bed combustor. If the OC materials are appropriately selected and designed, they are expected to have multi-functions, i.e. the functions of catalyst and OC, to achieve a more stable combustion with lower  $\text{NO}_x$  emission.

Currently, the most intensively studied OCs for OCAC are Fe- and Mn-based materials. Ilmenite is the most widely employed Fe-based OC. Due to its thermodynamic properties, ilmenite can be reduced by the fuels, mainly the gaseous fuels or the volatiles released from solid fuels, via the gas–solid reactions in the oxygen-deficient areas. This is the same case for Mn-based OCs at high temperatures, such as the typical temperature range of 800–1000 °C for a fluidized-bed combustor. In chemical looping technologies, certain types of OCs exhibit the ability to release molecular  $\text{O}_2$  in the oxygen-deficient reactor and to replenish the OCs with oxygen in an oxygen-enriched reactor. If the OC, which can release molecular  $\text{O}_2$  (i.e. gas-phase oxygen), is introduced into the OCAC process, the fuel combustion in the oxygen-deficient areas of the combustor can be achieved through not only gas–solid but also gas–gas reactions with a faster reaction rate. Therefore, it is expected that the promotional effect of OCAC can be further enhanced by employing OCs with the ability of reversible  $\text{O}_2$  release. To date, the Mn- and Cu-based materials are the well-known OCs with the ability of  $\text{O}_2$  release learned from the experience of chemical looping technologies. The drawback of the Mn-based OC is that it can release  $\text{O}_2$  at a high temperature but it can hardly be re-oxidized at such a temperature with a slightly lower oxygen pressure  $P_{\text{O}_2}$  [71]. This is due to the thermodynamic limit of manganese oxides, which has been widely studied by many researchers [72, 73]. However, such a drawback can be addressed by combining the ilmenite with Mn as guest species resulting in an OC of Mn-modified ilmenite [71]. The Mn-modified ilmenite contains an oxide pair between  $(\text{Fe}_{1-x}\text{Mn}_x)_2\text{O}_3$  and  $(\text{Fe}_{1-x}\text{Mn}_x)_3\text{O}_4$ , which endows the OC an ability of  $\text{O}_2$  release, at the same time, overcomes the thermodynamic limit of pure manganese oxide. On the contrary, the Cu-based OC materials have a favourable thermodynamic property for a reversible  $\text{O}_2$  release under OCAC-relevant conditions. However, it may impose a risk of bed agglomeration under the reaction condition of fluidized-bed combustor due to the low Tammann temperature of  $\text{Cu}/\text{CuO}_x$ . In general, it should be highly promising for employing OC materials with the ability of reversible  $\text{O}_2$  release in OCAC processes, and the design and searching for an OC with a suitable thermodynamic properties and sufficient physical strength under OCAC-relevant conditions is crucial.

## References

1. Hong J, Chaudhry G, Brisson JG, Field R, Gazzino M, Ghoniem AF (2009) Analysis of oxy-fuel combustion power cycle utilizing a pressurized coal combustor. *Energy* 34:1332–1340
2. Chen S, Yu R, Soomro A, Xiang W (2019) Thermodynamic assessment and optimization of a pressurized fluidized bed oxy-fuel combustion power plant with CO<sub>2</sub> capture. *Energy* 175:445–455
3. Cuenca MA, Anthony, EJ (2012) *Pressurized fluidized bed combustion*. Springer Science & Business Media
4. Darde A, Prabhakar R, Tranier J-P, Perrin N (2009) Air separation and flue gas compression and purification units for oxy-coal combustion systems. *Energy Procedia*. 1:527–534
5. Li L, Duan L, Yang Z, Zhao C (2020) Pressurized oxy-fuel combustion characteristics of single coal particle in a visualized fluidized bed combustor. *Combust Flame* 211:218–228
6. Pang L, Shao Y, Zhong W, Liu H (2018) Experimental investigation on the coal combustion in a pressurized fluidized bed. *Energy* 165:1119–1128
7. Lasek JA, Janusz M, Zuwała J, Głód K, Iluk A (2013) Oxy-fuel combustion of selected solid fuels under atmospheric and elevated pressures. *Energy* 62:105–112
8. Lasek JA, Głód K, Janusz M, Kazalski K, Zuwała J (2012) Pressurized oxy-fuel combustion: a study of selected parameters. *Energy Fuels* 26:6492–6500
9. Wang J, Duan Y, Duan L, Yan Y, Tong S, Zhao C (2019) Sulfur enrichment in particulate matter generated from a lab-scale pressurized fluidized bed combustor. *Energy Fuels* 33:603–611
10. Duan Y, Duan L, Wang J, Anthony EJ (2019) Observation of simultaneously low CO, NO<sub>x</sub> and SO<sub>2</sub> emission during oxy-coal combustion in a pressurized fluidized bed. *Fuel* 242:374–381
11. Li L, Duan Y, Duan L, Xu C, Anthony EJ (2018) Flow characteristics in pressurized oxy-fuel fluidized bed under hot condition. *Int J Multiph Flow* 108:1–10
12. Bao Z, Duan L, Wu K, Zhao C (2020) An investigation on the heat transfer model for immersed horizontal tube bundles in a pressurized fluidized bed. *Appl Therm Eng* 170:115035
13. Shi Y, Zhong W, Shao Y, Liu X (2019) Energy efficiency analysis of pressurized oxy-coal combustion system utilizing circulating fluidized bed. *Appl Therm Eng* 150:1104–1115
14. Soundararajan R, Gundersen T (2013) Coal based power plants using oxy-combustion for CO<sub>2</sub> capture: pressurized coal combustion to reduce capture penalty. *Appl Therm Eng* 61:115–122
15. Chen HT, Wu W (2015) Efficiency enhancement of pressurized oxycoal power plant with heat integration. *Int J Energy Res* 39:256–264
16. Zebian H, Gazzino M, Mitsos A (2012) Multi-variable optimization of pressurized oxy-coal combustion. *Energy* 38:37–57
17. Zebian H, Rossi N, Gazzino M, Cumbo D, Mitsos A (2013) Optimal design and operation of pressurized oxy-coal combustion with a direct contact separation column. *Energy* 49:268–278
18. Gopan A, Kumfer BM, Phillips J, Thimsen D, Smith R, Axelbaum RL (2014) Process design and performance analysis of a staged, pressurized oxy-combustion (SPOC) power plant for carbon capture. *Appl Energy* 125:179–188
19. Anthony EJ, Preto F (1995) Pressurized combustion in FBC systems. In: Cuenca MA, Anthony EJ (eds) *Pressurized fluidized bed combustion*. Springer, Dordrecht, pp 80–120
20. Rajan RR, Wen CY (1980) A comprehensive model for fluidized bed cool combustors. *AIChE J* 26:642–655
21. Hoffmann AC, Yates JG (1986) Experimental observations of fluidized beds at elevated pressures. *Chem Eng Commun* 41:133–149
22. Uusitalo MA, Vuoristo PMJ, Mäntylä TA (2002) High temperature corrosion of coatings and boiler steels in reducing chlorine-containing atmosphere. *Surf Coat Technol* 161:275–285
23. Glassman I, Yetter RA, Glumac NG (2014) *Combustion*. Academic Press
24. Pipitone G, Bolland O (2009) Power generation with CO<sub>2</sub> capture: technology for CO<sub>2</sub> purification. *Int J Greenhouse Gas Control* 3:528–534
25. Hughes R, Lu D, Symonds RT (2017) Improvement of oxy-FBC using oxygen carriers: concept and combustion performance. *Energy Fuels* 31:10101–10115

26. Assessment AD (2001) DOE/NETL-2001/1159 Tidd PFBC demonstration project
27. Mirer FE, Stellman JM (2008) Occupational safety and health protections. International Encyclopedia of Public Health
28. Hughes RW (2017) Co-firing of torrefied biomass and coal in oxy-FBC with Ilmenite bed material. 75th IEA-FBC technical meeting, Skive, Denmark, 23 Oct 2017
29. Hughes RW, Lu DY, Symonds RT, Ridha FN (2019) U.S. Patent Application No. 16/083,060
30. Follett WF, Fitzsimmons MA, Pisupati SV, Sonwane CG, Jovanovic S, Manley TW, Hiraoka D, Yows S (2015) Development of a pilot scale coal powered oxy-fired pressurized fluidized bed combustor with CO<sub>2</sub> capture. Power-Gen Europe Conference, 9–11 June 2015
31. Schwebel GL, Sundqvist S, Krumm W, Leion H (2014) Apparent kinetics derived from fluidized bed experiments for Norwegian ilmenite as oxygen carrier. *J Environ Chem Eng* 2:1131–1141
32. Adánez J, de Diego LF, García-Labiano F, Gayán P, Abad A, Palacios JM (2004) Selection of oxygen carriers for chemical-looping combustion. *Energy Fuels* 18:371–377
33. Lu X, Rahman RA, Lu DY, Ridha FN, Duchesne MA, Tan Y et al (2016) Pressurized chemical looping combustion with CO: reduction reactivity and oxygen-transport capacity of ilmenite ore. *Appl Energy* 184:132–139
34. Tan Y, Ridha FN, Duchesne MA, Lu DY, Hughes RW (2017) Reduction kinetics of ilmenite ore as an oxygen carrier for pressurized chemical looping combustion of methane. *Energy Fuels* 31:7598–7605
35. Tan Y, Ridha FN, Lu DY, Hughes RW (2017) Reduction kinetics of ilmenite ore for pressurized chemical looping combustion of simulated natural gas. *Energy Fuels* 31:14201–14210
36. NEDO (2015) Project finding research on CCUS project using oxyfuel technology in Canada. FY2014-FY2015 Final Report, June 2015
37. Symonds RT, Hughes RW, De Las Obras Loscertales M (2020) Oxy-pressurized fluidized bed combustion: configuration and options analysis. *Applied Energy* 262:114531
38. Ochs TL, Oryshchyn DB, Summers C, Gerdemann SJ (2008) Oxy-fuel combustion and integrated pollutant removal as retrofit technologies for removing CO<sub>2</sub> from coal fired power plants. DOE/NETL-IR-2008-062
39. Lind F, Corcoran A, Thunman H (2017) Validation of the oxygen buffering ability of bed materials used for OCAC in a large scale CFB boiler. *Powder Technol* 316:462–468
40. Lu D (2018) Enhancement combustion performance and emission control in oxy-FBC using oxygen carriers. In: 76th IEA-FBC meeting, Seoul, Korea, 13 May 2018
41. Wang X, Zhang J, Wang Z, Wang Y, Vujanović M, Li P, Tan H (2019) Experimental and kinetics study on SO<sub>3</sub> catalytic formation by Fe<sub>2</sub>O<sub>3</sub> in oxy-combustion. *J Environ Manage* 236:420–427
42. Malik MJ (2019) Formation and removal of SO<sub>x</sub> and NO<sub>x</sub> in pressurized oxy-fuel coal combustion. Master thesis, University of Waterloo
43. Pang L, Shao Y, Zhong W, Gong Z, Liu H (2020) Experimental study of NO<sub>x</sub> emissions in a 30 kW<sub>th</sub> pressurized oxy-coal fluidized bed combustor. *Energy* 194:116756
44. Thunman H, Lind F, Breitholtz C, Berguerand N, Seemann M (2013) Using an oxygen-carrier as bed material for combustion of biomass in a 12-MW<sub>th</sub> circulating fluidized-bed boiler. *Fuel* 113:300–309
45. Xu M, Yu D, Yao H, Liu X, Qiao Y (2011) Coal combustion-generated aerosols: formation and properties. *Proc Combust Inst* 33:1681–1697
46. Yao Q, Li SQ, Xu HW, Zhuo JK, Song Q (2010) Reprint of: studies on formation and control of combustion particulate matter in China: a review. *Energy* 35:4480–4493
47. Glarborg P, Jensen AD, Johnsson JE (2003) Fuel nitrogen conversion in solid fuel fired systems. *Prog Energy Combust Sci* 29:89–113
48. Stanmore BR, Tschamber V, Brilhac JF (2008) Oxidation of carbon by NO<sub>x</sub>, with particular reference to NO<sub>2</sub> and N<sub>2</sub>O. *Fuel* 87:131–146
49. Leckner B (1998) Fluidized bed combustion: mixing and pollutant limitation. *Prog Energy Combust Sci* 24:31–61
50. Leckner B, Åmand LE, Lücke K, Werther J (2004) Gaseous emissions from co-combustion of sewage sludge and coal/wood in a fluidized bed. *Fuel* 83:477–486

51. Lyngfelt A, Åmand L-E, Leckner B (1998) Reversed air staging—a method for reduction of  $N_2O$  emissions from fluidized bed combustion of coal. *Fuel* 77:953–959
52. Tourunen A, Saastamoinen J, Nevalainen H (2009) Experimental trends of NO in circulating fluidized bed combustion. *Fuel* 88:1333–1341
53. Lupiáñez C, Díez LI, Romeo LM (2014) Influence of gas-staging on pollutant emissions from fluidized bed oxy-firing. *Chem Eng J* 256:380–389
54. Arjunwadkar A, Basu P, Acharya B (2016) A review of some operation and maintenance issues of CFBC boilers. *Appl Therm Eng* 102:672–694
55. Ke X, Cai R, Zhang M, Miao M, Lyu J, Yang H (2018) Application of ultra-low NO<sub>x</sub> emission control for CFB boilers based on theoretical analysis and industrial practices. *Fuel Process Technol* 181:252–258
56. Cui J, Duan L, Zhou L, Zhao C (2018) Effects of air pollution control devices on the chlorine emission from 410 t/h circulating fluidized bed boilers co-firing petroleum coke and coal. *Energy Fuels* 32:4410–4416
57. Li S, Xu T, Peng S, Zhou Q, Tan H, Hui S (2008) NO<sub>x</sub> and SO<sub>x</sub> emissions of a high sulfur self-retention coal during air-staged combustion. *Fuel* 87(6):723–731
58. Ouyang Z, Zhu J, Lu Q (2013) Experimental study on preheating and combustion characteristics of pulverized anthracite coal. *Fuel* 113:122–127
59. Rydén M, Hanning M, Corcoran A, Lind F (2016) Oxygen carrier aided combustion (OCAC) of wood chips in a semi-commercial circulating fluidized bed boiler using manganese ore as bed material. *Appl Sci* 6(11):347
60. Rydén M, Hanning M, Lind F (2018) Oxygen carrier aided combustion (OCAC) of wood chips in a 12 MW<sub>th</sub> circulating fluidized bed boiler using steel converter slag as bed material. *Appl Sci* 8(12):2657
61. Moldenhauer P, Corcoran A, Thunman H, Lind F (2018) A scale-up project for operating a 115 MW<sub>th</sub> biomass-fired CFB boiler with oxygen carriers as bed material. In: 5th international conference on chemical looping, Park City, Utah, USA
62. Duan L, Li L, Liu D, Zhao C (2019) Fundamental study on fuel-staged oxy-fuel fluidized bed combustion. *Combust Flame* 206:227–238
63. Bujak J (2015) Thermal treatment of medical waste in a rotary kiln. *J Environ Manage* 162:139–147
64. Wey M-Y, Liu K-Y, Tsai T-H, Chou J-T (2006) Thermal treatment of the fly ash from municipal solid waste incinerator with rotary kiln. *J Hazard Mater* 137:981–989
65. Zhu J, Jiang X, Liu G, Yan J, Chi Y (2004) Discussion on the technology of waste disposal in rotary kiln. *Environ Eng* 5:57–61
66. Jiang X, Li Y, Yan J (2019) Hazardous waste incineration in a rotary kiln: a review. *Waste Dispos Sustain Energy*. 1:3–37
67. Pershing DW, Lighty JS, Silcox GD, Heap MP, Owens WD (1993) Solid waste incineration in rotary kilns. *Combust Sci Technol* 93:245–276
68. Yang Y, Pijnenborg M, Reuter M, Verwoerd J (2007) Analysis of transport phenomena in a rotary-kiln hazardous waste incinerator. *Progress in Computational Fluid Dynamics an International Journal*. 7:25
69. Huber F, Blasenbauer D, Mallow O, Lederer J, Winter F, Fellner J (2016) Thermal co-treatment of combustible hazardous waste and waste incineration fly ash in a rotary kiln. *Waste Manage* 58:181–190
70. Yang Y, Reuter MA, Verwoerd J (2004) Flow behaviour of shredded solid waste in a rotary kiln hazardous waste incinerator. In: 3rd international conference on combustion, incineration/pyrolysis and emission control. International Academic Publishers, pp 52–87
71. Sun Z, Lu DY, Hughes RW, Filippou D (2018) O<sub>2</sub> uncoupling behaviour of ilmenite and manganese-modified ilmenite as oxygen carriers. *Fuel Process Technol* 169:15–23
72. Larring Y, Braley C, Pishahang M, Andreassen KA, Bredesen R (2015) Evaluation of a mixed Fe–Mn oxide system for chemical looping combustion. *Energy Fuels* 29:3438–3445
73. Pérez-Vega R, Abad A, Izquierdo MT, Gayán P, de Diego LF, Adánez J (2019) Evaluation of Mn-Fe mixed oxide doped with TiO<sub>2</sub> for the combustion with CO<sub>2</sub> capture by chemical looping assisted by oxygen uncoupling. *Appl Energy* 237:822–835

**Open Access** This chapter is licensed under the terms of the Creative Commons Attribution 4.0 International License (<http://creativecommons.org/licenses/by/4.0/>), which permits use, sharing, adaptation, distribution and reproduction in any medium or format, as long as you give appropriate credit to the original author(s) and the source, provide a link to the Creative Commons license and indicate if changes were made.

The images or other third party material in this chapter are included in the chapter’s Creative Commons license, unless indicated otherwise in a credit line to the material. If material is not included in the chapter’s Creative Commons license and your intended use is not permitted by statutory regulation or exceeds the permitted use, you will need to obtain permission directly from the copyright holder.



# Chapter 7

## Perspectives on Future Research



The OCAC concept has been validated by operation of FB boilers on lab-scale, semi-industrial scale and full industrial scale [1–5]. Based on the current progress in the development of OCAC technology, it has been proven that the OCAC is a feasible technology showing obvious benefits in the applications on a CFB boiler [6]. However, there are still challenges remaining for more perspectives.

### 7.1 Fundamentals Regarding Transport Phenomena and Chemical Reactions

#### 7.1.1 Heat and Mass Transfer and Reactions

Although the OCAC concept has been proven to be effective in various thermal conversion processes, many basic principles are not clear, such as: (1) the effect of OC on the fluidization behaviour, heat and mass transfer, including in the dense bed, splash zone and transport zone, especially the transient character of bubbles, clusters and wall layers; (2) the influence of different redox atmospheres on the reaction characteristics of OC, including oxygen transfer mode, intermediate reaction processes, reaction rate, and the ratio of oxygen buffering; (3) the influence of different reaction conditions on particle temperature and microstructure, etc. Besides, it is difficult to analyze quantitatively the influence of various factors on the reaction process in a complex environment through experimental research; (4) the properties and existence of reducing/oxidizing regions should be further investigated. Therefore, multi-scale simulation studies including quantum chemical calculations, molecular-scale simulations, particle-scale models, and industrial-scale simulations, etc. can help to reveal the exact mechanism affected by different factors, which is rarely reported.



### **7.1.2 Problems Associated with Alkali Metals and S**

The absorption of alkali metals by an oxygen carrier may potentially be beneficial to alleviate a series of ash-related problems, such as bed agglomeration, ash deposition and corrosion on the heating surface and the formation and emission of PM in the flue gas, improve the efficiency and safety of the system. This is because the alkali metal contents not only diffuse into the OC bed particles but also forms compounds with high melting point [7]. For example, the ilmenite ore can absorb K and form a stable potassium-titanium compound [8–10]. However, the absorption mechanism of alkali metals and alkaline-earth metals (such as K, Ca and Na) by different oxygen carriers is still unclear and needs further study, which is of great significance for the optimization and selection of bed materials.

## **7.2 Pollutant Transformation Routes and Control Strategies**

### **7.2.1 $NO_x$ and $SO_x$ Formation and Emission Mechanism**

At present, the effect of the OC addition on  $NO_x$  emission is still divided, based on the results from bubbling beds and CFB boilers, and the influence of OCAC technology on  $NO_x$  formation and transformation is still unclear and needs to be investigated. In some studies, the presence of OC is found to bring several advantages to reduce  $NO_x$  in the FB system [3]. OC reduces the hot spots and volatile flames and so reducing NO formation. In addition, the active components, such as iron, in the OC shows a catalytic effect on the reduction of  $NO_x$  [11]. On the other hand, it also brings negative effects. The presence of OC consumes more reducing gases, thus, promotes  $NO_x$  formation. The oxidative OC may react with nitrogen-containing gas components, such as  $NH_3$  and HCN, generating more NO [12, 13]. In general, the influence of OC on  $NO_x$  formation and reduction mechanisms needs to be further studied.

In the application of OCAC technology, more uniformly distributed oxygen and temperature can promote the reactivity of a desulfurizing agent [14]. Besides, appropriate OCs, such as ilmenite ore, absorbs S [10, 15], which further reduces the emission of  $SO_x$  and alleviates the corrosion risk. However, studies on the absorption characteristics of OC over S along with the pathways of S migration and transformation are not clear. Furthermore, the  $SO_3$  emissions related to OCAC have not yet been reported, and this should be well studied since  $SO_3$  is corrosive to the heating surfaces at low temperatures.

### ***7.2.2 The Emissions of Cl and Dioxin***

Studies on chloride emissions in oxygen-carrier-aided air combustion have not been reported yet. However, for fuels with high Cl content, such as MSW, chloride emissions impose great risks of corrosion and ash deposition, and the Cl emission from the OCAC process needs to be paid special attention. In addition, Cl is an important source for the highly toxic dioxins. The dioxins are formed through precursors in the furnace and this formation is closely related to the temperature, residence time, and gas turbulence in the furnace, and the implementation of OCAC may potentially affect these factors which will subsequently have a significance in the convection pass outside the range of OCs. Therefore, the formation and emissions of dioxins should be considered during application of OCAC when burning fuels with high chlorine content such as MSW.

### ***7.2.3 Emissions of Mercury, Heavy Metals and PM***

The emission of mercury, heavy metals, PM and other pollutants in connection to OCs have not been investigated yet. The OCAC process improves the distribution of oxygen and temperature in the combustion system, the active OC particles may react with different forms of mercury and heavy metals to change their physico-chemical properties. Thereafter, the evolution process and emission rules of mercury and heavy metals might differ. Under OCAC operation, the flue gas has lower quantities of gaseous combustibles, which means that the flue gas may have lower carbon content, such as soot in fly ash. This not only affects the adsorption of mercury and heavy metals by fly ash, but also affects PM emissions related to soot. In addition, using OC as bed materials has the potential to adsorb alkali metals, which may be beneficial to reduce the formation and emission of PM related to alkali metals.

## **7.3 More Testing and Application of OCAC**

### ***7.3.1 More OC and Fuel Testing***

More fuel types (such as more types of coal, solid waste, hazardous waste, etc.), OC types (including natural ores, synthetic oxygen carriers, and industrial waste residues) and addition ratios of OC need to be tested. Currently, most of the research has focused on biomass fuels and only limited types of OCs are considered. The selection of different types of fuel and OC will have a significant impact on the OCAC process. For example, the ash content of biomass fuels is usually small, and the OC can be added periodically. However, during combustion of high-ash fuel (such as coal), the bed material of the CFB boiler needs to be discharged frequently,

so adding OC, maintaining the concentration of OC in the combustor, and recovering OC from the bottom ashes are all topics that need further study. In addition, since the use of OC implies a cost, the management of OC is very important for the application of OCAC technology to industrial CFB boilers [6]. At present, the study of OC regeneration and recycling on an industrial scale test facility is lacking, which is the next step to be carried out urgently. Such matters can accumulate the basic data of OCAC technology to cope with the application scenarios of multiple fuels and processes.

In addition, it should be noted that if this technology is applied to existing boilers, in principle, the introduced OC should avoid changing the original fluid-dynamic state of the boiler, that is, the mass distribution and particle size distribution of OC should match the flow characteristics of the original inert bed material. Otherwise, if the OCAC technology is applied to a newly built boiler, it will have a more flexible design scheme. According to the fuel characteristics, boiler load, and OCs type, the size distribution of a bed material can be flexibly adjusted to adapt different combustion requirements. For example, a higher proportion of fine OC particles can promote the oxidation of combustible gases in the dilute upper zone to improve combustion efficiency, which is especially meaningful for burning high-volatile fuels. This can also increase the heat-transfer coefficient of superheater and reheater resulting in the increase of boiler load.

### ***7.3.2 More Applications of OCAC Technology***

The existing research on OCAC technology focuses on the combustion and gasification in a fluidized bed reactor, while the application of OCAC in other processes has not been reported. However, OCAC technology may also potentially have applications in other conversion processes with poor mixing and reactivity. For example, OCAC technology can be applied to gasification-combustion coupling processes in two CFB reactor to achieve efficient, low-NO<sub>x</sub> combustion. It can also be used in the process of pyrolysis/gasification to produce activated carbon and combustible gas in a polygeneration process. In addition, OCAC technology can also be tried in reactor configurations, such as fixed bed, rotary kiln incinerator, grate furnace, and other furnaces to improve the oxygen distribution and to achieve a better heat and mass transfer.

## **7.4 Techno-economic Analysis of OCAC Technology**

Economic efficiency is a most important factor that determines whether a new technology can be commercially applied. Specific techno-economic analysis of the OCAC technology is important for the commercial application. However, no such

studies have been reported yet, to the best of our knowledge. The profit ( $P$ ) from the application of OCAC technology depends on economic benefit ( $B$ ) and cost ( $C$ ).

The  $B$  may come from: (1) The benefit from reduced power consumption of fan ( $B_1$ ). OCAC improves the efficiency of oxygen utilization and reduces the total amount of air, thus, reducing the energy consumption of the fan; (2) The benefit of higher combustion efficiency of boiler ( $B_2$ ). OCAC reduces the combustible gas concentration in the flue gas and the carbon content of fly ash; (3) The benefits of reducing the operating costs of flue gas purification units ( $B_3$ ). OCAC improves the in-furnace desulfurization efficiency and reduces the desulfurization cost. In addition, OCAC also may increase or reduce  $\text{NO}_x$  and PM emissions, which will effect the costs of gas purification units; (4) The benefit of improving continuous operation time of boiler ( $B_4$ ). OCAC not only can improve the stability and safety of the combustion system, but also may reduce the ash accumulation and corrosion of heat exchangers, thereby potentially increasing the continuous working time of the equipment. The  $C$  may come from: (1) The cost of OC ( $C_1$ ). The use of OC instead of inert bed material will bring about changes in the cost of bed material, which requires specific analysis. For example, if using synthetic OC or natural ore OC increases the cost of bed material to varying degrees, but if using industrial waste slag (such as steel slag, etc.) it may even reduce the cost of bed material.  $C_1$  is influenced of the degree of recovery. (2) The cost of OC recovery ( $C_2$ ). OC recovery requires additional equipment (such as screening system and magnetic separation system), and the investment and operating costs of the OC recovery system will be increased. In addition, different application scenarios mean different types, reactivity, the regeneration frequency, and mixing ratios of OC, which all will affect the cost.

Generally, the  $P$  can be calculated by the following formula:  $P = B_1 + B_2 + B_3 + B_4 - (C_1 + C_2)$ . All of these aspects need to be considered in the technical-economic analysis models. The quantitative discussion of the effect of the parameters involved should be based on process simulation to guide the low-cost application of OCAC technology.

## 7.5 Process Scale-Up and Optimization

### 7.5.1 Process Scale-Up

Most of the current research on OCAC technology is focused on small and medium-sized CFB boilers, and the application of OCAC on large-scale electric utility CFB boilers has not yet been involved. However, many technical details, such as furnace layout, gas-solid flow state, and heat-exchanger layout of large-scale CFB boilers are not the same as in small-scale CFB boilers. Therefore, the application of OCAC will not only bring about changes in temperature and oxygen distribution in the CFB system, but it also may affect the original flow state, heat-transfer characteristics, ash deposition and erosion characteristics of the furnace. All of these aspects need

further research. In addition, the experience and evaluation of the long-term operation of OCAC technology are insufficient. For example, has long-term operation so far unexpected effects on system and equipment? How does OCAC affect the variable load operation of large boilers? What effect does the application of OCAC have on the erosion characteristics in the furnace? All such questions require more and longer-term industrial testing and detailed evaluation to answer.

### **7.5.2 Process Optimization**

Based on the discussion and analysis of advantages and potential concerns, it is necessary to develop an economically optimal mode of operation. On the one hand, based on the relevant experience of experimental research and the sensitivity analysis of process simulation, a technically feasible and economically optimal operation scheme need to be formulated, including detailed operation parameters, such as the selection suitable OC species, blending ratios, flow regime, and outlet oxygen concentrations, etc.; on the other hand, minimize the cost increase due to the introduction and regeneration of OC to improve the economy of the whole process. This point can be divided into two parts: one is to develop efficient separation devices to recover and reuse OC from ash discharge, another is to strengthen the utilization of the discarded OC.

Although it is claimed that bed materials, such as natural OC ores, are not expensive, the cost is still higher than that of sand in conventional processes. Therefore, according to the physical and chemical characteristics of different types of oxygen-carrier, it is necessary to develop a specific OC recovery device for the reuse of OC to reduce the cost. For example, in addition to the magnetic separator developed according to the magnetic characteristics of ilmenite ore, one can also develop separators according to the density difference (flotation method) and the size difference (mechanical screening). However, it should be noted that due to attrition and aging, the OC's life is limited. Therefore, the cost can be further reduced by recycling and utilizing related elements in the discarded OC. Taking ilmenite ore as an example, the contents of Ti (due to the attrition of the iron-rich layer on the surface of OC), K and S (absorption from the fuel) in the regenerated bed material increases significantly, and the recovery and utilization of Ti and K from discarded OC in a controlled manner is a challenge. Furthermore, it is also conducive to the harmless treatment of OC.

## References

1. Wang P, Leion H, Yang H (2017) Oxygen-carrier-aided combustion in a bench-scale fluidized bed. *Energy Fuels* 31:6463–6471
2. Garcia E, Liu H (2022) Ilmenite as alternative bed material for the combustion of coal and biomass blends in a fluidised bed combustor to improve combustion performance and reduce agglomeration tendency. *Energy* 239:121913
3. Thunman H, Lind F, Breitholtz C, Berguerand N, Seemann M (2013) Using an oxygen-carrier as bed material for combustion of biomass in a 12-MW<sub>th</sub> circulating fluidized-bed boiler. *Fuel* 113:300–309
4. Gyllén A (2019) Oxygen carrier aided combustion: implementation of oxygen carriers to existing industrial settings. Doctoral dissertation, Chalmers University of Technology
5. Lind F, Corcoran A, Andersson B-Å, Thunman H (2017) 12,000 hours of operation with oxygen-carriers in industrially relevant scale. *VGB PowerTach*
6. Störner F, Lind F, Rydén M (2021) Oxygen carrier aided combustion in fluidized bed boilers in Sweden—review and future outlook with respect to affordable bed materials. *Appl Sci* 11(17):7935
7. Morris JD, Daood SS, Chilton S, Nimmo W (2018) Mechanisms and mitigation of agglomeration during fluidized bed combustion of biomass: a review. *Fuel* 230:452–473
8. Corcoran A, Marinkovic J, Lind F, Thunman H, Knutsson P, Seemann M (2014) Ash properties of ilmenite used as bed material for combustion of biomass in a circulating fluidized bed boiler. *Energy Fuels* 28:7672–7679
9. Corcoran A, Knutsson P, Lind F, Thunman H (2018) Mechanism for migration and layer growth of biomass ash on ilmenite used for oxygen carrier aided combustion. *Energy Fuels* 32:8845–8856
10. Vigoureaux M, Knutsson P, Lind F (2020) Sulfur uptake during oxygen-carrier-aided combustion with ilmenite. *Energy Fuels* 34:7735–7742
11. Li L, Duan L, Yang Z, Wang Y, Xiang W (2021) Experimental study on in-situ denitration using catalyst in fluidized bed reactor. *Fuel Process Technol* 216(3):106742
12. Song T, Shen L, Xiao J, Chen D, Gu H, Zhang S (2012) Nitrogen transfer of fuel-N in chemical looping combustion. *Combust Flame* 159:1286–1295
13. Mayrhuber S, Normann F, Yilmaz D, Leion H (2021) Effect of the oxygen carrier ilmenite on NO<sub>x</sub> formation in chemical-looping combustion. *Fuel Process Technol* 222:106962
14. Lu D. Enhancement combustion performance and emission control in oxy-FBC using oxygen carriers. In: 76th IEA-FBC meeting, Seoul, Korea, 13 May 2018
15. Hanning M, Corcoran A, Lind F, Rydén M (2018) Biomass ash interactions with a manganese ore used as oxygen-carrying bed material in a 12 MW<sub>th</sub> CFB boiler. *Biomass Bioenergy* 119:179–190

**Open Access** This chapter is licensed under the terms of the Creative Commons Attribution 4.0 International License (<http://creativecommons.org/licenses/by/4.0/>), which permits use, sharing, adaptation, distribution and reproduction in any medium or format, as long as you give appropriate credit to the original author(s) and the source, provide a link to the Creative Commons license and indicate if changes were made.

The images or other third party material in this chapter are included in the chapter's Creative Commons license, unless indicated otherwise in a credit line to the material. If material is not included in the chapter's Creative Commons license and your intended use is not permitted by statutory regulation or exceeds the permitted use, you will need to obtain permission directly from the copyright holder.

